

Dissertation

**The Role of the M₃-Muscarinic Receptor (M₃-R) in Bile
Formation and Cholangiopathies**

Submitted by

Dr.med.univ. Franziska Baumann-Durchschein

for the Academic Degree of

Doctor of Medical Science

Dr. scient. med.

at the

Medical University of Graz
Division of Gastroenterology and Hepatology

under the Supervision of

Univ. Prof. Dr. Peter Fickert

2017

Declaration

I hereby declare that this thesis is my own original work and that I have fully acknowledged by name all of those individuals and organisations that have contributed to the research for this thesis. Due acknowledgement has been made in the text to all other material used. Throughout this thesis and in all related publications I followed the guidelines of "Good Scientific Practice and Ombuds Committee at the Medical University of Graz".

Part of this thesis has been published in Durchschein F, Krones E, Pollheimer M, Zollner G, Wagner M, Raufmann JP, Fickert P: Genetic loss of the muscarinic m3 receptor (m3-r) markedly alters bile formation and cholestatic liver injury in mice. *Hepatology Research*. 2017; in press (1)." I have obtained permission to reproduce figures and tables published in Durchschein F, Krones E, Pollheimer M, Zollner G, Wagner M, Raufmann JP, Fickert P: Genetic loss of the muscarinic m3 receptor (m3-r) markedly alters bile formation and cholestatic liver injury in mice. *Hepatology Research*. 2017; in press from John Wiley & Sons Australia, ("Wiley").

14.07.2017

TABLE OF CONTENTS

TABLE OF CONTENTS	3
ABBREVIATIONS:	5
ABSTRACT	7
KURZFASSUNG	8
1 INTRODUCTION	10
2 ANATOMIC STRUCTURE OF LIVER INNERVATION	11
2.1 The Sympathetic and Parasympathetic Innervation of the Liver	11
2.2 The Efferent and Afferent Innervation of the Liver	14
2.3 The Intrahepatic Liver Innervation	16
2.4 Neurotransmitters of Liver Innervation	19
3 INTERSPECIES VARIATIONS OF HEPATIC INNERVATION	21
4 THE LIVER-BRAIN INFLAMMATION AXIS: A FEEDBACK MECHANISM REGULATING IMMUNE RESPONSE	22
5 ALTERED HEPATIC INNERVATION IN LIVER DISEASES	25
6 REGULATION OF LIVER REGENERATION BY THE AUTONOMOUS NERVOUS SYSTEM	26
7 MUSCARINIC RECEPTORS	28
8 REGULATION OF CHOLANGIOCYTE'S FUNCTION BY THE PARASYMPATHETIC NERVOUS SYSTEM:	28
9 POTENTIAL PATHOGENETIC ROLE OF THE M ₃ -R IN HUMAN CHOLESTATIC LIVER DISEASES	30
10 STATUS OF RESEARCH	34
10.1 What is Known about the Liver Phenotype and Biliary Physiology in M ₃ -R Knockout Mice?	34
10.2 What is Known about M ₃ -R Function and Alterations in Cholangiopathies?	34
10.3 Hypotheses	35
11 MATERIAL AND METHODS:	36
12 RESULTS	41
12.1 Aim (1): Determine the Physiological Role of M ₃ -R in Bile Formation	41
12.1.1 Comparison of bile flow in M ₃ -R ^{-/-} mice and WT controls:	41
12.1.2 Comparison of bile flow in M ₃ -R ^{-/-} mice and WT controls after intraperitoneal (i.p.) N-butyl-scopolamine injection:	42

12.1.3	Comparison of bile flow in $M_3-R^{-/-}$ mice and WT controls after <i>norUDCA</i> feeding:	43
12.2	Aim (2): Determine the Pathophysiological Role of the M_3-R in Mouse Models for Cholangiopathies and Biliary Fibrosis	45
12.2.1	Comparison of $M_3-R^{-/-}$ and WT mice after 17 days 3,5-diethoxycarbonyl - 1,4 -dihydrocollidine (DDC) feeding:.....	45
12.2.2	Comparison of $M_3-R^{-/-}$ and WT mice after CBDL for 5 days:	50
12.2.3	Comparison of $M_3-R^{-/-}$ and WT after 1% cholic acid (CA) feeding for 7 days:	53
12.2.4	Comparison of $M_3-R^{-/-}$ and WT after 1% lithocholi acid (LCA) feeding	55
12.2.5	Comparison WT after DDC feeding with sham operation versus vagotomy:..	57
12.2.5	Comparison of $Mdr2^{-/-}$ mice treated with vagotomy for 4 and 8 weeks versus sham operated mice:	61
12.2.6	Comparison of liver injury in $Mdr2^{-/-}$ after 4 weeks treatment with bethanechol (M_3 -agonist) versus controls:.....	67
12.2.7	Comparison of bile flow in $Mdr2^{-/-}$ mice after 1 week treatment with bethanechol (M_3 -Agonist) versus untreated controls:	70
12.2.8	Comparison of liver phenotyp in „aged“ $M_3-R^{-/-}$ compared to WT mice:	71
13	DISCUSSION	72
12	REFERENCES	84

ABBREVIATIONS:

ACh	Acetylcholine
AChE	Acetylcholinesterase
AE2	Cl ⁻ /HCO ⁻³ anion exchanger 2
ALT	Alanine aminotransferase
AP	Alkaline phosphatase
ASH	Alcoholic steatohepatitis
BA	Bile acids
BA	Bile acid
BD	Bile duct
BEC	Biliary epithelial cell
BW	Bodyweight
CA	Cholic acid
cAMP	Cyclic adenosine monophosphate
CBDL	Common bile duct ligation
CBDL	Common bile duct ligation
CCC	Cholangiocarcinoma
CFTR	Cl ⁻ channel cystic fibrosis transmembrane regulator
CGRP	Calcitonin Gene-Related Peptide
CHB	Chronic hepatitis C
CHC	Chronic hepatitis C
CK-19	Cytokeratin-19
D₂ receptor	Dopamine 2 receptor
DAG	Diacylglycerol
DDC	3,5-diethoxycarbonyl-1,4-dihydrocollidine
DDC	3,5-diethoxycarbonyl-1,4-dihydrocollidine
DNA	Deoxyribonucleic acid
DRG	Dorsal root ganglia
DSS	dextran sodium sulphate
EGF	Endothelial growth factor
EpCAM	Epithelial cell adhesion molecule
GJ	Gap type junctions
GLP	Glucagon, glucagon- like peptide
H/E	Hematoxylin/Eosin
HA	Hepatic artery
HCC	Hepatocellular carcinoma
HGF	Hepatocyte growth factor
hmAChR M₃	Human muscarinic acetylcholine receptor of the M ₃ type
HPC	Hepatic progenitor cells
HSC	Hepatic stellate cells
i.p.	Intraperitoneal
IHC	Immunohistochemistry
IHF	Immunofluorescence
IL	Interleukin
IP3	Inositol triphosphate
LCA	Lithocholic acid
LPS	Lipopolysaccharide
LTX	Liver transplantation
M₃-R	Muscarinic receptor of the M ₃ type
mRNA	Messenger Ribonucleic acid

NfκB	Nuclear factor kappa B
norUDCA	24- <i>nor</i> ursodeoxycholic acid
NPY	Neuropeptide Y
NSE	neuron-specific enolase
OHDA	6-hydroxydopamine
PBC	Primary biliary cirrhosis
PH	Partial hemihepatectomy
PKA	Proteinkinase A
PSC	Primary sclerosing cholangitis
PV	Portal vein
SC	Sclerosing cholangitis
SSC-CIP	Secondary sclerosing cholangitis in critically-ill patients
SSC-CIP	Sclerosing cholangitis of critically ill patients
TGF α	Transforming growth factor α
TNF α	Tumor necrosis factor α
TRPV4	transient receptor channel protein vanilliod 4
VCAM	Vascular cell adhesion molecule
VIP	Vasoactive intestinal peptide
WT	Wild type
α7nAChR	α 7 subunit nicotinic receptor
αSMA	α-smooth muscle antigen

ABSTRACT

Cholangiopathies remain the major black box in modern hepatology since their etiology and pathophysiology are almost enigmatic. Therefore, medical treatment modalities for prototypic cholangiopathies such as primary sclerosing cholangitis (PSC), secondary sclerosing cholangitis of critically ill patients (SSC-CIP), and primary biliary cirrhosis (PBC) are limited in their efficacy and consequently there is a frequent need for liver transplantation in such difficult to treat patients. Since cholangiocytes represent both victims and therapeutic targets in cholangiopathies, physiology of these highly specialized epithelial cells lining up bile ducts is of major interest. Cholangiocytes secretory function and regenerative capacity is regulated by numerous transport proteins, specific receptors for cytokines/chemokines, growth factors, hormones, and neurotransmitters. The muscarine 3 receptor (M_3 -R) represents the primary cholangiocyte receptor for the afferent parasympathetic innervation.

Therefore, we aimed to determine the specific role of the M_3 -R in bile formation and models for cholestatic liver disease in mice. We compared bile flow and composition in M_3 -R knock-out mice (M_3 -R^{-/-}) and wild type littermates (WT). Liver function and morphology in aged M_3 -R^{-/-} mice were compared to respective aged WT controls. For the second aim we compared liver injury in both genotypes in different cholestatic models (3,5-diethoxycarbonyl-1,4-dihydrocollidine (DDC) feeding, lithocholic acid (LCA) feeding and common bile duct ligation (CBDL)); these experimental interventions represent well-characterized preclinical models of cholestatic liver disease. To analyze the possible role of the M_3 -R as a therapeutic target, we treated 4 weeks-old $Mdr2$ ^{-/-} mice, a preclinical model for sclerosing cholangitis, with the M_3 -R agonist bethanechol for 4 and 8 weeks. Besides we performed hepatic vagotomy in different cholestatic models (DDC-feeding, $Mdr2$ knockout mice) to determine the effect of the parasympathetic nervous system in general on cholestasis.

Our experimental findings show that M_3 -R-signalling significantly influences bile formation. M_3 -R^{-/-} mice showed significantly reduced bile flow compared to WT mice, most likely due to decreased biliary HCO_3^- secretion. However, even aged M_3 -R^{-/-} mice did not spontaneously develop liver injury or cholestasis. M_3 -R^{-/-} and WT littermates show different susceptibility in the used cholestatic mouse models, which highlights the important role of this receptor. Since treatment of $Mdr2$ ^{-/-} mice with a M_3 -R agonist decreases liver injury, M_3 -R signaling may represent a novel therapeutic target in specific cholangiopathies.

KURZFASSUNG

Ätiologie und Pathogenese chronischer Gallenwegserkrankungen (Cholangiopathien) wie der primär sklerosierenden Cholangitis (PSC), der primär biliären Zirrhose (PBC) und der sekundär sklerosierenden Cholangitis kritisch-kranker Patienten (SSC-CIP) sind weitgehend unklar. Das fehlende grundlegende pathobiologische Verständnis erklärt die bislang nur sehr limitierten medikamentös-therapeutischen Möglichkeiten bei diesen Krankheitsbildern. Das Fortschreiten dieser Erkrankungen kann zu einer Leberzirrhose führen, welche oftmals eine Lebertransplantation notwendig macht. Da Gallengangsepithelzellen (Cholangiocyten) sowohl Opfer als auch therapeutische Ziele bei Cholangiopathien darstellen, ist die Physiologie dieser hoch spezialisierten Epithelien von großem potentiell therapeutischem Interesse. Sekretion und regenerative Kapazität von Cholangiocyten werden durch spezielle Rezeptoren und Transportproteine, Cytokine/Chemokine, Wachstumsfaktoren, Hormone und Neurotransmitter reguliert und gesteuert. Die parasympatische Innervation von Cholangiocyten erfolgt über Fasern des Nervus vagus dessen Endigungen über Freisetzung von Acetylcholin den Muskarin 3 Rezeptor (M_3 -R) an der basolateralen Membran von Cholangiocyten aktivieren. Da die parasympatische Innervation von Speicheldrüsen von essentieller Bedeutung für die Steigerung der Sekretionsleistung und die Zusammensetzung des gebildeten Sekrets ist, könnte der M_3 -R von Gallengangsepithelien auch eine zentrale Rolle bei der duktalem Gallebildung spielen und Störungen des M_3 -R Signalweges in der Pathogenese von Cholangiopathien von Bedeutung sein.

Daher war das Ziel dieser Arbeit die Rolle des M_3 -R für die Gallebildung sowie dessen pathophysiologische Relevanz in Tiermodellen für Cholangiopathien zu untersuchen. Hierzu wurde in M_3 -R Gen knockout Mäuse (M_3 -R^{-/-}) und entsprechenden Kontrollmäusen der Gallefluß gemessen. Desweiteren wurden beide Gruppen in verschiedenen Mausmodellen für Cholangiopathien miteinander verglichen (3,5-diethoxycarbonyl-1,4-dihydrocollidine (DDC)-Fütterung, Lithocholsäure (LCA)-Fütterung and Gallengansligatur (CBDL)). Desweiteren wurden $Mdr2$ ^{-/-} mit dem M_3 -R Agonisten Bethanechol behandelt, um den Nutzen des M_3 -R als therapeutischen Angriffspunkt zu klären.

Unsere Ergebnisse zeigen, dass der M_3 -R die Gallebildung beeinflusst. M_3 -R^{-/-} Mäuse besitzen im Vergleich zu den Kontrollmäusen einen signifikant geringeren Gallefluß. Desweiteren unterscheidet sich ihre Anfälligkeit in den verwendeten murinen Cholestasemodellen gegenüber den Wildtyp Tieren, was auf einen Einfluss des parasympathischen Nervensystems bei Cholangiopathien hin deutet. Da die Behandlung von $Mdr2$ ^{-/-} mit einem M_3 -Agonist zu einem geringeren Leberschaden führt, könnte die

Aktivierung des M₃-R eine neue Therapieoption in der Behandlung der Cholangiopathien darstellen.

1 INTRODUCTION

Since the landmark discovery of the important role of nerves in controlling digestive secretion by Ivan Petrovitch Pawlow in the 19th century (2), the knowledge on the autonomous nervous system in regulating gastrointestinal function has been engrossed (3). Based on the observation approximately 150 years ago that “wounding” of the fourth ventricle’s floor in brain stimulates hepatic glucose release by Claude Bernard, detailed morphological studies showed intense hepatic nervous innervation (4). However, the exact structure and function of hepatic innervation is still not fully understood (5).

Studies in neurohepatology in the last decades indicate that the autonomous system plays a pivotal role in regulating liver metabolism, hemodynamic and regeneration. Activation of the sympathetic nervous system leads to hepatic glucose production, whereas stimulation of the parasympathetic nervous system induces hepatic glucose uptake (6). Interruption of the parasympathetic innervations by hepatic branch vagotomy suppresses liver regeneration after partial hepatectomy (7). By contrast, vagal stimulation following hepatectomy results in an increased liver regeneration (8).

In particular, the parasympathetic nervous system is an important modulator of gastrointestinal functions. Acetylcholine (ACh) stimulation results in gastric acid secretion, duodenal bicarbonate (HCO_3^-) secretion, stimulation of gut motility, and affects the renewal rate of the intestinal epithelium. In the alimentary tract almost each function involves muscarinic receptor activation. In the liver cholangiocytes and hepatic progenitor cells (HPCs) express the muscarinic M_3 receptor (M_3 -R) (8). Activation of the M_3 -R on HPCs results in an enhanced liver regeneration (8). However the role of the M_3 -R expressed on cholangiocytes is still unknown.

The aim of our study was to evaluate the function of the M_3 -R in bile formation and cholangiopathies. To accomplish these goals we compared bile flow and composition in M_3 -R knock-out mice (M_3 -R^{-/-}) and wildtype (WT) littermates. Besides we compared both mouse groups in different cholestatic models.

2 ANATOMIC STRUCTURE OF LIVER INNERVATION

2.1 The Sympathetic and Parasympathetic Innervation of the Liver

Hepatic innervation is a complex network of sympathetic and parasympathetic nerve fibers. Despite technological progress with improved neuro-imaging and high resolution, the exact structure of liver innervation is until now not fully understood. In general, the autonomic nervous system consists of two branches: the sympathetic nervous system and the parasympathetic nervous system (9, 10). Typically these two branches act in a reciprocal fashion with an increase in activity in one branch coincident to a decline in activity of the other (10, 11). The majority of peripheral tissues are innervated by both systems (10).

In the past many researchers tried to analyse liver innervations in detail. In 1875 Karl Wilhelm von Kupffer looked for nerve fibers in the liver lobule. However he was unable to demonstrate hepatic nerves and described instead the "Sternzelle" which is now known as the Kupffer cell, meaning the liver resident macrophages. He wrote in his notations: "Im Verlauf der andauernden und immer noch vergeblichen Bemühungen Nerven in den Leberläppchen nachzuweisen" (12). One of the first who described the distribution of hepatic nerves was Eduard Pflüger in 1869 (13). In 1928 Lothar Riegele demonstrated the close relationship between nerves, blood vessels and parenchymal cells in mammalian livers (13). In the 1960s and 1970s, morphological observations postulated that the liver is a very sparsely innervated organ. This was confirmed by the observation that a transplanted and consequently total denervated liver is able to function well without any significant problems. However, studies in the last two decades demonstrate that this long-standing view is subject to revision (14). Systematic neural ablation has emphasized the importance of the hepatic innervation in physiological and pathological processes (15-17).

The liver is innervated by the sympathetic and parasympathetic system (s. figure 1) (15). In most mammalian species, large nerve fibers can be identified at the hilum of the liver. These nerve fibers originate from the celiac plexus, lower thoracic ganglia, right phrenic nerve and the vagal nerves (18). The vagal nerves divide into an anterior (left) and posterior (right) branch as they proceed from the thorax into the abdomen (18). The anterior vagus splits into a cephalic and a hepatic division, which runs through the gastrohepatic ligament to innervate the liver and is responsible for the parasympathetic innervation. Sympathetic innervation derives predominantly from the celiac plexus as well as from the thoracic splanchnic nerves

(18). The sympathetic innervation is postganglionic and arises in the celiac and superior mesenteric ganglia, which receive preganglionic fibers from the intermediolateral column of spinal cord (T₇-T₁₀) (17, 19). By contrast, the parasympathetic branch of the vagal nerves innervates the liver either directly as preganglionic fibers developing in the dorsal motor nucleus of the brainstem located at the hepatic hilus (17). Before entering the liver, the sympathetic and parasympathetic fibers form two separated but intercommunicating plexus in close position to the portal vein and the hepatic artery: an anterior hepatic plexus around the hepatic artery and a posterior hepatic plexus around the portal vein and the common bile duct (20, 21).

The smaller anterior hepatic plexus is located in the hepatoduodenal ligament and is in close contact with the hepatic artery (19, 22). It consists of parasympathetic fibers of the vagal nerves: direct hepatic branches of the anterior vagal trunk, branches from the main nerves of the lesser curvature of the stomach and fibers originating predominantly from the posterior vagal trunk via the celiac plexus (22). Sympathetic nerves arise from the celiac plexus, which consists of celiac ganglia and fibers from the splanchnic nerves (19, 22). The nerve fibers of the anterior hepatic plexus supply the liver, the bile ducts and the gallbladder (22).

The larger posterior hepatic plexus is located behind the portal vein and is generally associated with it. The parasympathetic fibers predominantly derive from the posterior vagal trunk (22). The sympathetic fibers come from the celiac plexus. In some species parasympathetic fibers also originate from the right phrenic nerve (19). For instance, in cat and man, the right phrenic nerve appears not to contribute consistently to the innervation of the liver (21). However, some nerve fibers do not follow hepatic vessels and enter the liver *via* the small omentum (23).

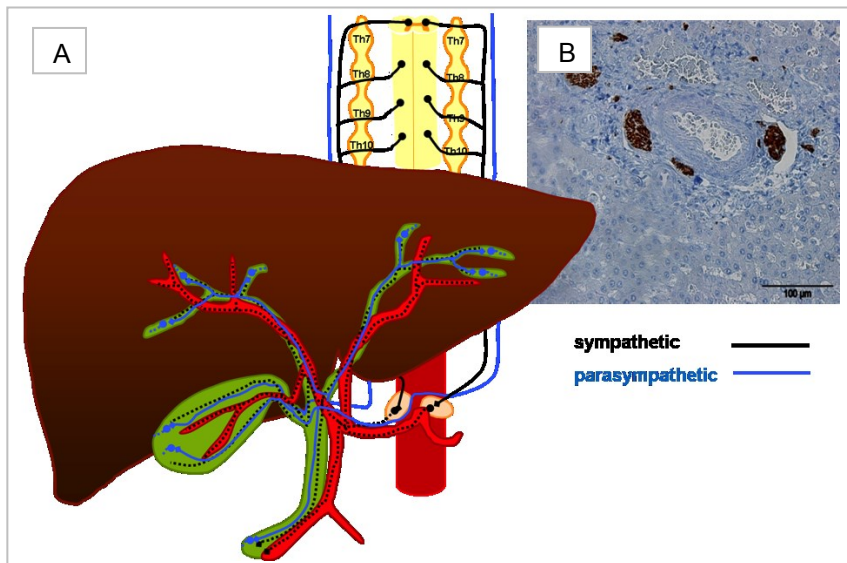


Figure 1: Liver innervation

A: The liver is innervated by sympathetic and parasympathetic fibers. In most mammalian species, large nerve fibers can be identified at the hilum of the liver. They form two separate but intercommunicating plexuses in close contact to the portal vein and the hepatic artery: The anterior plexus around the hepatic artery and a posterior plexus around the portal vein and the common bile duct. These bundles consist of sympathetic fibers from Th7-Th10 (black line) via the coeliac ganglia and parasympathetic nerves (blue line) from the posterior and anterior vagal nerves. **B:** Liver histology illustrating nerve fibers, immunohistochemical stained for neurofilament (brown), which follow the branches of the A. hepatica.

2.2 The Efferent and Afferent Innervation of the Liver

The hepatic neural network cannot only be divided in sympathetic and parasympathetic nerve fibers, but also in afferent and efferent fibers (21). These nerves arise from or terminate in nuclei of the central nervous system (22). The central regulator of these afferent and efferent signals is the hypothalamus (24). After receiving signals from afferent nerves, the hypothalamus transmits informations to the peripheral organs including the liver (24).

The hypothalamus can be classified into three areas: lateral, medial and the periventricular area (24). Each area consists of several nuclei (24). There are two significant nuclei and one area in the hypothalamus navigating the neural autonomic information of the liver: the ventromedial hypothalamic nucleus (VMH) in the medial area, the lateral hypothalamic area (LHA) and the periventricular hypothalamic nucleus (PVN) in the periventricular area (24). VMH transmits sympathetic signals to the liver via the celiac ganglia, the LHA sends parasympathetic signals to the liver via the vagal nerve, and the PVN sends both, sympathetic and parasympathetic information (24).

The **efferent** hepatic innervations is a complicated network of parasympathetic and sympathetic fibers: The parasympathetic efferent innervation is controlled by the PVN and LHA (24). These structures are directly associated to parasympathetic cell groups of the nucleus vagus and to the medullary reticular cell group (25). These areas supply efferent preganglionic parasympathetic nerves to the liver (24, 26). The sympathetic efferent signals are controlled by the PVN and VMH. The descending projections are connected to the intermediolateral cell column in the thoracolumbar spinal cord and preganglionic neurons finally send signals to the liver via the celiac ganglia (24, 27). This complex efferent innervation regulates intrahepatic haemodynamic, bile flow, control of carbohydrate and lipid metabolism as well as parenchymal cell regeneration (19, 28). For example stimulation of the VMH promotes glycogenolysis, whereas stimulation of the LHA promotes glycogenesis (19, 22, 29). A scheme of the efferent liver innervation is given in figure 2 (24).

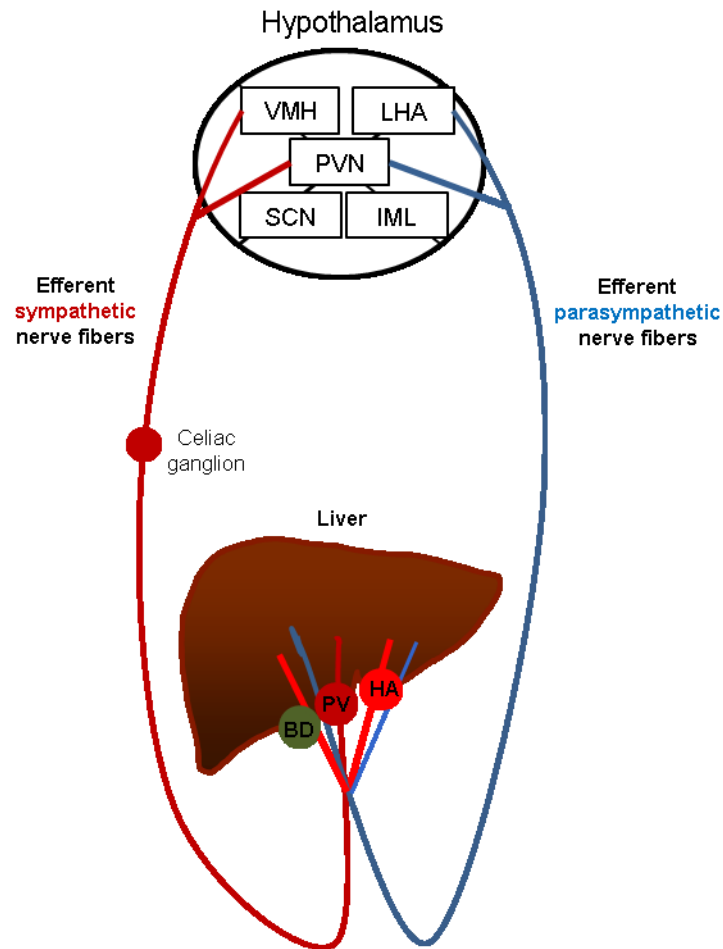


Figure 2: Scheme of efferent nerve pathways between hypothalamus and the liver

The liver is innervated by efferent sympathetic (red line) and parasympathetic (blue line) nerve fibers. This generates a direct link between liver and brain (hypothalamus) to regulate the intrahepatic haemodynamic, bile flow, carbohydrate and lipid metabolism as well as parenchymal cell regeneration.

VMH: ventromedial hypothalamic nucleus; **LHA:** lateral hypothalamic area; **PVN:** periventricular hypothalamic nucleus; **SCN:** suprachiasmatic nucleus; **IML:** intermediolateral column; **BD:** bile duct; **PV:** portal vein; **HA:** hepatic artery

Adapted from Uyama et al. Anat Rec A Discov Mol Cell Evol Biol. 2004

Additionally to the efferent innervation, the liver is also supplied by **afferent** sympathetic and parasympathetic nerves. There are approximately ten times more vagal afferents than efferents (30). Afferent nerves can be detected near the peribiliary glands of the larger intra- and extrahepatic bile duct and the portal vein adventitia (24, 30, 31). From the liver, they follow the vagal and splanchnic nerves, which project to the tractus solitarius (19, 24, 31). Afferent nerve fibers are directly linked to chemo-, osmo- and baroreceptors and play a key role as hepatic sensors (24). By sending signals to the brain, the afferent hepatic innervation helps to regulate a number of metabolic pathways. The liver is exposed to alimental and solute load entering the body from the gut before this reaches the systemic circulation. Therefore hepatic afferent innervation is an essential feedback mechanism modulating

water intake, glomerular filtration rate, natriuresis, glucose homeostasis, appetite and gastric emptying (19). For example, hepatic neurons depend on osmotically activated ion channels like the transient receptor channel protein vanilloid 4 (TRPV4) (32). Detection of hypo-osmolality by this channel is transmitted to the brain via afferent hepatic fibers (32). Liver-transplant recipients exhibit lower plasma norepinephrine levels after water intake compared to those of control transplant recipients (like kidney transplants) (33). Besides, liver transplant patients show an elevated plasma osmolality and a decreased sympathetic response to water intake (17, 33). Next to blood osmolality, a number of studies have revealed glucose sensing by the liver (17). Decreased portal glucose concentrations stimulate vagal afferent activity, which triggers increased food intake (17, 34). A scheme of hepatic afferent innervation is illustrated in figure 3 (24).

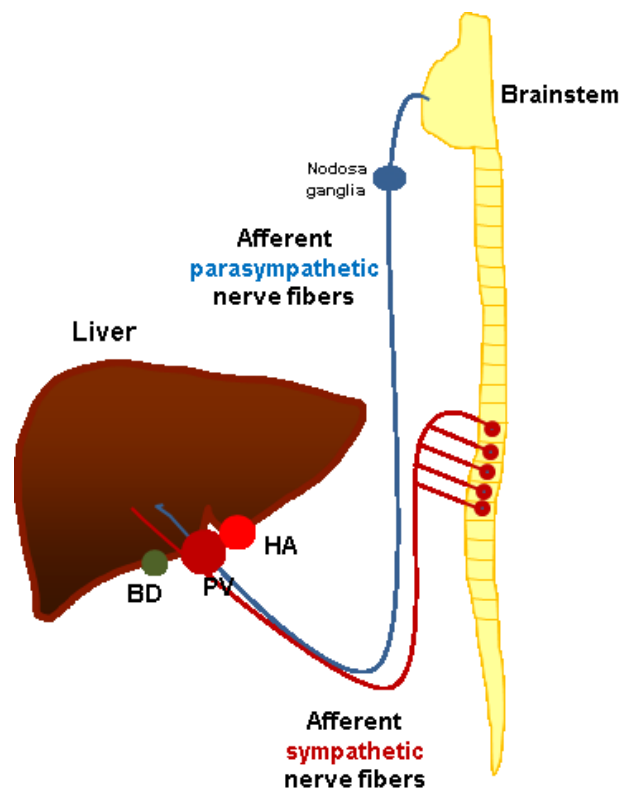


Figure 3: Scheme of afferent nerve pathways between the hypothalamus and the liver

Afferent nerve fibers play a key role as sensors in peripheral organs and send signals to the brain. These fibers can be found terminates near the peribiliary glands of bile ducts and the portal vein adventitia. From the liver, the afferent nerve fibers follow the vagus and splanchnic nerves. By sending signals to the brain, hepatic afferent innervation represents a feedback mechanism, which modulate water intake, glomerular filtration rate, natriuresis, glucose homeostasis, appetite and gastric emptying. **BD:** bile duct; **PV:** portal vein; **HA:** hepatic artery;

Adapted from Uyama et al. *Anat Rec A Discov Mol Cell Evol Biol.* 2004

2.3

The Intrahepatic Liver Innervation

Various methods have been used to study the intrahepatic nerves in more detail (22). However the exact distribution of nerves in the liver is incompletely understood and differs according to species (23). Moreover there is also an uneven distribution of fibers between different lobules (22). While intrahepatic fibers expand throughout the lobule, they predominate in the periportal region (35). Here they are in close contact to vessels, hepatocytes, bile ducts and sinusoidal cells (19, 35). In the portal and centrolobular spaces, naked endings without a Schwann sheath reach some mesenchymal cells such as fibroblasts, myofibroblasts, and smooth muscle cells, which form part of the adventitial wall of blood vessels and bile ducts (36). Nerve endings in the intralobular spaces are situated mainly in the space of Disse (36). Electron microscopic studies have detected nerve terminals along the space of Disse, where nerve endings are closed to sinusoidal and perisinsoidal cells (10, 22, 37). Here, nerve terminals can interact with sinusoidal endothelial cells, Kupffer cells, hepatocytes and hepatic stellate cells (23, 38, 39). Due to this dense neural network, liver regeneration, fibrosis and hepatic hemodynamics may be regulated by the autonomic nervous system. Next to parenchymal cells, nerve fibers can also be detected in the biliary tree. In the normal liver, extrahepatic bile ducts and peribiliary glands have parasympathetic and sympathetic nerve fibers in their walls (40). S-100- and NSE-positive nerves can be found in the walls of intrahepatic large, medium-sized and septal bile ducts as well as in the intralobular connective tissue of peribiliary glands (10, 41). Intrahepatic peribiliary glands secrete mucous glycoproteins into bile ductal lumina (41) as well as bicarbonate ion (HCO_3^-), electrolytes and water (42). As vagal stimulation increases biliary secretory activity (41-43), peribiliary glands might be targeted by the parasympathetic nervous system (41). However the density of nerve fibers in the biliary tract is much lower than in blood vessels (41).

Hepatic nerve fibers contain classical neurotransmitters, like noradrenaline and acetylcholine (ACh) (19). Numerous hepatic functions are regulated by these neurotransmitters, which activate different receptors expressed by parenchymal and non-parenchymal cells. Hepatocytes express α_1 - and α_2 - as well as β_1 - and β_2 - adrenergic receptors. The liver is activated by epinephrine and norepinephrine released from intrahepatic nerve endings but also derived through the blood from the adrenal glands (23). By stimulating the α_1 -receptor noradrenalin can affect the glucose metabolism of hepatocytes (44). Norepinephrine released from nerve endings can activate the formation of prostanoids in non-parenchymal liver cells modulating hepatocyte metabolism (23). Besides noradrenalin can stimulate the proliferation and collagen synthesis of hepatic stellate cells (HSC) (45) and can suppress

apoptosis in hepatocytes (46). Moreover, sympathetic activity alters hepatic progenitor cell (HPC) accumulation in damaged livers and alters liver regeneration (47).

Nerve fibers communication with hepatocytes can be divided into three different mechanisms (23): First, hepatocytes can be influenced directly by neuropeptides. Second, signals can be intercellularly transmitted by using gap type junctions (GJ). GJ regulate the transmission of information to neighboring cells, achieving functional integration of hepatocytes. GJ density is different among species and are more numerous in rats and mice compared to human liver (23). In mouse and rat livers, only a few hepatocytes have a neural supply but exhibit numerous GJ (22, 23). Consequently the lack of innervation could possibly be compensated by direct intercellular communicative GJ (12, 22). Third, sinusoidal cells innervation can result in activation of hepatocytes by releasing eicosanoids (like prostaglandins, leukotrienes), cytokines (like necrotic factor or IL-6) and other chemical mediators (like endothelin or nitric oxide) (23).

Next to hepatocytes, cholangiocytes also express a number of different receptors, which can be activated by neurotransmitters. Proliferating cholangiocytes express α_1 - and α_2 - as well as β_1 - and β_2 - adrenergic receptors influenced by sympathetic nerve terminals (48, 49). Additionally, the muscarinic M_3 receptor (M_3 -R) can be found at their basolateral membrane (50) as well as the D_2 -dopaminergic receptor (51). It was shown that the secretin-induced ductal secretion in BDL rats was inhibited by the D_2 dopaminergic agonist quinlorane (51), supporting the role of the dopaminergic innervation in biliary physiology.

Altogether, these data suggest that the autonomic innervation plays a substantial role in regulating liver function. The parenchymal as well as the non-parenchymal cells of the liver seem to be directly regulated by sympathetic as well as parasympathetic nerve fibers. In general, there are fewer cholinergic than adrenergic fibers in the human liver (41).

2.4 Neurotransmitters of Liver Innervation

Hepatic innervation is a complex network of sympathetic and parasympathetic nerve fibers with afferent and efferent, aminergic, cholinergic and peptidergic components (21). These nerves contain not only classical neurotransmitters, but also regulatory peptides such as substance P, somatostatin, Calcitonin Gene-Related Peptide (CGRP), neuropeptide Y (NPY), vasoactive intestinal peptide (VIP), glucagon, glucagon-like peptide (GLP), neurotensin, serotonin or galanin or bombesin (52). They are released locally by autonomic nervous fibers and are involved in the regulation of liver hemodynamics as well as liver function. The distribution of these fibers differs among species.

Aminergic positive fibers associated with hepatic arteries are denser than those linked to the portal veins and bile ducts (21, 24, 35). Central and sublobular hepatic veins lack innervation but aminergic nerves can be found in the walls of the larger hepatic veins (35, 53). Furthermore, as numerous parenchymal cells of the perisinusoidal and sinusoidal space are connected to nerve terminals, aminergic nerves may directly regulate not only hepatic parenchymal metabolism but also the tone of the sinusoidal wall (35, 54).

Cholinergic nerves form a plexus, which is separate from aminergic nerves and courses adjacent to the vasculature in portal areas (35, 55). Acetylcholinesterase-(AChE)-positive fibers can be found in both hepatic arteries and bile ducts (21). There are inconsistent findings concerning the presence of intralobular cholinergic fibers (35). However, some cholinergic fibers are not associated with the vasculature and course adjacent to the hepatic cells that abutted the portal area (35). Besides, the cholinergic innervation is more prevalent in rat and mice compared to humans (21).

Neuropeptides have been colocalized with neurotransmitters in both aminergic and cholinergic nerves (35). They are associated with the branches of the portal vein, hepatic artery and bile ducts in the connective tissue of portal tracts (21, 35). NPY has been localized in aminergic nerves supplying all segments of the portal venous, arterial and biliary system of the liver (56). NPY-positive fibers are more dense around portal vein and hepatic artery branches compared to bile ducts in the periportal area. However, they can be detected in the larger extrahepatic bile ducts. Here these fibers are involved in the modulation of biliary secretion, suggesting an endocrine-paracrine control of bile flow (40). Additionally, a dense NPY-immunoreactive network can be found near hepatocytes: the nerve terminals can be detected close to endothelial cells of blood vessels and in the space of Disse (19, 57). NPY has direct vasoconstrictor properties and potentiates the effect of noradrenalin (58). Consequently, these fibers might help to regulate hepatic hemodynamics. Besides, NPY can

inhibit cholangiocarcinoma growth (59) and promote the proliferation of HSCs (45). Other peptidergic nerves, like substance P and somatostatin positive fibers, follow a similar distribution like NPY-positive fibers (35). Somatostatin positive fibers are located around the portal vein and hepatic artery in the periportal and perisinusoidal region (24). These nerve terminals are in close contact with sinusoidal liver cells (60). Besides, somatostatin receptors can be found in cholangiocytes and in activated HSCs (61, 62). Studies showed, that somatostatin can inhibit basal and secretin-induced ductal bile secretion as well as the proliferation of cholangiocytes induced by bile duct ligation (61, 62). Somatostatin might also regulate contraction of HSCs as well as hepatic microcirculation (24). The number of somatostatin positive nerve are decreased in patients with alcoholic cirrhosis compared to normal livers (56), arguing for a role of the autonomous nervous system in liver diseases.

Substance P positive fibers are not as numerous as NPY-positive nerves (21). They are more common in the periportal (21) and intralobular regions of the liver, where their terminals are associated with HSCs (63). Substance P containing nerves often inclose the neurotransmitter CGRP (24, 64). CGRP-positive nerve fibers are located in the periportal region but not in the intralobular area (21). Additionally, these nerve fibers can be detected adjacent to bile ducts with a high density in humans (19, 21, 65).

Like CGRP, VIP-positive nerve fibers are located around vessels and bile ducts in the periportal area, but not in the intralobular area (21, 66). Compared to NPY or substance P positive fibers, the number of VIP-positive nerves in the liver is much lower (24). However, VIP positive nerves seem to regulate biliary secretion. VIP infusion results in a significantly increase of human biliary HCO_3^- output (67). Besides VIP stimulates the HCO_3^- secretion in cultured cholangiocytes via a cAMP-independent pathway (68).

3 INTERSPECIES VARIATIONS OF HEPATIC INNERVATION

The intrahepatic distribution of nerves is highly species-dependent (12). Even within one species, there are remarkable variations in the pattern of innervation (19, 21). As rats, mice and guinea pigs are mostly used in animal experiments, hepatic innervation of these species will be compared to human livers (21). In most species, parasympathetic and sympathetic nerve fibers can be detected around the hepatic artery, portal vein and bile ducts, indicating general innervation of these structures by a variety of neuron subtypes (17).

In the human liver, nerve endings are disseminated all over the hepatic lobules from the portal spaces to the centrilobular spaces (36), by contrast to mice and rats with a less dense hepatic innervation. Among mammals, the human liver has the highest density of intralobular nerves (24). Immunohistochemical studies on the development of nerves in the human fetal liver showed, that a few neurofilament-containing fibers can be detected at the hilum of an eight week human fetal liver (69). During embryonic growth, the liver is sparsely innervated and does not contain intrinsic neurons by contrast to the developing gastrointestinal tract (70). Portal tract innervation is not detected before twelve weeks (19). There is however a progressive rise in density in neural fibers towards term (19). Consequently, the fetal human liver might not need broad neural control to develop. However after gestation the role of hepatic innervation changes as reflected in its more complex innervation pattern (70). Intrahepatic fibers in human liver seem to be only partly surrounded by Schwann cells (19). In normal human livers neuron-specific enolase (NSE)- immunoreactive fibers (which are positive for neuronal axons) can be found around hepatic arteries, portal veins and bile ducts in the portal areas and less frequently in the parenchyma (71).

Guinea pigs show an intralobular innervation similar to the human one (23). By contrast, rodents have only little or no intralobular innervation (23, 35). In rats and mice only hepatic cells in the portal region seem to be in close contact with intrahepatic nerve endings (23). Intrahepatic tight-junctions help to transmit electrochemical and hormonal signals from the periportal area to hepatocytes and to the intrahepatic vasculature (72). This effect is more pronounced in livers of rats and mice compared to humans (73).

There are also numerous interspecies differences concerning the aminergic, cholinergic and peptidergic hepatic innervations (table 1) (24). Intralobular distribution of aminergic nerve fibers shows significant species variation. Aminergic nerves are not detected in the

parenchyma of mouse and rat livers, but are found in the hepatic parenchyma of guinea pigs and humans (21). In humans and guinea pigs these intralobular aminergic nerves course from the portal region to the space of Disse. Here they are in close contact with hepatocytes and sinusoidal endothelial cells (21). By contrast, in rats and mice fine aminergic nerve fibers can be observed only along the border between the parenchyma and stroma (21, 35).

Cholinergic nerves, showing acetylcholinesterase (AChE) activity, can be detected in portal areas of rat, mouse, guinea pig and human (21, 74). There is less or no cholinergic innervation in the hepatic parenchyma of mouse and rat compared to human and guinea pig (24). The peribiliary plexus of guinea pig and human however is supplied by a dense cholinergic innervation (50).

Rat and mouse livers show less adrenergic innervation of hepatocytes, with fibers contacting cells only in the periportal region compared to humans or guinea pigs (75). Additionally, norepinephrine concentration in liver tissue is equivalent in guinea pigs and humans, but decreased in livers of rat and mouse (21, 76).

	Periportal region			
	HA	PV	BD	Parenchyma
Adrenergic nerves				
Rat	++	+	+	-
Mouse	++	+	+	-
Guinea pig	+++	++	+	++
Man	++	+	+	+
Cholinergic nerves				
Rat	+++	+	++	-
Mouse	+++	+	++	-
Guinea pig	+	+	+	-
Man	++	+	+	-

Table 1: Distribution of adrenergic and cholinergic nerves in the liver in different species; **BD:** bile duct; **PV:** portal vein; **HA:** hepatic artery

Adapted from Uyama et al. Anat Rec A Discov Mol Cell Evol Biol. 2004

4 THE LIVER-BRAIN INFLAMMATION AXIS: A FEEDBACK MECHANISM REGULATING IMMUNE RESPONSE

Electron microscopy studies have revealed, that nerve endings are not only closed to hepatic parenchymal cells, but also in the surroundings of immune cells (77). Synapse-like structures created by nerve endings have been determined in the near of T –, B cells and macrophages expressing receptors for ACh, catecholamines, neuropeptides, and other neurotransmitters (77). Besides immune cells are able to release and synthesize neurotransmitters (78). Research in neuroimmunology has shown that the autonomous nervous system and the immune system communicate during inflammation (78). There is an anti-inflammatory effect of the parasympathetic nervous system and an immune stimulating effect of the sympathetic nervous system (79).

The so-called “antiinflammatory cholinergic effect” describes an interaction between the vagus nerve and peripheral immune cells, resulting in an attenuation of inflammation (80). The central nervous system is protected by the blood-brain barrier, which cannot be crossed by hydrophilic cytokines. However cytokines can directly activate vagal nerve afferents, as they express cytokine receptors, such as the IL-1 receptor (81). Consequently proinflammatory cytokines in the periphery are detected by vagal afferents, resulting in a vagal efferent response with an reduction of cytokines (82). Activation of vagal afferent signaling after LPS-induced peritoneal inflammation results in an increase of c-Fos expression (c-FOS= transcription factor; a marker for activation in many cell types including many neurons) in the nucleus solitarius and the parabrachial and hypothalamic paraventricular nuclei (83). This raise can be attenuated by subdiaphragmatic vagotomy, which resulted in a reduction in c-Fos expression (84, 85). The cholinergic anti-inflammatory pathway is an effective mechanism for sensing inflammation via sensory pathways to the brain. Additionally excessive inflammation is counteracted in a localized and rapid way through ACh release by the efferent vagus nerve (86). Electrical stimulation of the vagus nerve has shown to attenuate inflammation and improve outcome in several animal models (78, 87). In an ischemia-reperfusion injury model of rats, vagal nerve stimulation reduces hepatic tissue necrotic factor synthesis and systemic shock (88). Furthermore, experimental induced colitis in animal models for inflammatory bowel disease improved after sympathectomy as well as after administration of parasympathomimetics (80, 89, 90). M₃-R knock-out mice (M₃-R^{-/-}) treated with dextran sodium sulphate (DSS) developed more severe colitis than DSS-treated WT littermates (91). In an animal model of amoebic liver abscess in hamsters, vagotomy resulted in an increased inflammatory response, a greater production of collagen fibres and larger abscess size (79, 92). In contrast adrenergic stimulation favors the release of pro-inflammatory mediators and the recruitment of leukocytes (78). The balance between the parasympathetic and sympathetic nervous system seem to regulate the inflammatory response towards pro- and anti-inflammatory outcome (78). Studies have

shown that this effect is mainly based on interactions between ACh and the $\alpha 7$ subunit nicotinic receptor ($\alpha 7nAChR$) on macrophages (93). Activation of this receptor results in an inhibition of the synthesis of pro-inflammatory mediators such as TNF- α , IL-1, IL-6 and IL-18 (78, 79). The vagus also alters lymphocyte trafficking and mast cell numbers (94, 95). Several studies have analysed the anti-inflammatory effect of nAChR, whereas the role of the muscarinic acetylcholine receptors, especially the M_3 -R, remain not fully understood (96). ACh plays an important role in smooth muscle contraction, especially in the gastrointestinal tract. Consequently M_2 - and M_3 -R are thought to be involved in contractile activity. In inflammatory conditions, like bacterial infections or Crohn's disease, motor function may be altered by direct interactions of proinflammatory cytokines with M_3 -R function. In dogs with colitis motility was reduced due to decreased M_3 -R density (97). In a model of nematode infection-induced gut inflammation smooth muscle contractility was increased, whereas in experimental bowel obstruction, hemorrhagic shock or peritonitis smooth muscle contractility was decreased. The observed discrepancies in regard to the motor function activity in these model systems may be due to differences in cytokine profiles (98). Akiho et al. examined the effect of different cytokines on smooth muscle contractility in the gut. He showed that Th_1 compared to Th_2 immune response have opposing effects on muscle contractility. Th_2 cytokines, like IL-4, IL-13, enhance muscle contractility, whereas Th_1 cytokines, like IFN γ , decreases muscle contractility (99). Next to the gastrointestinal tract, ACh also regulates bronchial secretion, airways tone and airway obstruction. In the bronchial system activation of M_3 -R results in smooth muscle contraction and stimulates the production of prostanoids and various other inflammatory mediators from epithelial cells (100). In patients with COPD the M_3 -R expression is increased and ACh stimulation increases leukotriene release. Besides, anticholinergic drugs are the treatment of choice in the management of COPD (101) and glucocorticoid treatment decreases muscarinic receptor expression in airway smooth muscle (99). This indicates that muscarinic receptors are directly involved in airway inflammation.

The autonomous nervous system interacts with the inflammatory immune response (98). Consequently, the M_3 -R expressed on cholangiocytes might be involved in biliary inflammation and modulation of the parasympathetic system could represent a new therapeutic option in liver diseases to decrease inflammation.

5 ALTERED HEPATIC INNERVATION IN LIVER DISEASES

Studies in the last two decades have shown that hepatic innervation is altered in liver diseases. In normal liver tissue nerve fibers can be found in the portal area and the parenchyma. (10). However, in chronic liver disease nerve fibers seem to proliferate in the portal area and to penetrate the parenchyma accompanied by fibrotic tissue (10). The number of NSE, S-100 and NPY positive nerve fibers is increased in the fibrous septa of cirrhotic livers compared to non-cirrhotic livers (10, 36). By contrast, hepatic parenchymal nerves are reduced in precirrhotic liver disease and are missing in regenerating hepatic nodules in established cirrhosis (102). There is also a complete absence of intrasinusoidal nerve fibers in established cirrhosis. Although there is sufficient proliferation of hepatocyte and sinusoidal cell in cirrhotic livers, ingrowth of nerve fibers into the regenerative nodules is not stimulated (102). The change in liver innervation is irrespective of the aetiology of the cirrhosis (19, 102) and mechanisms responsible for this loss of parenchymal nerves are not fully understood. In alcoholic liver disease, nerve fiber density is increased in fibrous portal tracts as well as around portal veins (103, 104). In severe chronic hepatitis B and C or autoimmune hepatitis the number of nerves/mm² in stromal areas is 10-fold increased compared to normal liver (104). By contrast in various forms of acute liver injury there is a normal or only slightly increase in nerve fibre density (105). Furthermore, patients with liver cirrhosis show an increased sympathetic activity and higher expression levels of proinflammatory cytokines compared to normal livers (70). In an experimental rat model of liver cirrhosis, sympathectomy prevents bacterial translocation and decreases incidence and severity of infections with *Escherichia coli* (70). Carvediol, which can block the sympathetic nervous system, seems to be protective against the development of hepatosteatosis in rats with alcoholic fatty liver disease (70). Consequently, inhibiting sympathetic innervation could represent a therapeutic option for prevention bacterial translocation in advanced cirrhosis. In addition, hepatic stellate cells (HSCs), which derived from the neuroendocrine compartment within the liver like HPCs, are also controlled by the nervous system. Quiescent HSCs can differentiate into an activated phenotype and play a central role in fibrogenesis. HSCs are in close contact with nerve endings in normal liver. As these contacts are reduced in cirrhosis, the autonomous nervous system may effect fibrogenesis in liver disease (39).

Changes in the distribution of nerve fibers not only cause anatomical changes, but seem to impair hepatic efferent and afferent nerve functions (10). As afferent innervation regulates baro-, osmoreception and functions as metabolic sensors, changes in hepatic innervation

may contribute to circulatory and systemic fluid disturbances in cirrhotic livers (102). As nerve fibers have direct contact to sinusoidal cells, altered hepatic innervation might contribute to changes in liver blood flow in liver diseases. Furthermore, the release of neurotransmitters might modulate fibrogenic cells and regulate liver fibrosis (104). The adrenergic antagonist 6-hydroxydopamine (OHDA), a toxin that destroys noradrenergic fibers, was shown to reduce experimental induced liver fibrosis (106). After common bile duct ligation (CBDL) in guinea-pigs, an increase in nerve fibres in portal tracts and in fibrous septa was observed (19, 107), which mainly affects cholinergic nerve fibers (19, 39). In the parenchymal nodules, no alteration of the innervation was detected (19). Besides nerve fibers of the intrahepatic biliary system are slightly increased in extrahepatic obstructive jaundice (108). The altered biliary innervation might cause changes in biliary physiology (108, 109) contributing to development or progression of cholangiopathies.

6 REGULATION OF LIVER REGENERATION BY THE AUTONOMOUS NERVOUS SYSTEM

The liver is unique among mammalian organs in its ability to regenerate (70). Liver regeneration is a very complex process involving multiple cytokines and growth factors, which control cell growth and proliferation (70). In the rat, reconstruction of hepatic mass is completed in 5–7 days following seventy percent partial hepatectomy (PH) (70, 110). Furthermore, original liver architecture is restored in 10–14 days (111). This process of liver regeneration can be repeated several times in animal models (112). In a study of Yokoyama et al (5), liver regeneration in mice after PH was studied continually through the following 6 months. The left lobes showed a rapid increase in weight soon after operation, so that the original percentage of liver to body weight was restored after six days. A peak in mitotic activity of parenchymal cells could be detected on the third day. The original liver weight was recovered until the eighth day (113). Besides, after 95% PH in young mice hepatocytes replicated between 30 and 60 hours (114).

The successful use of the liver living donation or the possibility of liver resection in clinical medicine shows that these animal models reflect the efficiency of the human liver to regenerate (112). The pathomechanism behind this feature is still unknown. Many factors like hormones, peptides and cytokines are thought to be involved. An important step in preparing hepatocytes to regenerate is “priming”. Priming depends on the inflammatory cytokines IL-6 and tumor necrosis factor α (TNF α), that activate the expression of genes and transcriptional factors like nuclear factor kappa B (NF κ B) (114). Finally cytokines like EGF (endothelial

growth factor), TGF α (transforming growth factor α) and HGF (hepatocyte growth factor) act as growth factors and activate hepatocytes to proliferate (115). Nonparenchymal cells like Ito cells, Kupfer cells and endothelial cells in the liver release HGF. During the first 4-6 h after hemihepatectomy an intensely increase of serum levels of HGF can be observed (114). Besides cytokines, the autonomous nervous system seems to play a pivotal role in liver regeneration (111). Selective hepatic branch vagotomy attenuates liver regeneration in partially hepatectomized rats (7, 116). Besides studies in CBDL rats with concomitant cervical vagotomy showed a significant decrease in ductal mass and enhanced apoptosis of cholangiocytes compared to CBDL treated animals without vagotomy (117). By contrast vagal stimulation activates liver regeneration after partial hepatectomy (118, 119).

Parasympathetic nerves can stimulate DNA synthesis and liver regeneration after partial hepatectomy. By contrast, sympathetic nerves seem to suppress these processes (120). The exact effect of autonomic denervation on liver regeneration is still unknown, but an alteration in the control of the hepatic vascular system might play a role (120). Furthermore, HPCs are involved in liver regeneration and are regulated by the autonomous nervous system (118). These cells are related to terminal biliary ductules and the canals of Hering. They can differentiate into both hepatocytes and cholangiocytes (118) and express the M₃-R (118). The expression of the M₃-R decreases upon differentiation of HPCs towards the hepatocytic lineage, while it is preserved upon differentiation towards the biliary lineage (118). An interplay between vagal secreted ACh, the M₃-R expressed by HPCs and the enzyme acetylcholinesterase was previously postulated (118). Acetylcholinesterase is secreted by hepatocytes and clears the parasympathetic neurotransmitter ACh. Under physiological conditions, HPCs are surrounded by a sufficient number of hepatocytes, which inhibits binding of ACh to the M₃-R by producing acetylcholinesterase (16). In pathological conditions with reduced hepatocytes mass, the level of acetylcholinesterase falls and ACh activates the M₃-R of HPCs resulting in liver regeneration until restoration of an adequate hepatocyte mass (118). Interruption of the cholinergic innervation by vagotomy induces a marked decline in total bile duct mass (121). Besides, in transplanted human liver with hepatitis the number of HPCs is significantly decreased in contrast to control liver with hepatitis and normal innervation (70). Lesage et al. explained this decrease by an impaired cholangiocyte proliferation capacity and intracellular cAMP levels as well as enhanced cell death by apoptosis (121). The chronic administration of forskolin, which increases intracellular cAMP levels, prevents the effect of vagotomy on cholangiocyte proliferation (121). Hepatic vagal nerves may activate HPCs in an injured liver, probably through ACh release stimulating the M₃-R (70). Enhanced proliferation by ACh binding to the M₃-R was observed in human colon cancer cells (122) and human astrocytoma cells (123). By contrast, sympathetic nervous system stimulation induces hepatic fibrosis and attenuated liver regeneration (70).

This indicates a key role of the parasympathetic nervous system in controlling hepatic regeneration. However, the effect of the M₃-R on cholangiocytes still unknown. Activation might play a role in cholangiocyte proliferation, regeneration as well as apoptosis.

7 MUSCARINIC RECEPTORS

ACh muscarinic receptors (mACh-R) are classified into five major subtypes (M₁-M₅-R) with different tissue distribution, pharmacology and functions. Each receptor subtype is the product of a specific gene. All mACh-R are members of the superfamily of seven-transmembrane G-protein coupled receptors and can be grouped into two major functional classes. Whereas M₁, M₃ and M₅-Rs are selectively linked to G-proteins of the G_q family, the M₂ and M₄-Rs are coupled to G-proteins of the G_i type (124). M₁-R, M₃-R and M₅-R are usually coupled to hydrolysis of phosphoinositide, while M₂-R and M₄-R are linked to the inhibition of the adenylate cyclase activity (125). Activation of the G_q protein results in activating phospholipase C, which generates the second messenger inositol triphosphate (IP₃) and diacylglycerol (DAG). IP₃ then causes the release of calcium from intracellular stores and DAG induces influx of extracellular Ca²⁺. By contrast G_i protein activation inhibits adenylate cyclase, which results in reduction in cAMP levels (125). Most tissues and cell types express different mAChR types. In glandular parenchymal tissue the subtype M₁-R and M₃-R are expressed, in smooth muscles of the gut and the bladder M₂-R and M₃-R subtypes can be found. Luo et showed that hepatocytes express all of the five mACh-R (96). In bile duct epithelial cells and hepatic progenitor cells M₃-R is widely detected (3, 100). Compared to other M-Rs, M₃-R is relatively low expressed in the central nervous system. During differentiation of HPCs towards the hepatic cell line, the M₃-R expression decreases, whereas during differentiation towards cholangiocytes the M₃-R expression persists (118). M₃-R is expressed on cholangiocytes independent of bile duct size (3). By contrast to the secretin receptor, which is only expressed on large bile ducts (118, 126). Furthermore, M₃-R seems to be located at invaginations of the cell membrane suggesting a process of receptor-mediated endocytosis (4).

8 REGULATION OF CHOLANGIOCYTE'S FUNCTION BY THE PARASYMPATHETIC NERVOUS SYSTEM:

In the liver two types of epithelia contribute to bile secretion: hepatocytes and cholangiocytes (127, 128). Also contributing only 3 to 5% to the total liver cell mass, cholangiocytes account for 30-60% of daily bile production (129-131). These epithelial cells line the hepatic biliary tree forming a three-dimensional network of interconnecting ducts of different size (132). The bile duct system extends from the canals of Hering to the large extrahepatic ducts (133). Hepatic as well as ductular transport mechanisms regulate bile volumen and composition (127, 134). The biliary duct system can be classified into three segments based on duct size (135). This classification differs extrahepatic bile ducts, large bile ducts and intrahepatic small bile ducts or ductules (128, 134, 136-138). They are equipped with a number of different transporters to modify bile. Furthermore, micovilli on the apical pole of cholangiocytes facilitate the secretory and absorptive properties of the hepatic biliary epithelium (139). They can absorb glucose, bile acids (BA) and amino acids from bile (127). By contrast different secretory components like IgA or organic solutes are transported into bile generating an osmotic gradient (129, 140).

These secretory and absorptive properties of cholangiocytes are regulated by a number of different factors including nerves (3), enzymes (3, 141), peptides (68), bile salts (127) and gastrointestinal hormones (62, 142). Secretin for example, increases biliary HCO_3^- secretion and this increase in bile flow is proportional to the dose of secretin (127). The secretin receptor is expressed on the basolateral membrane of cholangiocytes. Its activation leads to an increase of intracellular cAMP, which is followed by a stimulation of the intracellular protein kinase A (PKA) (3, 143). This results in an opening of the Cl^- channel cystic fibrosis transmembrane regulator (CFTR). The following transport of Cl^- into the ductular lumen induces a Cl^- -gradient favoring the activation of the apically located $\text{Cl}^-/\text{HCO}_3^-$ exchanger. It transports Cl^- back from the ductular lumen to intracellular by exchanging Cl^- with HCO_3^- . Additionally, the Na-HCO_3^- symport is activated due to depolarisation caused by Cl^- - efflux, which potentiates biliary HCO_3^- secretion (133, 134, 144). This secretin-induced biliary HCO_3^- seems to be important, as an increased hepatic secretin receptor expression can be observed after PH or CBDL in rats (3, 145-147).

By contrast to secretin, the hormone serotonin inhibits bile flow as well as cholangiocytes' proliferation (148). Activation of the serotonin 1A or 1B receptor, which is expressed on cholangiocytes, results in an increase of intracellular Ca^{2+} , IP_3 and PKC with a reduction of the intracellular cAMP levels and PKA activity (148). Serotonin is commonly synthesized and secreted by endochromaffin cells. Endochromaffin cells are widely distributed in the epithelium of the gastrointestinal tract. These cells can be detected in the epithelium of the stomach, small intestine, colon and also in bile ducts (149). During

cholestasis biliary cells start to express markers of endochromaffin cells (150). Consequently, enterochromaffin cells in the bile duct system or even cholangiocytes themselves might regulate ductal secretion by secreting the hormone serotonin.

In addition to hormones, the autonomous nervous system can alter bile flow (3, 50). Experimental evidence suggests that vagal stimulation increases bile flow and biliary bicarbonate excretion, while experimental vagotomy decreases basal bile flow and bicarbonate output (121, 151). Electrical vagal stimulation increases intracholedochal pressure, suggesting a central role of the vagal nerves in bile secretion (152). Intrahepatic parasympathetic terminations release ACh, which interacts with the M₃-R expressed on the basolateral membrane of cholangiocytes. This potentiates the secretin-stimulated cAMP synthesis and Cl⁻/HCO₃⁻ exchanger activity by a Ca²⁺-calcineurin-mediated, PKC-independent modulation of adenylate cyclase (3, 127). However, single ACh stimulation of cholangiocytes (without secretin) failed to raise fluid secretion (127, 153). Similar to ACh, epinephrine and norepinephrine potentiate the effect of secretin on cholangiocytes, whereas dopamine inhibits the secretin-induced ductal secretion (148).

Next to bile flow and cholangiocyte proliferation, the parasympathetic nervous system seems to regulate bile composition. Witz et al. studied the effect of vagotomy on bile composition in patients treated for duodenal ulcer with vagotomy. After vagotomy the patients showed a significant increase in relative cholesterol content and lithogenic index compared before surgery (154). By contrast a reduced biliary cholesterol saturation was noticed in an other study (155). Fletcher *et al.* reported a reduction in bile-salt concentration in vagotomized dogs, especially biliary cholate concentration (156, 157). By contrast, the gallbladder filling and storage capacity measured by quantitative cholescintigraphy was normal in patients who have had vagotomy (155).

9 POTENTIAL PATHOGENETIC ROLE OF THE M₃-R IN HUMAN CHOLESTATIC LIVER DISEASES

Cholangiocytes have to face a potential hazardous environment on their apical cell surface due to exposure to millimolar concentrations of potentially toxic bile acids. In contrast, acquired or inborn defects in bile formation can result in cholangiopathies (158). Based on these findings a recently published hypothesis by Beuers et al. supposes that AE2-mediated HCO₃⁻ secretion by BECs forms a "HCO₃⁻ umbrella" on the outer surface of the apical

membrane of BECs (159, 160). A negative surface charge located at the extracellular membrane side attracts protons, which cause a more acidic pH close to the apical surface of BECs. Due to this acidic environment most of the bile acids are available as apolar hydrophobic protonated molecules, which are able to pass cell membranes by simple diffusion. HCO_3^- secretion by BECs increases the pH of luminal bile near the apical surface of BECs. By this pH change hydrophobic bile acids are deprotonated and lose their ability to permeate membranes in an uncontrolled way. This “ HCO_3^- umbrella” might be a protective key mechanism of cholangiocytes against toxic hydrophobic protonated bile acids. Since the cholangiocellular M_3 -R is engaged in HCO_3^- excretion this receptor may also be critically involved in protecting BECs. Consequently conditions of disturbed HCO_3^- secretion may lead or contribute to the development of cholangiopathies. However, this concept has not been studied in detail.

Periductal fibrosis in cholangiopathies: Since vagal stimulation in a rat liver ischemia-reperfusion injury model attenuates tissue necrotic factor (TNF) synthesis and systemic shock (161) and experimental colitis in dogs inhibits muscarinic signaling with reduced colonic motility due to decreased M-R density (162), M-Rs seem to be direct targets of inflammation and critically engaged in its regulation (163). Consequently, it is tempting to hypothesize that portal inflammation triggers impairment of cholangiocellular M_3 -R function and contributes to the initiation or progression of human cholangiopathies. More specifically, in sclerosing cholangitis (SC) a thickened periductal fibrotic shield could lead to impaired M_3 -R activation via an increased length of way for neurotransmitter diffusion. Therefore periductal fibrosis and mediators of inflammation might hinder ACh to bind to the M_3 -R. Taken together it is reasonable to assume that the alterations of M_3 -R pathway may be involved in the pathogenesis of cholangiopathies and its sequel biliary fibrosis, however such a concept has not been investigated.

Primary biliary cirrhosis (PBC): is a chronic cholestatic condition, which may progress to liver fibrosis and cirrhosis (164). Studies showing an altered transepithelial HCO_3^- transport of BECs in PBC patients indicate that an impaired “ HCO_3^- umbrella” may be also involved in the pathogenesis of PBC. In PBC patients hepatic and salivary gland AE2 gene expression is decreased and the response of AE2 to secretory stimuli is impaired (164). In addition, recent studies also showed the presence of autoantibodies against the human muscarinic acetylcholine receptor of the M_3 type (hmAChR M_3) in PBC patients (165). Autoantibodies to hmAChR M_3 are also involved in the pathogenesis of Sjögren’s Syndrome (166) frequently accompanying PBC.(164) Taken together, in PBC HCO_3^- secretion seems to be impaired via

altered AE2 function and impaired M₃-R function may contribute to PBC development and progression, but detailed knowledge on possible M₃-R malfunction in PBC is lacking.

Secondary sclerosing cholangitis in critically-ill patients (SSC-CIP): SSC-CIP represents a progressive cholangiopathy frequently leading to end-stage liver disease. Bile cast formation with enigmatic pathomechanism, lining the intra-, and extrahepatic bile duct system, seems to embody a pivotal pathogenetic step.(167) It is assumed that relative bile duct ischemia lead to cholestasis in such patients. Since previous studies showed decreased hepatic bile acid transporter activity in sepsis (168), bile duct hypoxia may also negatively impact on BECs transporter function leading to impaired biliary HCO₃⁻ secretion. In addition, high-dose administration of vasoactive drugs may negatively impact on M₃-R function, which may render the bile duct susceptible for exogenous and endogenous injury. However, there are no mechanistic studies on the role of M₃-R function in SSC-CIP pathogenesis.

Liver transplantation (LTX):

Hepatic innervation regulates many physiological effects. Therefore, it is surprising that hepatic function following liver transplantation in man appears to be relatively normal (28). The fact that hepatic innervation is not necessary for life is clearly shown by the observation that the liver can be transplanted successfully. During liver transplantation, extrinsic nerves supplying the donor liver are transected (71). The allograft has no connection to the nervous system of the recipient and consequently is completely denervated (118). In the transplanted human liver the parenchymal nerve fibres disappear shortly after orthotopic liver transplantation, while the disappearance of portal fibres is less rapid. However also the latter are undetectable by six weeks (19, 28). There is a total loss of the normal sinusoidal innervation and an almost complete loss of small portal tract innervation soon after liver transplantation (28). Reinnervation of some portal tracts may take place as early as 32 – 61 weeks post-transplant, but the majority of the liver appears to remain denervated (71, 169). In a normal human liver nerve fibers can be easily detected following blood vessels and bile ducts by immunohistostaining for example for NSE and Protein gene product 9.5 (PGP 9.5) (71). Nerve fibres identify in this way diminish within 5 days after transplantation (71). Only a few scanty nerves can be detected between days 13 and 8 months. After 8 months post-transplantation, small portal nerves can be again identified with both markers (71). This reinnervation might be explained by extrinsic nerves reinnervation or proliferation of intrinsic (peribiliary) nerves. In other transplanted organs, like after heart transplantation, there is a kind of reinnervation after some time (71).

Bile ducts represent the Achilles' heel of the transplanted liver since anastomotic and non-anastomotic strictures are frequent problems following LTX with significant morbidity and mortality. Besides affecting the microcirculation as well as glycemic regulation, hepatic denervation significantly alters the physiology of cholangiocytes and bile formation. Bile ducts of transplanted livers show significantly increased susceptibility to ischemia (e.g. due to hepatic artery thrombosis). Interestingly, animal studies using the model of hepatic denervation in rats and dogs showed reduced biliary cholesterol and phospholipid secretion and a decrease in M_3 -R on cholangiocytes as well as a reduction in intracellular cAMP levels (170). In addition, denervated human liver grafts with hepatitis contain significantly less HPCs, activated by vagal nerves and critically engaged in liver regeneration, compared to control livers (170). Taken together, it is tempting to speculate that the increased vulnerability of the liver graft may be related to a lacking innervation of the liver. More specifically, the lack of M_3 -R activation may alter graft physiology and result in an enhanced susceptibility for bile duct injury; however this hypothesis has not been addressed so far.

10 STATUS OF RESEARCH

As outlined above the M₃-R may play an essential role in biliary physiology and consequently cholangiopathies. However the specific role of the M₃-R in these regards is not well defined.

10.1 What is Known about the Liver Phenotype and Biliary Physiology in M₃-R Knockout Mice?

Cholangiopathies are chronic progressive diseases with variable clinical course and pathogenetic studies in liver disease widely depend on the availability of liver tissue, which is hard to access, especially in the case of medium- or large-sized bile ducts. Therefore, well-characterized animal models allowing longitudinal time course studies are indispensable to investigate their pathophysiology. Our group previously successfully established mouse models for cholangiopathies (e.g. Mdr2^{-/-} (Abcb4 knock out) mice, and 3,5-diethoxycarbonyl-1,4-dihydrocollidine (DDC) -, and lithocholic acid (LCA) -intoxicated mice (171-175). As the use of mouse models has several advantages over other mammalian animal models, we aim to define the role of the M₃-R in specific mouse models for cholangiopathies and biliary fibrosis.

M₃ knockout mice (M₃R^{-/-}) are viable, fertile and do not show any obvious behavioral deficits (176, 177). Although the M₃-R is predominantly expressed in smooth muscle cells, tissues contractility was only inconsistently reduced in M₃R^{-/-} (177). Severe urinary retention due to smooth muscle dysfunction was observed in male knockout mice, whereas gastrointestinal complications were not detected (177). This indicates that in addition to the M₃-R alternative muscarinic receptors contribute to smooth muscle contractility. Despite some physiological studies in M₃-R^{-/-} mice, information on biliary physiology or a possible liver phenotype is lacking. As this receptor is expressed in liver specifically on cholangiocytes, altered biliary physiology can be expected. With the aid of M₃-R^{-/-} mice we want to determine the specific impact of genetic M₃-R loss on bile formation.

10.2 What is Known about M₃-R Function and Alterations in Cholangiopathies?

Recent studies showed the presence of autoantibodies against the hmAChR M₃ in patients with PBC (165). M₃-R function may be impaired in human cholangiopathies due to

inflammation-driven downregulation, dysfunction or decreased innervation of the bile ducts due to a thickening periductal fibrotic shield. In addition, it is tempting to speculate that M₃-R malfunction may render bile ducts more vulnerable due to reduced biliary HCO₃⁻-secretion. Moreover, altered distribution of ACh- positive receptors in cirrhotic livers was previously postulated (24, 118). In cirrhotic nodules ACh- positive nerves were shown to be located in vicinity of myofibroblasts. The observation that ACh potentially stimulates the proliferation and collagen production of HSCs indicates that cholinergic nerves could affect liver fibrosis (24). Taken together these arguments call for the concept of M₃-R dysfunction or alterations in human cholangiopathies, which has not been addressed so far.

10.3 Hypotheses

Based on the data from the literature, we aimed to investigate two hypotheses in this thesis:

1. M₃-R plays a major role in bile formation
2. M₃-R impacts on the cholestatic phenotype in mouse models for cholangiopathies

11 MATERIAL AND METHODS:

Animal Experiments:

Experiments were performed in 2-month-old and 50-week-old, male $M_3-R^{-/-}$ mice and wild type (WT) littermates (25–30 g). $M_3-R^{-/-}$ mice were kindly provided by Dr. Jürgen Wess (Laboratory of Biological Chemistry, NIDDK, NIH). Animals were housed with a 12:12 hour light : dark cycle and permitted ad libitum consumption of water as well as chow diet (SSNIFF, Soest, Germany). $M_3-R^{-/-}$ mice were housed in the same room as WT mice. Experimental protocols were approved by the local animal care and use committee (BMWF-66.010/0030-II/3b/2014; BMWF-66.010/0075-WF/V/3b/2017) according to the criteria outlined in the Guide for the Care and Use of Laboratory Animals prepared by the U.S. National Academy of Science (National Institutes of Health publication 86-23, revised 1985) (1).

Routine serum biochemistry and bile acid measurements:

Blood was collected at harvesting and after centrifugating, it was stored at -80°C until analysis. Assays for alanine aminotransferase and alkaline phosphatase were routinely measured, whereas serum bile acid concentration were determined by using Bile Acid Kit (Ecoline S + from DiaSys Diagnostic Systems GmbH, Holzheim, Germany in a Hitachi 917 analyser (Boehringer Mannheim, Mannheim, Germany) (1).

Bile Flow and Composition: Mice were anesthetized and a longitudinal incision of the abdomen was performed. The common bile duct was ligated, and the gallbladder was cannulated for collection of bile. After a 10-minute equilibration period, bile was collected for 1 hour in test tubes under mineral oil for determination of HCO_3^- , total carbon dioxide and pH using an automatic blood gas analyzer (AVL 995 hp, AVL, Graz, Austria; COBAS Mira plus, Roche). For bile flow measurements and further bile analysis, bile was collected for the following 30 minutes in preweighed test tubes. Bile flow was determined gravimetrically and normalized to liver weight. Biliary glutathione (GSH) concentrations were determined after protein precipitation in 5% metaphosphoric acid by using the Glutathione Assay Kit (Calbiochem) according to the manufacturer's instructions. Biliary bicarbonate, total carbon dioxide, and pH concentration were measured with an automatic blood gas analyzer (AVL 995 hp; AVL, Graz, Austria). Biliary phospholipid concentration was determined using a commercially kit (Phospholipid B; Wako, Neuss, Germany). In detail, 5 μl of bile was mixed with 750 μl of color reagent and incubated for 10 minutes at 37°C and measured at 505 nm.

Concentrations were determined using the standard solution of the kit. Biliary cholesterol concentrations were determined using a commercially available kit (cholesterol liquicolor; Human, Wiesbaden, Germany) according to the manufacturer's instructions. For cholesterol extraction, 5 μ l of bile and 95 μ l of distilled water were mixed with 400 μ l of chloroform:methanol (2:1) and centrifuged 5 minutes at 14,000 \times *g*. The lower phase was concentrated, and the obtained pellet was dissolved in 5 μ l of methanol. After the addition of 500 μ l of color reagent and incubation at 37°C for 5 minutes, probes were measured at 500 nm. Concentration was determined using the standard solution of the kit. For biliary glutathione, proteins in bile were precipitated with 5% metaphosphoric acid (2.5 μ l of bile in 50 μ l of metaphosphoric acid), and glutathione analysis was performed using the glutathione assay kit (Calbiochem, San Diego, CA), according to the manufacturer's instructions. Biliary bile acid concentration required bile to be diluted 1:300 in physiological saline and analyzed using a 3 α -hydroxysteroid dehydrogenase assay (Ecoline S⁺; DiaSys, Holzheim, Germany) according to the manufacturer's instructions. Equipment and conditions used for extraction, electrospray mass spectrometry, and gas chromatography-mass spectrometry were the same as previously described (1).

Common bile duct ligation (CBDL): This well-characterized model system is broadly accepted in the scientific community (173, 178, 179) and was used to study the effect of genetic M₃-R loss on initiation of cholangitis, pericholangitis, ductular reaction and biliary fibrosis using respective M₃-R^{-/-} mice and wild type controls. For performing the CBDL, after longitudinal incision of the abdomen, the common bile duct was ligated under general anesthesia (inhalational anaesthesia with isoflurane) close to the liver hilum immediately below the bifurcation. In addition, cholecystectomy was performed after ligation of the cystic duct. Controls underwent sham operation with exposure but without ligation of the common bile duct and removal of the gallbladder.

Lithocholic acid (LCA) intoxicated mice show segmental bile duct obstruction caused by LCA crystals, destructive cholangitis, bile duct infarcts as well as periductal fibrosis within days. The hydrophobic bile acid LCA alters tight junctions of cholangiocytes (172) and permits bile to leak causing cell damage, chemotaxis of neutrophil granulocytes, activation of cholangiocytes to proliferate and activation of periductular myofibroblasts leading to periductular fibrosis within days (172). Mice treated with 1% LCA show numerous bile infarcts beginning at day 2. Around days 3 and 4, animals developed a dense neutrophilic-granulocytic infiltrate around small interlobular as well as larger bile ducts and pronounced periductal edema in larger ducts (172). Comparative studies using M₃-R^{-/-} mice and respective controls were performed to determine the specific role of the M₃-R in bile acid-induced acute cholangitis.

Chronic feeding of 3,5-diethoxycarbonyl-1,4-dihydrocollidine (DDC) is a model for xenobiotic-induced Cholangitis with ductular proliferation and onion-skin type-like periductular fibrosis. DDC induces segmental subtotal mechanical bile duct obstruction via porphyrine plugs and can transform cholangiocytes into a reactive phenotype, secreting proinflammatory / chemotactic cytokines. Consequently, neutrophils infiltrate the portal fields, periductal myofibroblasts are activated leading to a ductular reaction and sclerosing cholangitis in the presence of regular biliary phospholipid secretion (171). Comparative studies using $M_3-R^{-/-}$ mice and controls were performed to determine the specific role of the M_3-R in porphyrine induced sclerosing cholangitis and biliary type of liver fibrosis (1).

Chronic feeding of 3 α ,7 α ,12 α -trihydroxy-5 β -cholan-24-oic acid (CA): Cholic acid is a primary bile acid and is with chenodesoxycholic acid the main bile acid in the human bile. In mice, CA feeding results in a disseminated hepatocyte necroses, increased liver cell size, an increased number of mitotic figures, and dilatation of interlobular bile ducts (172, 180). Besides CA feeding significantly stimulates bile flow in mice. Comparative studies using $M_3-R^{-/-}$ mice and respective controls were performed to determine the specific role of the M_3-R in bile acid-induced acute cholangitis.

Mdr2 knockout mice present a genetic model for sclerosing cholangitis and biliary fibrosis. In these mice the lack of biliary phospholipids results in a decreased micelle formation and consequently increased biliary concentration of monomeric bile acids (158) leading to bile duct injury and chronic sclerosing cholangitis with periductal inflammation and onion-skin like periductular fibrosis already at an age of 4 weeks (174, 181). The increased level of free bile acids in $Mdr2^{-/-}$ mice results in destruction of tight junctions and basement membranes of bile ducts. Consequently toxic bile acids leak into the periductal area and cause inflammation, chemotaxis and activation of myofibroblasts, which form a periductular fibrous ring. This ring disconnects cholangiocytes from the peribiliary plexus, resulting in atrophy and death of cholangiocytes (174). Human liver diseases like primary and secondary sclerosing cholangitis show comparable histological, biochemical, and cholangiographic features to $Mdr2^{-/-}$ mice. Comparative studies using $Mdr2^{-/-}$ mice with vagotomy versus sham operation were performed to determine the effect of the parasympathetic nervous system in chronic sclerosing cholangitis. To determine if the liver phenotype in $Mdr2^{-/-}$ mice can be altered by treatment with a muscarinic M_3-R agonist, 4-week-old $Mdr2^{-/-}$ mice and respective controls ($Mdr2^{+/+}$ mice) received bethanechol (400 μ g/ml) via the drinking water for 4 weeks (182). We compared these mice with an untreated control group of $Mdr2^{-/-}$ mice and WT littermates. Mice were freely allowed to drink water with or without bethanechol (without gavage) for 4

weeks. Volumes of water consumed by each group were measured weekly and were not significantly different between the groups during the study period. In addition, to determine whether bethanechol treatment alters bile flow and biliary HCO_3^- secretion, 8-week-old $\text{Mdr}2^{-/-}$ mice and respective controls ($\text{Mdr}2^{+/+}$ mice) received bethanechol (400 $\mu\text{g/ml}$) via the drinking water for 1 week. Thereafter, bile flow and biliary HCO_3^- output was measured. We compared bile flow of these mice with an untreated control group of $\text{Mdr}2^{-/-}$ mice and WT littermates ($\text{Mdr}2^{+/+}$ mice) (1).

Vagotomy was performed under general anaesthesia (inhalational anaesthesia with isoflurane). After performing a longitudinal incision the retroperitoneum was located. Afterwards the abdominal part of the esophagus was prepared and nerve fibers around the esophagus were coloured with trypanblue. After 2 minutes the colouring was remarkable. Parasympathetic denervation was achieved by selective section of the hepatic branch of the vagus nerve branching from the left main vagal trunk. In sham operated mice all procedures including colouring with trypanblue were performed without nerval cutting.

Liver histology: For conventional light microscopy, livers were fixed in 4% neutral-buffered formaldehyde solution and embedded in paraffin. Sections (4- μm thick) were stained with H&E or Trichrome stain (1).

Measurement of Hepatic Hydroxyproline Content: Quantification of liver fibrosis was carried out by measurement of hepatic hydroxyproline concentration by a calorimetric method. In brief, mouse liver lobe 3 (left liver lobe) was homogenized in 6N HCl and hydrolyzed overnight at 110 °C. Afterward hydrolysates were filtered, neutralized with NaOH and oxidized with chloramine-T. This was followed by a reaction with perchloric acid and p-dimethylaminobenzaldehyde resulting in the formation of a chromophore quantified photometrically at 565 nm wavelength. Rate of liver fibrosis were identified by both measurement of hydroxyproline content and Sirius red staining (1).

Immunohistochemistry for Cytokeratin 19 (CK19): Immunohistochemistry for CK19 was performed on cryosections fixed with a modified formalin/methanol/acetone fixation. Sections were fixed in 4% buffered formaline for 5 minutes and then fixed with methanol for 5 minutes at -20°C and with acetone for 3 minutes at -20°C . CK19 was detected using the monoclonal rat anti-Troma-III antibody (developed by Rolf Kemler, Max Planck Institute, Freiburg, Germany), which was obtained from the Developmental Studies Hybridoma Bank (developed under the auspices of the National Institute of Child Health and Human Development and maintained by the University of Iowa, Iowa City, IA). Binding of the antibody was detected using the ABC system (Dako) with AEC (Dako) as substrate (1).

Immunohistochemistry for Proliferation Marker Ki-67 Immunohistochemistry for Ki-67 was performed on microwave-treated paraffin sections (4 µm thick) using 0.01 mmol/L citrate buffer (pH 6.0) and a polyclonal rabbit anti-Ki-67 antibody (dilution 1:500; Novocastra, Newcastle on Tyne, UK). Binding of the antibody was detected using the ABC system (Dako) with AEC (Dako) as substrate.

Immunohistochemistry for vascular cell adhesion molecule (VCAM) and α-smooth muscle antigen (αSMA): To investigate hepatic inflammation immunohistochemical studies of vascular cell adhesion molecule (VCAM) and α-smooth muscle antigen (αSMA) were performed. Immunohistochemistry for Ki-67 was performed on microwave-treated paraffin sections (4 µm thick) using 0.01 mmol/L citrate buffer (pH 6.0) and a polyclonal rabbit anti-Ki-67 antibody (dilution 1:500; Novocastra, Newcastle on Tyne, UK). Binding of the antibody was detected using the ABC system (Dako) with AEC (Dako) as substrate. Immunohistochemistry for vascular cell adhesion molecule (VCAM)-1 was performed on acetone-fixed cryosections by using the monoclonal rat anti-CD106 (VCAM-1; dilution 1:30; PharMingen, San Diego, CA), and binding of the antibody was detected with the ABC system (Dako) with AEC (Dako) as a substrate.

Immunostaining for active caspase-3: To determine the role of apoptotic cell death, active caspase-3 staining was performed. After removal of paraffin, PBS washing, and microwave treatment, formaldehyde-fixed sections were incubated with 4 µg/mL rabbit polyclonal antibodies to active caspase-3 (AF835; R&D Systems, Abingdon, United Kingdom). Binding of the caspase-3 antibody was detected using the ABC system (Dako, Glostrup, Denmark).

12 RESULTS

12.1 Aim (1): Determine the Physiological Role of M₃-R in Bile Formation

We wanted to determine the physiological role of the M₃-R in bile formation and its potential pathophysiological and therapeutic role in cholangiopathies. Studies in animal models revealed that stimulation of the vagus nerve increases bile flow and biliary HCO₃⁻ excretion, whereas vagotomy decreased basal bile flow and HCO₃⁻ output. Moreover, ACh was shown to potentiate the stimulatory effect of secretin on bile secretion. Taken together these findings argue for a direct involvement of the M₃-R in bile formation and more specifically engagement in biliary HCO₃⁻ secretion.

12.1.1 Comparison of bile flow in M₃-R^{-/-} mice and WT controls:

To determine the role of the M₃-R in bile formation, we compared bile flow and bile composition in M₃-R^{-/-} mice and WT littermates under standard conditions. M₃-R^{-/-} mice had reduced bile flow, most likely due to reduced biliary HCO₃⁻ secretion (bile flow 1.7±0.3 vs. 2.4±0.3 µl/gLW/min; biliary HCO₃⁻ output 65.5±9.7 vs. 97.6±16.2 nmol/gLW/min, M₃R^{-/-} vs. WT, *p*<0.05) (table 2) (1). In contrast, biliary BA, phospholipid and cholesterol secretion were similar in both genotypes (table 2) (1). These findings suggest that reduced bile flow in M₃-R^{-/-} mice is primarily related to defective HCO₃⁻ secretion and that M₃-R loss does not alter the secretion of other bile constituents (1).

Variable	M ₃ R ^{-/-} (n=4)	WT (n=6)
Bile flow (µl/gLW/min)	1.73 ± 0.25 *	2.40 ± 0.31
Bicarbonate output (nmol/gLW/min)	65.47 ± 9.69 *	97.61 ± 16.22
Bile acid output (nmol/gLW/min)	64.01 ± 29.03	57.24 ± 12.78
Phospholipid output (nmol/gLW/min)	8.74 ± 2.39	6.91 ± 2.40
Cholesterol output (nmol/gLW/min)	1.01 ± 0.24	0.75 ± 0.27

Table 2: Genetic loss of M₃-R results in reduced biliary HCO₃⁻ secretion. M₃-R^{-/-} showed a significantly reduction in bile flow due to a significantly reduced biliary HCO₃⁻ secretion. Reproduced from Durchschein F et al. Hepatology Research. 2017; in press with permission of John Wiley & Sons Australia, ("Wiley") (1).

12.1.2 Comparison of bile flow in $M_3-R^{-/-}$ mice and WT controls after intraperitoneal (i.p.) N-butyl-scopolamine injection:

In order to investigate the influence of the parasympathetic antagonist scopolamine on bile flow, we injected N-butyl scopolamine (S7882 Sigma: Scopolamine N-butyl bromide) i.p. (2mg/kgKG) and started measuring bile flow after 30 minutes. We used N-butyl-scopolamine, because it does not cross the blood brain barrier. As control group we measured bile flow in $M_3-R^{-/-}$ and WT mice after i.p. injection of 0.9% sodium chloride solution (NaCl).

In the NaCl treated group, $M_3-R^{-/-}$ mice showed a significant reduction in biliary HCO_3^- output compared to WT mice (biliary HCO_3^- secretion 48.6 ± 8.5 vs. 76.0 ± 16.0 mmol/l, $M_3R^{-/-}$ vs. WT, $p < 0.05$) (figure 4). After i.p. injection of N-butyl-scopolamine, there was a reduction in biliary HCO_3^- output in WT mice without reaching statistical significance (biliary HCO_3^- secretion 55.09 ± 7.7 vs. 64.70 ± 12.22 mmol/l, WT treated with scopolamine vs. WT treated with NaCl, $p > 0.05$). After i.p. injection of N-butyl-scopolamine in $M_3-R^{-/-}$ mice, biliary HCO_3^- output did not change compared to $M_3-R^{-/-}$ mice treated with i.p. injection of NaCl (biliary HCO_3^- secretion 41.2 ± 7.4 vs. 48.6 ± 8.5 mmol/l, $M_3-R^{-/-}$ treated with N-butyl-scopolamine vs. $M_3-R^{-/-}$ treated with NaCl, $p > 0.05$).

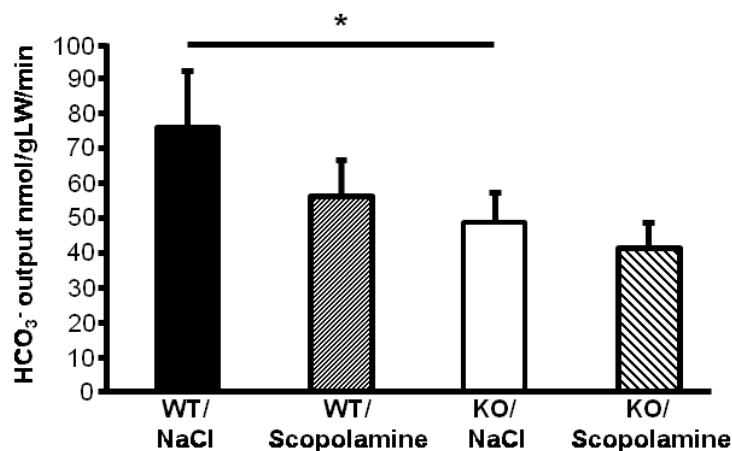


Figure 4: $M_3-R^{-/-}$ mice showed a significant reduction in biliary HCO_3^- output compared to WT littermates. I.p. injection of N-butyl-scopolamine reduced biliary HCO_3^- output in WT mice without reaching a statistical significance. I.p. injection of N-butyl-scopolamine had no effect on biliary HCO_3^- output in $M_3-R^{-/-}$ mice. * $P < 0.05$ versus control.

12.1.3 Comparison of bile flow in $M_3-R^{-/-}$ mice and WT controls after *norUDCA* feeding:

Rationale: Raufmann et al. determined that lithocholytaurine is a partial muscarinic receptor agonist (183, 184). Lithocholytaurine has a similar molecular structure like ACh. Both molecules contain a tetrahedral atom with the quaternary ammonium group in ACh and the sulfonic acid part in lithocholytaurine. Due to the structural similarity between the taurine and choline part of lithocholytaurine and ACh, lithocholytaurine can interact with muscarinic receptors. *In vitro* experiments showed, that lithocholytaurine stimulates pepsinogen secretion in gastric chief cells. This effect was abolished by adding the cholinergic antagonist atropine (185). By contrast, lithocholycholine, a created molecule combining the steroid nucleus of lithocholic acid with a choline part as is present in ACh, is a muscarinic receptor antagonist (184). Consequently some BAs seem to interact with muscarinic receptors and alter postreceptor signaling (184). 24-*nor*ursodeoxycholic acid (*norUDCA*) is a side chain-modified ursodeoxycholic acid derivative. In animal models for sclerosing cholangitis and biliary fibrosis *norUDCA* demonstrated a therapeutic superiority compared to UDCA (186). This molecule is reabsorbed from bile by cholangiocytes and resecreted by hepatocytes undergoing a cholehepatic shunting. By this process *norUDCA* induces a rich hypercholeresis (186). As some BAs seem to affect the M_3-R , we investigated if *norUDCA* induces biliary HCO_3^- secretion via the M_3-R . Therefore, we fed $M_3-R^{-/-}$ and WT mice with 0.5% *norUDCA* for 3 days and compared bile flow in both groups. As control group we compared bile flow in untreated WT and $M_3-R^{-/-}$ mice.

After 0.5% *norUDCA* feeding WT mice showed a significant increase in biliary HCO_3^- output compared to chow fed WT mice (biliary HCO_3^- secretion 319.6 ± 102.3 vs. 70.8 ± 6.7 mmol/l, *norUDCA* fed WT vs. chow fed WT, $p < 0.05$) (figure 5). In the $M_3-R^{-/-}$ group, *norUDCA* feeding resulted in a significant increase of biliary HCO_3^- output compared to chow fed $M_3-R^{-/-}$ mice (biliary HCO_3^- secretion 213.6 ± 88.6 vs. 40.9 ± 18.0 mmol/l, *norUDCA* fed $M_3-R^{-/-}$ vs. chow fed $M_3-R^{-/-}$, $p < 0.05$). Comparing chow fed animals, $M_3-R^{-/-}$ mice showed a significant reduced biliary HCO_3^- output compared to WT mice (biliary HCO_3^- secretion 40.9 ± 18.0 vs. 70.8 ± 6.7 mmol/l, chow fed $M_3-R^{-/-}$ vs. chow fed WT, $p < 0.05$).

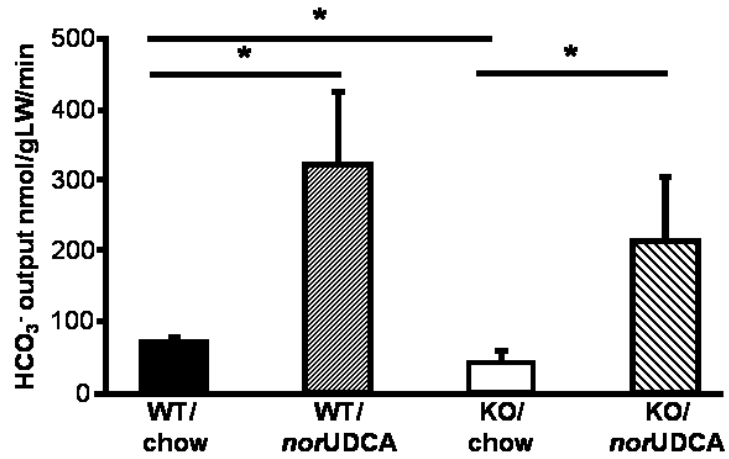


Figure 5: *norUDCA* feeding increases HCO₃⁻ output in M₃-R^{-/-} and WT mice. 0.5% *norUDCA* feeding for 3 days resulted in a significant increase of biliary HCO₃⁻ output in M₃-R^{-/-} as well as WT. Untreated M₃-R^{-/-} mice showed a significant reduction in biliary HCO₃⁻ output compared to WT. *P<0.05 versus control

To sum up, *norUDCA*-induced hypercholeresis is independent of the M₃-R activity.

12.2 Aim (2): Determine the Pathophysiological Role of the M₃-R in Mouse Models for Cholangiopathies and Biliary Fibrosis

Rationale: Since M₃-R seems to regulate biliary HCO₃⁻ secretion, which may protect cholangiocytes in their toxic environment; alterations in M₃-R function might predispose individuals for cholangiopathies. It is therefore tempting to hypothesize that M₃-R^{-/-} mice show increased susceptibility in experimental models for cholangiopathies. Therefore, we compared WT and M₃-R^{-/-} mice in different cholestatic models in regard to their cholestatic and fibrotic phenotype combining numerous read outs such as serum biochemical tests (e.g. ALT, AP, serum BA levels), liver morphology (H&E stained liver sections) and quantification of liver fibrosis (i.e. hepatic hydroxyproline content, sirius red-stained liver sections).

12.2.1 Comparison of M₃-R^{-/-} and WT mice after 17 days 3,5-diethoxycarbonyl -1,4-dihydrocollidine (DDC) feeding:

We next challenged mice with DDC to test the hypothesis that M₃-R^{-/-} mice are more vulnerable to bile duct injury. M₃-R^{-/-} and WT control mice were fed 0.1% DDC-supplemented diet for 17 days to determine whether loss of M₃-R function increases susceptibility to porphyrin-induced chronic cholangitis and the biliary type of liver fibrosis (171).

After 17 days DDC feeding M₃-R^{-/-} mice showed significantly higher serum ALT (2324±613 vs. 1823±257 U/l, M₃-R^{-/-} vs. WT, *p*<0.05), serum BAs (1138±358 vs. 370±208 μmol/l, M₃-R^{-/-} vs. WT, *p*<0.05), and bilirubin levels (3±1 vs. 1±0 mg/dl, M₃-R^{-/-} vs. WT, <0.05) compared to WT mice (figure 6) (1).

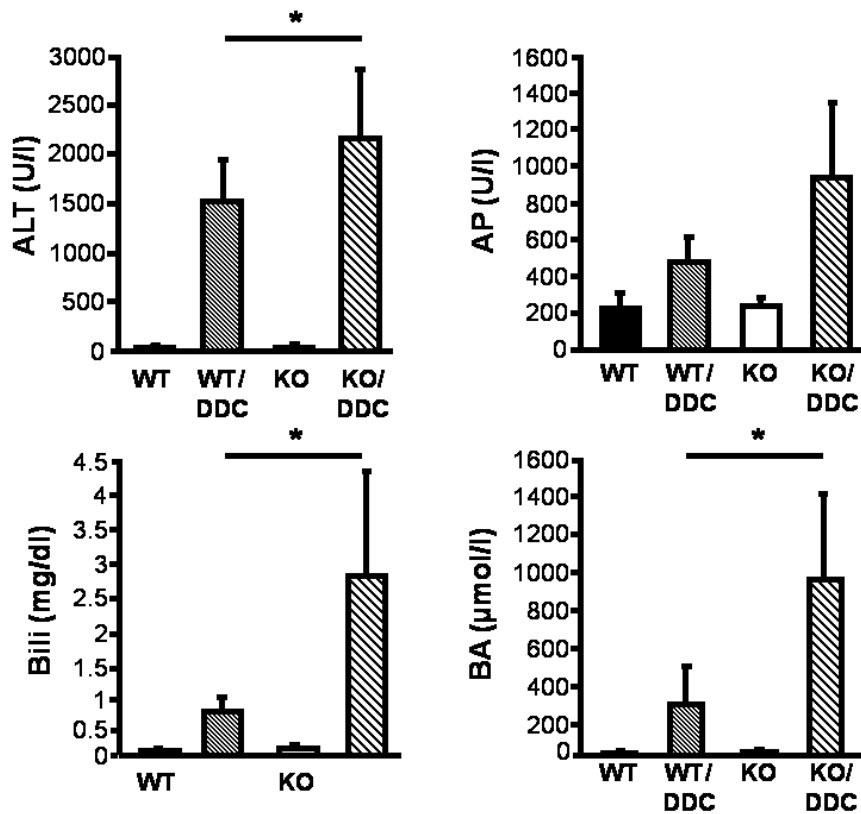


Figure 6: $M_3-R^{-/-}$ mice were more susceptible to liver injury after DDC feeding compared to WT. $M_3-R^{-/-}$ mice showed significantly higher serum ALT, Bilirubin and BA levels compared to WT mice after 17 days DDC feeding. * $P < 0.05$ versus control. Reproduced from Durchschein F et al. Hepatology Research. 2017; in press with permission of John Wiley & Sons Australia, ("Wiley") (1).

Liver histology of DDC-fed $M_3-R^{-/-}$ and WT control mice showed comparable ductular reaction (figure 7A) (1). However, livers of $M_3-R^{-/-}$ mice contained more and larger porphyrin plugs compared to WT mice (black arrows figure 7A/B) (1). Differences in liver fibrosis between the two genotypes as suggested by Sirius red staining (figure 7B) did not translate into significant differences in hepatic hydroxyproline levels (figure 8B) or mRNA levels of col1a1 (figure 8C). Between the two groups no difference could be detected analysing TGF β and F4/80 (figure 8C) (1).

After 17 days DDC feeding $M_3-R^{-/-}$ lost more bodyweight (BW) compared to WT (BW start 25.24 ± 0.7 g; BW after DDC feeding 17.39 ± 0.8 g vs. BW start 25.5 ± 2.92 g; BW after DDC feeding 24.7 ± 2.7 $M_3-R^{-/-}$ vs. WT, $p < 0.05$) (figure 8A) (1).

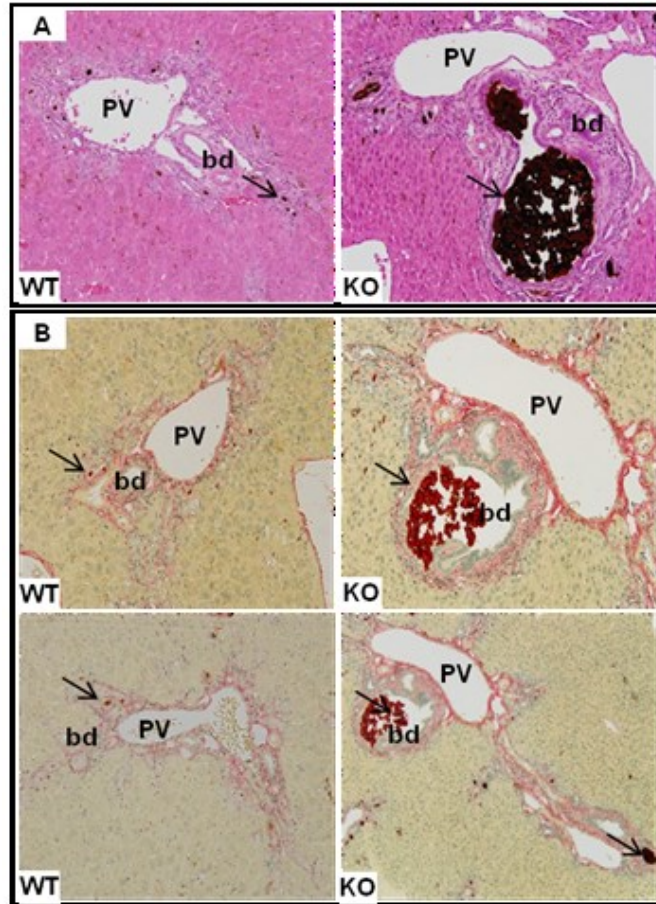


Figure 7: (A) Hematoxylin/Eosin and (B) Sirius Red staining of $M_3-R^{-/-}$ (KO) and WT mice after 17 days DDC feeding. Ductular reaction and liver fibrosis were similar in both groups. Note that there is subtotal obstruction of bile ducts by porphyrin plugs as well as increased porphyrin accumulation in bile duct lumina of $M_3-R^{-/-}$ compared to WT mice (arrow). Original magnification, x 20. **pv**, portal vein, **bd**, bile duct. Reproduced from Durchschein F et al. *Hepatology Research*. 2017; in press with permission of John Wiley & Sons Australia, ("Wiley") (1).

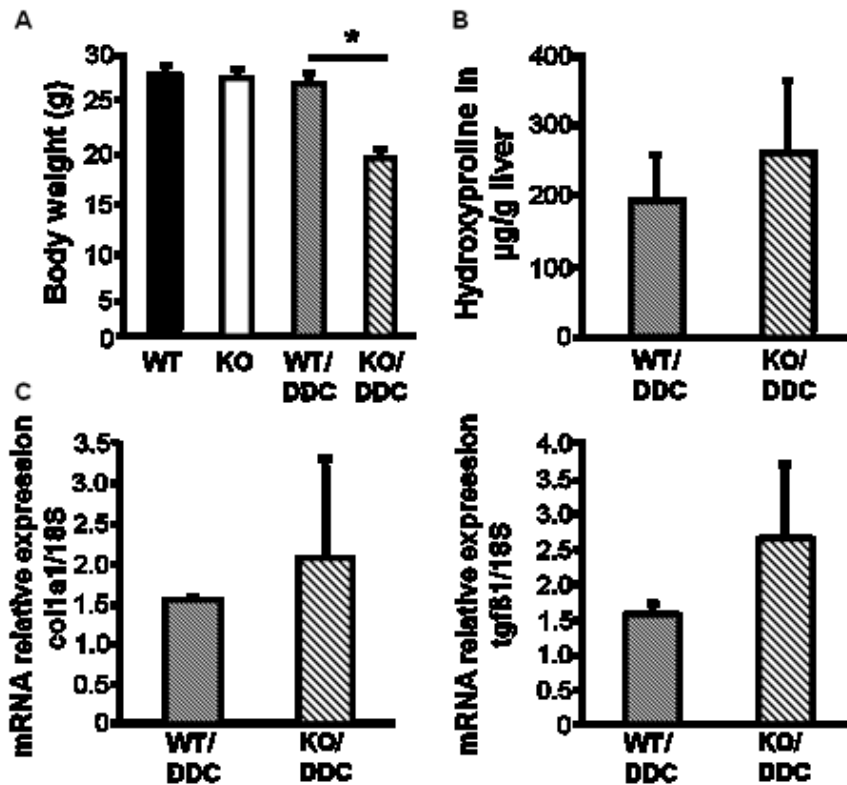


Figure 8: A) Comparison of body weight (BW) of $M_3-R^{-/-}$ (KO) and WT mice before and after DDC feeding. $M_3-R^{-/-}$ lost significantly more BW after 17 days DDC feeding compared to WT. B) Hepatic hydroxyproline of $M_3-R^{-/-}$ and WT mice after 17 days DDC feeding show increased liver fibrosis of $M_3-R^{-/-}$ mice without reaching statistical significance. C) Hepatic mRNA expression of col1a1 and tgf β 1 after 17 days DDC-feeding of WT and $M_3-R^{-/-}$ mice showing no difference between the two groups. * $p < 0.05$ versus control.

Reproduced from Durchschein F et al. Hepatology Research. 2017; in press with permission of John Wiley & Sons Australia, ("Wiley")(1).

We also compared both mouse groups for ductular proliferation by using immunohistochemistry (IHC) and immunofluorescence (IHF) for CK-19 (figure 9A/B) and for apoptosis by using IHC for caspase 3 (figure 9C/D). IHC for CK-19 and caspase-3 however did not show significant differences in ductular proliferation and apoptosis comparing $M_3-R^{-/-}$ mice and WT littermates under the used experimental conditions.

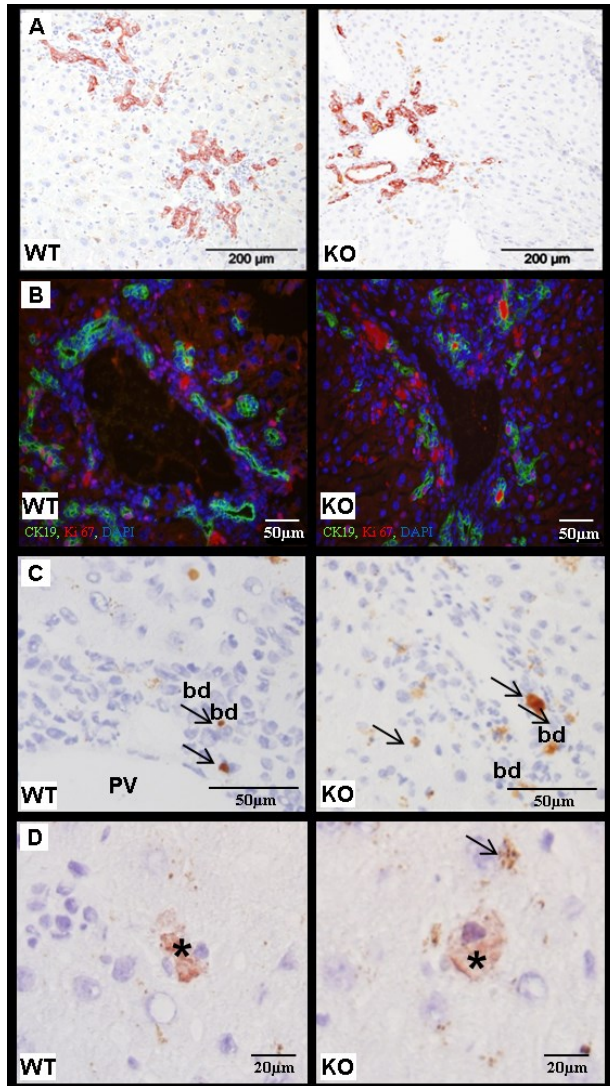


Figure 9: After 17 days DDC-feeding $M_3-R^{-/-}$ (KO) and WT show similar ductular proliferation. A) IHC for **CK-19** demonstrating similar **CK-19** expressing on bile duct epithelial cells in WT and $M_3-R^{-/-}$ (KO) mice after 17 days DDC-feeding. B) IF microscopy for **CK19/Ki-67/DAPI** showing similar staining of **CK19** and **Ki-67** in both groups. C and D) IHC for caspase-3 determine only a few apoptotic cells (*) in both genotypes. Note that $M_3-R^{-/-}$ show increased porphyrin accumulation in bile duct lumina compared to WT mice (arrow). Under the used experimental conditions, the immunohistochemical analysis does not show significant difference in ductular proliferation and apoptosis comparing $M_3-R^{-/-}$ mice and WT littermates. **pv**, portal vein, **bd**, bile duct.

12.2.2 Comparison of M₃-R^{-/-} and WT mice after CBDL for 5 days:

Complete obstructive cholestasis was surgically induced by CBDL for 5 days to determine the effects of genetic M₃-R loss on cholangitis, bile infarcts, ductular reaction and liver fibrosis of the biliary type (178). The CBDL testing however showed inconsistent findings: Of the total four CBDL trials we performed, only two experiments revealed an increased susceptibility of M₃-R^{-/-} compared to WT littermates. After 5 days CBDL M₃-R^{-/-} mice showed significantly higher ALT (3507±564 vs. 564±243 U/l, M₃-R^{-/-} vs. WT, *p*<0.05), serum BA (3624±664 vs. 1341±400 μmol/l, M₃-R^{-/-} vs. WT, *p*<0.05), and bilirubin levels (23.4±3.9 vs. 12.7±2.9 mg/dl, M₃-R^{-/-} vs. WT, <0.05) compared to WT mice (figure 10). There was no significant difference comparing serum AP levels of M₃-R^{-/-} and WT mice (1911±79 vs. 1460±25 U/l, M₃-R^{-/-} vs. WT, *p*>0.05) (figure 10).

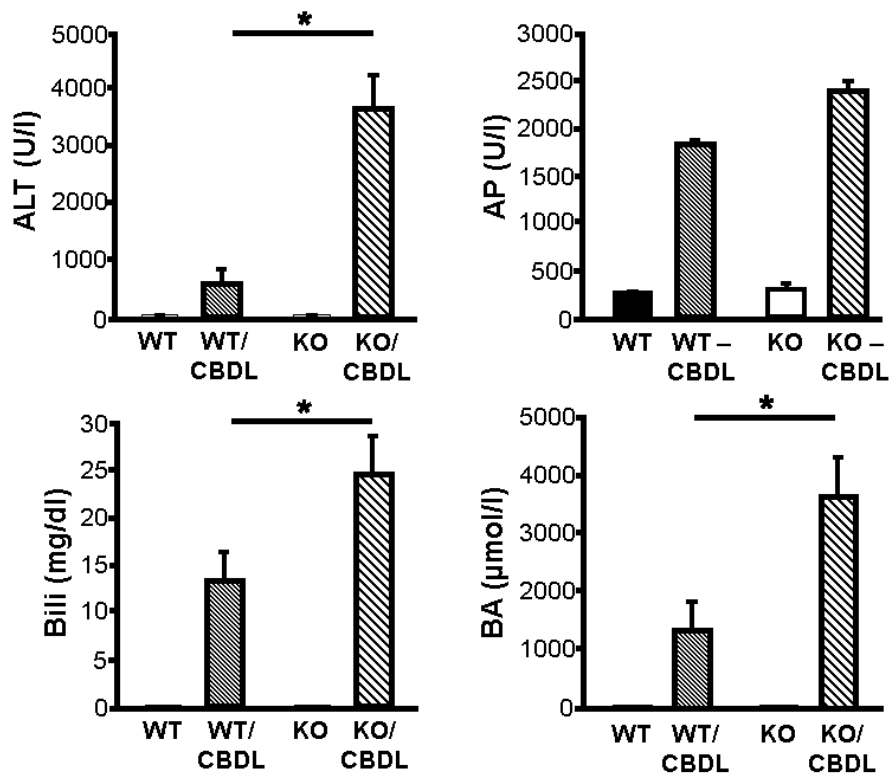


Figure 10: Serum parameters of M₃-R^{-/-} and WT mice after after 5 days CBDL. M₃-R^{-/-} showed significantly higher serum ALT, Bilirubin and BA levels compared to WT mice after 5 days CBDL. M₃-R^{-/-} mice seem to be more susceptible to liver injury after CBDL compared to WT. **P*<0.05 versus control.

In the following two CBDL experiments WT and M₃-R^{-/-} mice however showed similar liver injury and the initial increased susceptibility of the M₃-R^{-/-} mice after 5 days CBDL was not longer obvious. Comparing serum liver enzymes of the two genotypes no difference was detectable (serum ALT (1410±1648 vs. 417±158 U/l, M₃-R^{-/-} vs. WT, *p*>0.05), serum AP

(1027 ± 691 vs. 1543 ± 83 U/l, $M_3-R^{-/-}$ vs. WT, $p > 0.05$), serum BA (1900 ± 1386 vs. 1220 ± 251 $\mu\text{mol/l}$, $M_3-R^{-/-}$ vs. WT, $p > 0.05$), serum bilirubin levels (19 ± 5 vs. 12 ± 1 mg/dl, $M_3-R^{-/-}$ vs. WT, > 0.05) (figure 11).

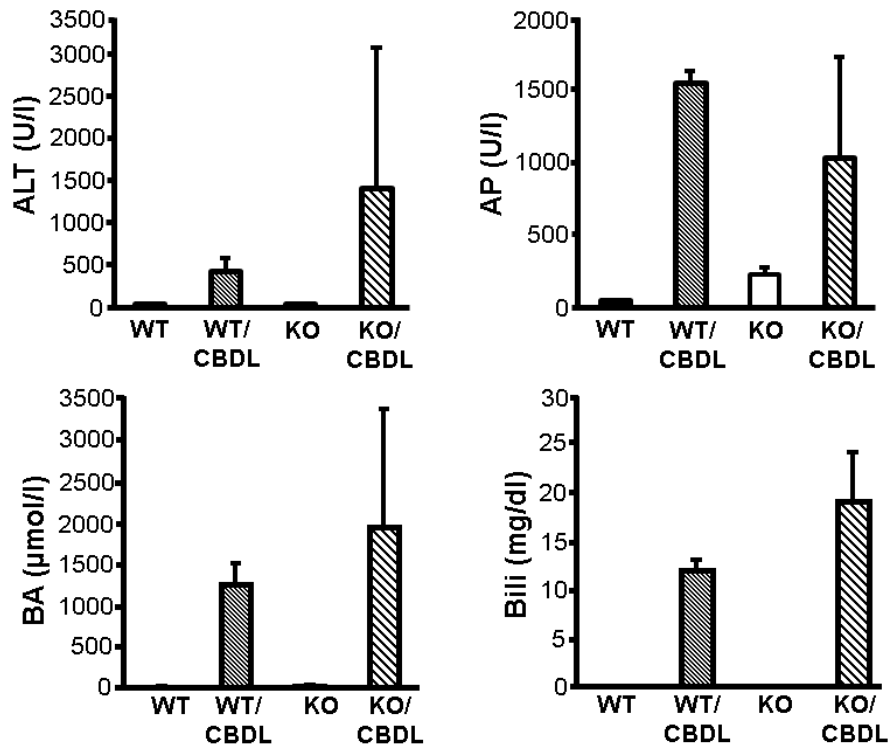


Figure 11: Serum parameters of $M_3-R^{-/-}$ and WT mice after 5 days CBDL. Compared to the first experiment, $M_3-R^{-/-}$ mice showed similar serum ALT, AP, bilirubin and BA levels compared to WT mice after 5 days CBDL.

Besides no difference in body weight or liver fibrosis was detectable comparing the two groups after 5 days CBDL (figure 12A/B).

Taken together, the effect of the M_3-R in the cholestatic model of CBDL is unclear.

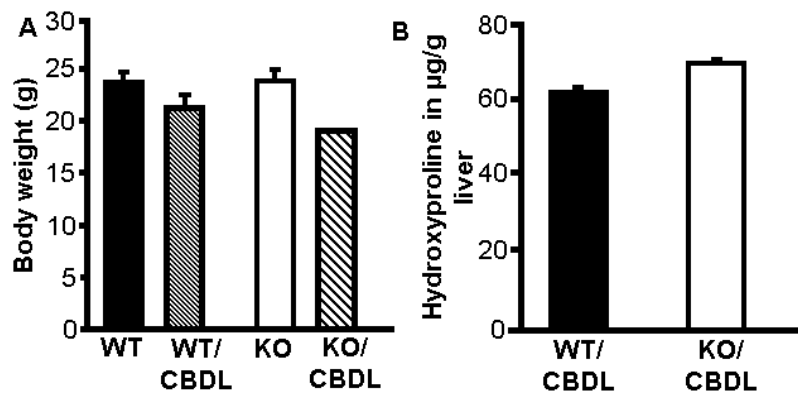


Figure 12: A) $M_3-R^{-/-}$ and WT mice lost similar BW after 5 days CBDL. B) Hepatic hydroxyproline of $M_3-R^{-/-}$ and WT mice after 5 days CBDL showing similar liver fibrosis.

12.2.3 Comparison of M₃-R^{-/-} and WT after 1% cholic acid (CA) feeding for 7 days:

Feeding a CA-supplemented diet does not induce SC in WT mouse strains (180). We compared the effects of 1% CA-supplemented diet for 7 days in M₃-R^{-/-} mice and WT littermates to determine whether loss of M₃-R function increases bile duct susceptibility to biliary secreted bile acids such as CA.

Both genotypes were fed with 1% CA for 7 days. There was a significant increase of serum ALT, AP, bilirubin and BA in both mouse strains after 7 days CA feeding (figure 13). Comparing M₃-R^{-/-} and WT mice, serum BA (374.12±109 vs. 392.8±174µmol/l, M₃-R^{-/-} vs. WT, *p*>0.05) and bilirubin (0.36±0.16 vs. 0.49±0.36µmol/l, M₃-R^{-/-} vs. WT, *p*>0.05) levels were similar. However, WT showed significant higher serum ALT levels compared to M₃-R^{-/-} after 7 days CA feeding (121.64 vs. 233.5±70µmol/l, M₃-R^{-/-} vs. WT, *p*>0.05). By contrast, M₃-R^{-/-} showed significant higher serum AP levels compared to WT (303.4±47.8 vs. 250.0±36µmol/l, M₃-R^{-/-} vs. WT, *p*>0.05) (figure 13).

Furthermore we compared bodyweight (BW) of WT and M₃-R^{-/-} after CA feeding. At the start of the experiment, M₃-R^{-/-} mice showed significant lower BW compared to WT (23.8±2.6 vs. 33.1±1.8µmol/l, M₃-R^{-/-} vs. WT, *p*>0.05). However, both groups lost similar BW during the experiment and at the end of the study, the BW of M₃-R^{-/-} was still significant lower compared to WT (20.6±2.6 vs. 29.2±1.1µmol/l, M₃-R^{-/-} vs. WT, *p*>0.05) (figure 14).

To sum up, M₃-R^{-/-} and WT mice showed similar susceptibility towards CA feeding. No difference comparing serum levels of liver injury, liver fibrosis (measuring hydroxyproline levels), BW or liver histology between the two groups was detectable.

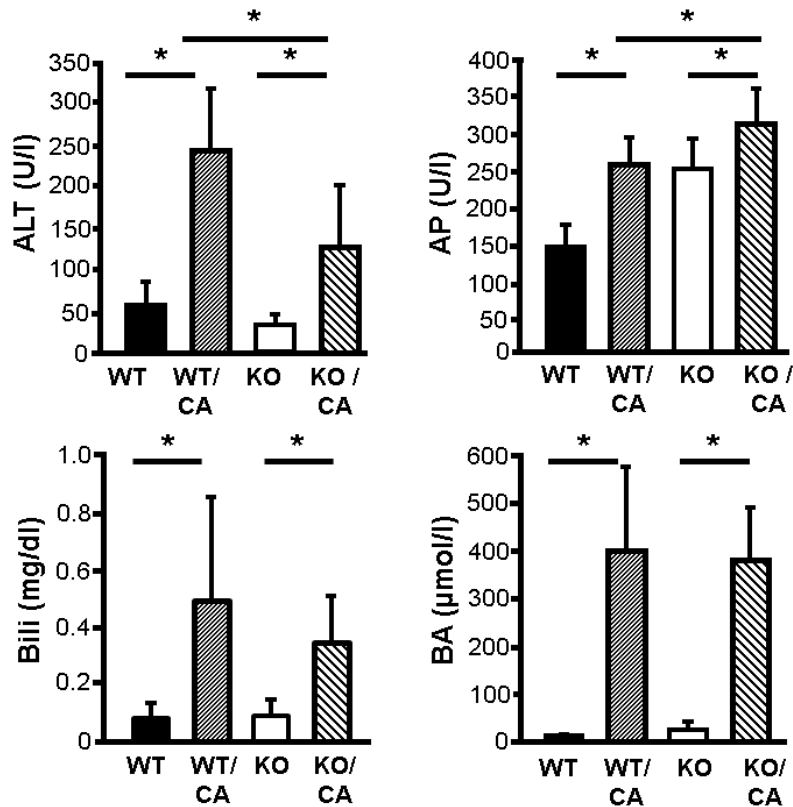


Figure 13: Serum parameters of $M_3-R^{-/-}$ and WT mice after 7 days 1% CA feeding showing similar liver injury after 7 days CA feeding. There is a significant increase of serum ALT, AP, bilirubin and BA after CA feeding in both groups. However, comparing WT and $M_3-R^{-/-}$ mice after 7 days CA feeding no difference was detectable. * $P < 0.05$ versus control.

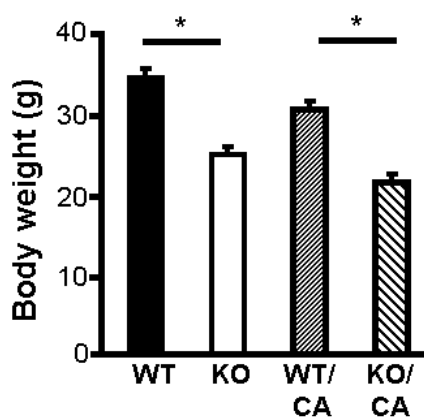


Figure 14: WT and $M_3-R^{-/-}$ mice lost similar BW after 7 days CA feeding. At the start of the experiment $M_3-R^{-/-}$ showed significant lower BW compared to WT mice. However both groups lost similar percentage of BW during the CA feeding. * $P < 0.05$ versus control.

12.2.4 Comparison of $M_3-R^{-/-}$ and WT after 1% lithocholic acid (LCA) feeding

Feeding LCA-supplemented diet induces acute destructive cholangitis in mice via physicochemical injury of BECs via LCA crystals. For determining whether the M_3-R is critically engaged in protecting bile ducts from bile acid-induced SC (172), we fed $M_3-R^{-/-}$ mice and WT controls with 1% LCA feeding for 10 days.

After 10 days 1% LCA WT mice showed significantly higher serum ALT (3267.5 ± 843.1 vs. 110 ± 57.7 U/l, WT vs. $M_3-R^{-/-}$, $p < 0.05$), serum AP (1047.5 ± 216.5 vs. 245.0 ± 117.6 WT vs. $M_3-R^{-/-}$), serum BA (273.1 ± 84.21 vs. 27.5 ± 22.9 $\mu\text{mol/l}$, WT vs. $M_3-R^{-/-}$, $p < 0.05$), and serum bilirubin levels (2.36 ± 1.35 vs. 0.7 ± 0.7 mg/dl, WT vs. $M_3-R^{-/-}$, < 0.05) compared to $M_3-R^{-/-}$ mice (figure 15).

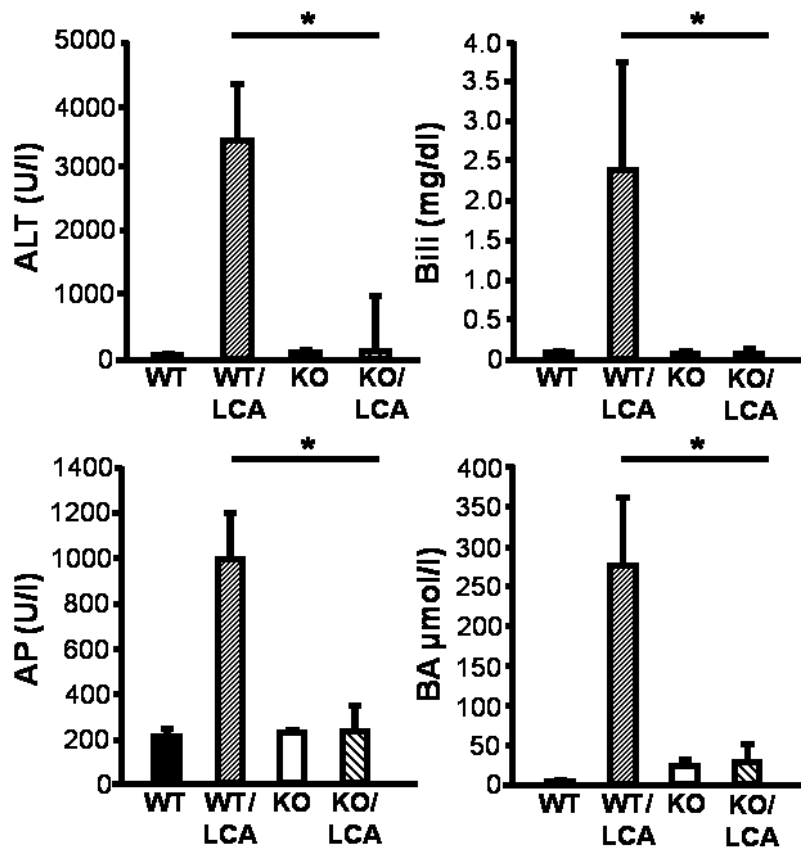


Figure 15: WT showed significantly higher serum ALT, Bilirubin, AP and BA levels compared to $M_3-R^{-/-}$ after 10 days LCA-feeding. WT seem to be more susceptible to liver injury after LCA feeding compared to $M_3-R^{-/-}$. * $P < 0.05$ versus KO.

Histologically, bile infarcts were detectable throughout the liver in both groups (figure 16A; black star). However ductular proliferation was more prominent in the WT group compared to the $M_3-R^{-/-}$ group (16B/; black arrow; 17A). In order to quantify liver fibrosis hepatic hydroxyproline content was determined in liver homogenates from $M_3-R^{-/-}$ mice and WT controls after 10 days LCA-supplemented diet. WT mice show similar hydroxyprolin levels compared to $M_3-R^{-/-}$ (134 ± 25 vs. 125 ± 47 μg Hydroxyprolin/g liver, WT vs. $M_3-R^{-/-}$, >0.05 (figure 16C).

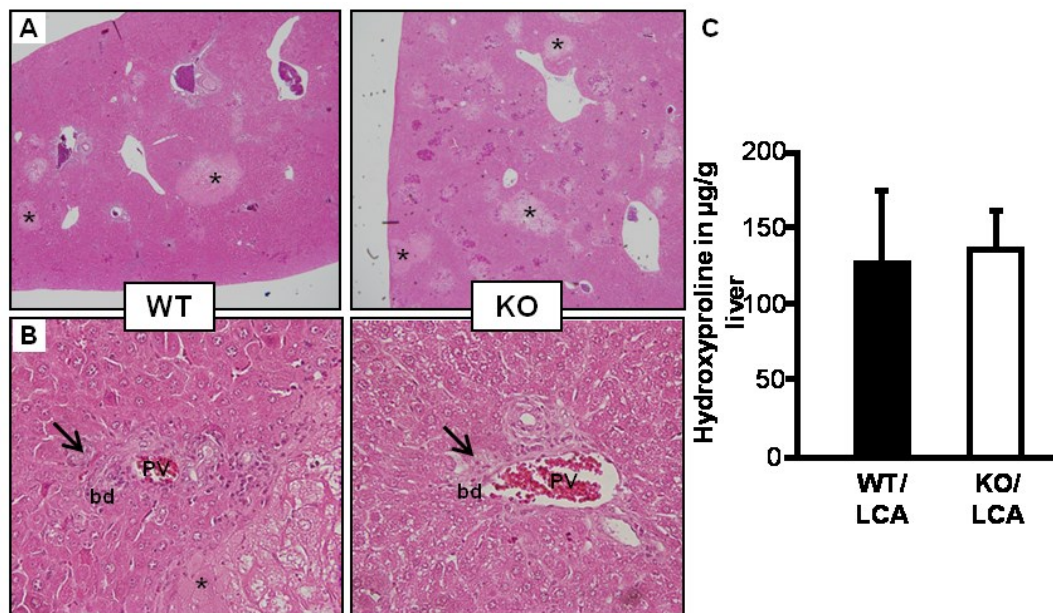


Figure 16: A/B: Hematoxylin / eosin staining, of $M_3-R^{-/-}$ and WT mice after 10 days LCA feeding. A) $M_3-R^{-/-}$ show similar liver injury compared to WT. Bile infarcts were detectable throughout the liver in both genotypes; bile infarcts (*), (Original magnification, 4x). B) Ductular proliferation (black arrow) was more prominent in WT mice compared to $M_3-R^{-/-}$ mice; (Original magnification, 20x). C) Hepatic hydroxyproline of $M_3-R^{-/-}$ and WT mice after 10 days LCA feeding showing no difference between the two groups. **pv**, portal vein, **bd**, bile duct.

We compared both mouse groups for ductular proliferation by using immunohistochemical staining for CK-19 (figure 17A). WT showed more ductular proliferation compared to $M_3-R^{-/-}$. Furthermore during 10 days LCA feeding WT lost more body weight (BW) compared to $M_3-R^{-/-}$ (5.9 ± 0.43 vs. 3.8 ± 1.7 g loss of BW after LCA feeding WT vs. $M_3-R^{-/-}$, $p = 0.05$) (figure 17B). We also compared $M_3-R^{-/-}$ and WT mice concerning inflammation and liver fibrosis on the mRNA level after 10 days LCA-feeding. WT showed significant higher mRNA levels of F4/80 and TGF α compared to $M_3-R^{-/-}$ (figure 17C).

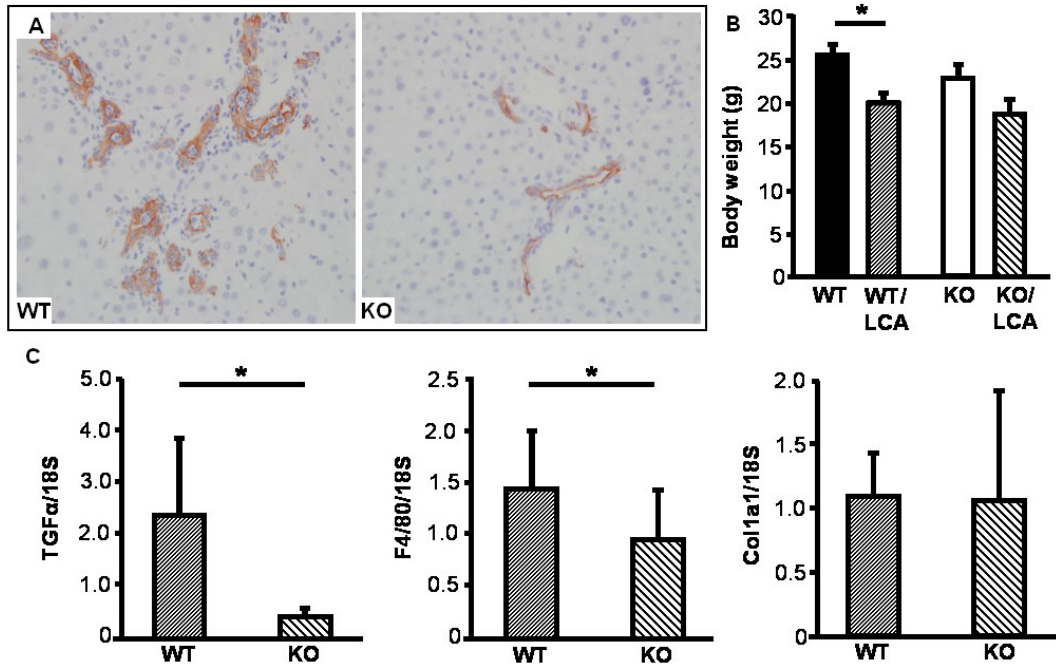


Figure 17: **A)** Immunohistochemical staining of bile duct epithelial cells by using anti-CK19 antibody in WT and $M_3-R^{-/-}$ mice after 10 days LCA feeding (Original magnification, 20x). There is significant less ductular proliferation in $M_3-R^{-/-}$ mice compared to WT mice. **B)** WT mice lost significant more BW compared to $M_3-R^{-/-}$. **C)** Hepatic overexpression of TGF α , and F4/80 in response to LCA feeding. Expression levels of all transcripts are normalized to the housekeeping gene, S18. * $P < 0.05$ versus $M_3-R^{-/-}$.

12.2.5 Comparison WT after DDC feeding with sham operation versus vagotomy:

To study the effect of the parasympathetic nervous system on cholestasis in general, we performed hepatic vagotomy in different cholestatic mouse models and compared liver injury with sham-operated mice. To determine whether loss of the parasympathetic innervation increases susceptibility to porphyrine-induced chronic cholangitis similar to the knockout mouse model, we performed hepatic vagotomy in WT mice and fed these animals after 3 days of recovery with 0.1% DDC for 17 days. We compared liver injury with sham operated control mice. Compared to the sham operated mice, WT with vagotomy showed similar serum ALT (1343 ± 472 vs. 1490 ± 447 U/l, WT/sham vs. WT/vagotomy, serum AP (399.9 ± 41.9 vs. 393.7 ± 35.7 U/l, WT/sham vs. WT/vagotomy $p > 0.05$), serum BA (214 ± 90 vs. 175 ± 76 $\mu\text{mol/l}$, WT/sham vs. WT/vagotomy, $p > 0.05$), and bilirubin levels compared to $M_3\text{-R}^{-/-}$ mice (0.7 ± 0.2 vs. 0.7 ± 0.05 mg/dl WT/sham vs. WT/vagotomy, $p > 0.05$) (figure 18).

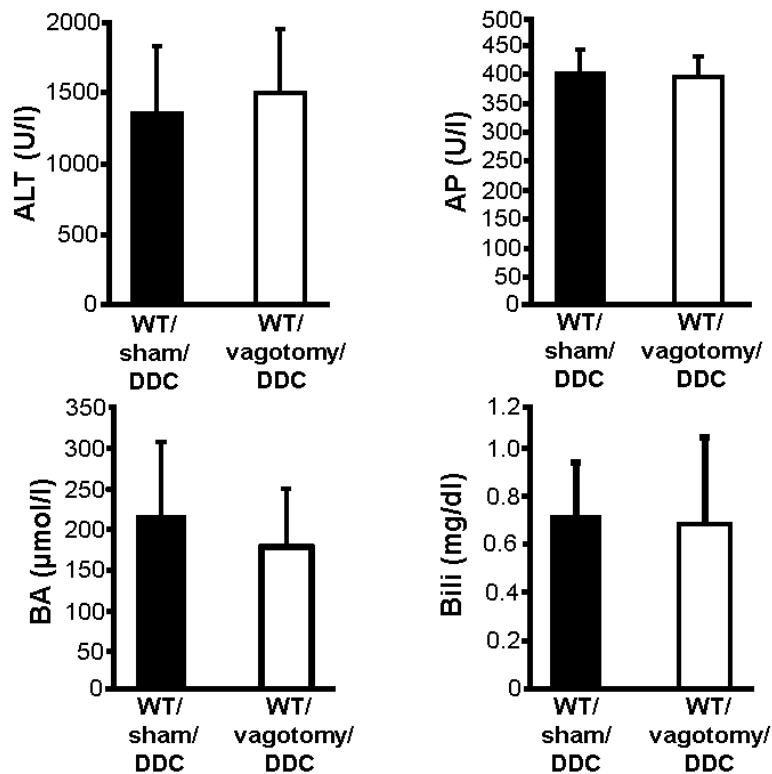


Figure 18: Serum parameters of sham operated WT mice versus vagotomized WT mice and DDC-feeding for 17 days. Vagotomized mice showed similar serum ALT, AP, bilirubin and BA levels compared to sham-operated mice.

Comparing liver histology of WT/sham versus WT/vagotomy after DDC-feeding, both groups showed similar liver injury (figure 19A). Besides, hydroxyproline levels and change of BW were similar in the two groups (figure 19B/20).

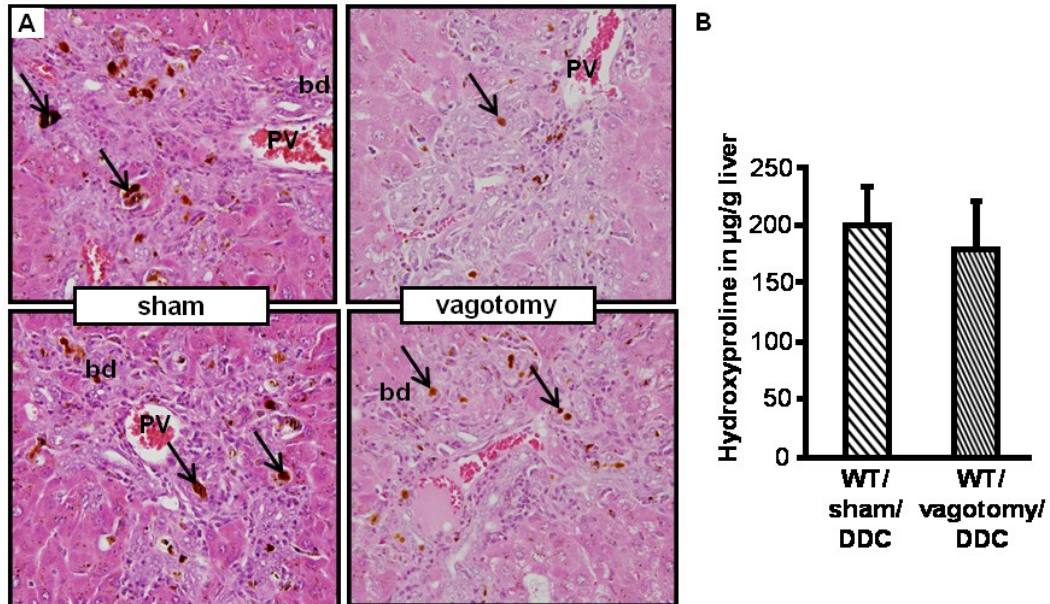


Figure 19: A) Hematoxylin / eosin staining of DDC fed WT treated with sham operation versus vagotomy showing no difference in liver injury. Vagotomized mice showed similar ductular proliferation and porphyrin plugs (black arrows) after DDC-feeding compared to sham-operated mice. B) Hepatic hydroxyproline of DDC fed WT treated with sham operation or vagotomy showed no difference between the two groups. Original magnification, x 20. **pv**, portal vein, **bd**, bile duct.

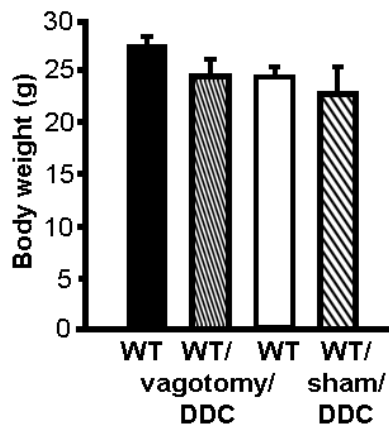


Figure 20: Body weight of WT mice after 17 days DDC-feeding with vagotomy versus sham operation. Both mouse groups lost similar amount of BW during the experiment.

The comparison of serum liver enzymes of the knock out mouse model with the data of the vagotomy experiments after DDC-feeding are illustrated in figure 21. $M_3-R^{-/-}$ mice showed increased susceptibility after DDC-feeding compared to WT mice. Vagotomy did not result in a change of susceptibility in WT mice towards DDC induced cholestasis (figure 21).

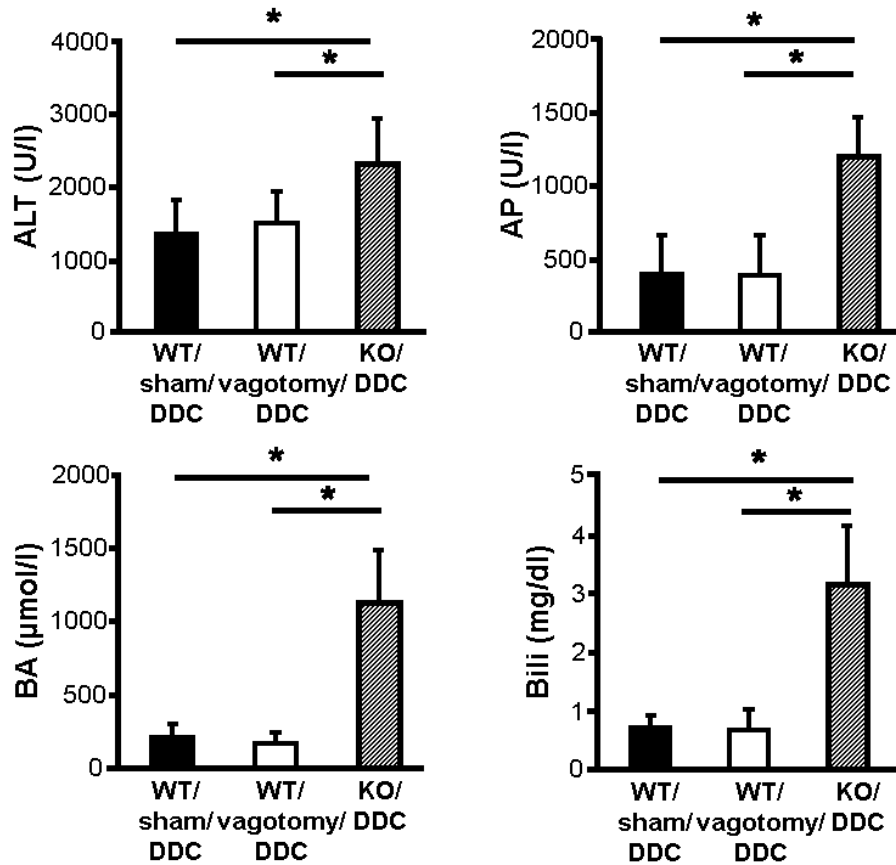


Figure 21: Comparison of serum parameters of WT/sham/DDC versus WT/vagotomy/DDC versus $M_3-R^{-/-}$ /DDC for 17 days. Compared to WT mice, $M_3-R^{-/-}$ show significant higher serum ALT, AP, bilirubin and BA levels. $M_3-R^{-/-}$ seemed to be more susceptible towards DDC-induced cholestasis compared to sham operated WT or vagotomized WT. Vagotomized WT mice showed similar serum ALT, AP, bilirubin and BA levels compared to sham-operated mice. * $P < 0.05$ versus $M_3-R^{-/-}$.

12.2.5 Comparison of Mdr2^{-/-} mice treated with vagotomy for 4 and 8 weeks versus sham operated mice:

Mdr2 knockout mice (Mdr2^{-/-}) present a genetic mouse model for sclerosing cholangitis and biliary fibrosis (158). We compared Mdr2^{-/-} mice after vagotomy for 4 and 8 weeks versus sham operation mice to determine whether loss of parasympathetic innervation aggravates liver injury in this cholestatic model. After 4 weeks vagotomy, Mdr2^{-/-} mice showed decreased serum ALT levels compared to sham operated mice but without reaching statistical significance (436±239 vs. 258±171 U/l, Mdr2^{-/-} + sham vs. Mdr2^{-/-}+ vagotomy, $p>0.05$). Serum AP levels were similar in both groups (119.0±28.9 vs. 100.0±49.4 U/l, Mdr2^{-/-} + sham vs. Mdr2^{-/-}+ vagotomy, $p>0.05$) Besides vagotomized Mdr2^{-/-} mice showed significantly lower serum BA compared to sham operated mice (59±15 vs. 29±14 µmol/l Mdr2^{-/-} + sham vs. Mdr2^{-/-}+ vagotomy, $p<0.05$). Serum bilirubin levels were also significantly lower in Mdr2^{-/-} mice with vagotomy compared to sham operated mice (0.11±0.02 vs. 0.06±0.02 mg/dl, Mdr2^{-/-} +sham vs. Mdr2^{-/-}+ vagotomy, $p<0.05$) (figure 22).

Comparing liver histology of both experimental groups, no difference could be detected. The vagotomized mice showed similar liver histology compared to the sham-operated mice (figure 23A). During the 4 weeks experiment both groups gain similar amount of BW (1.42±1.9 vs. 1.7±1.4 g gain of BW after 4 weeks Mdr2^{-/-} sham operation vs. Mdr2^{-/-} vagotomy, $p>0.05$) (figure 23B).

In order to quantify liver fibrosis hepatic hydroxyproline content was determined in liver homogenates from the two mouse groups. Mdr2^{-/-} after 4 weeks vagotomy showed similar hydroxyproline levels compared to sham operated Mdr2^{-/-} mice (134±25 vs. 125±47 µg hydroxyproline/g liver, sham vs. vagotomy, >0.05) (figure 23C).

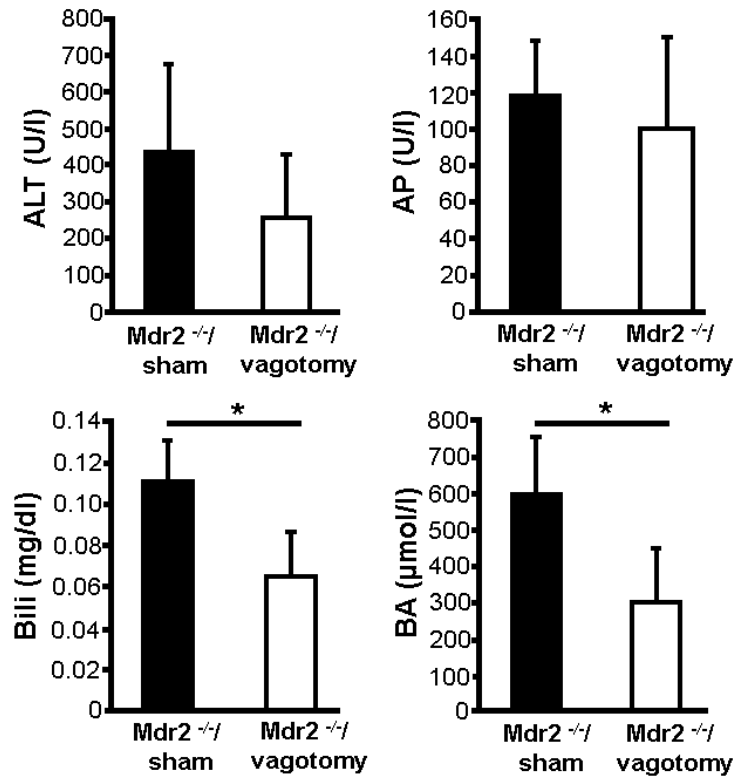


Figure 22: Serum parameters of Mdr2^{-/-} treated with sham operation versus vagotomy for 4 weeks. After 4 weeks vagotomy, mice showed significant lower serum bilirubin and BA levels compared to sham operated mice. There was no difference detectable comparing serum ALT and AP levels of both groups. *P<0.05 sham versus vagotomy.

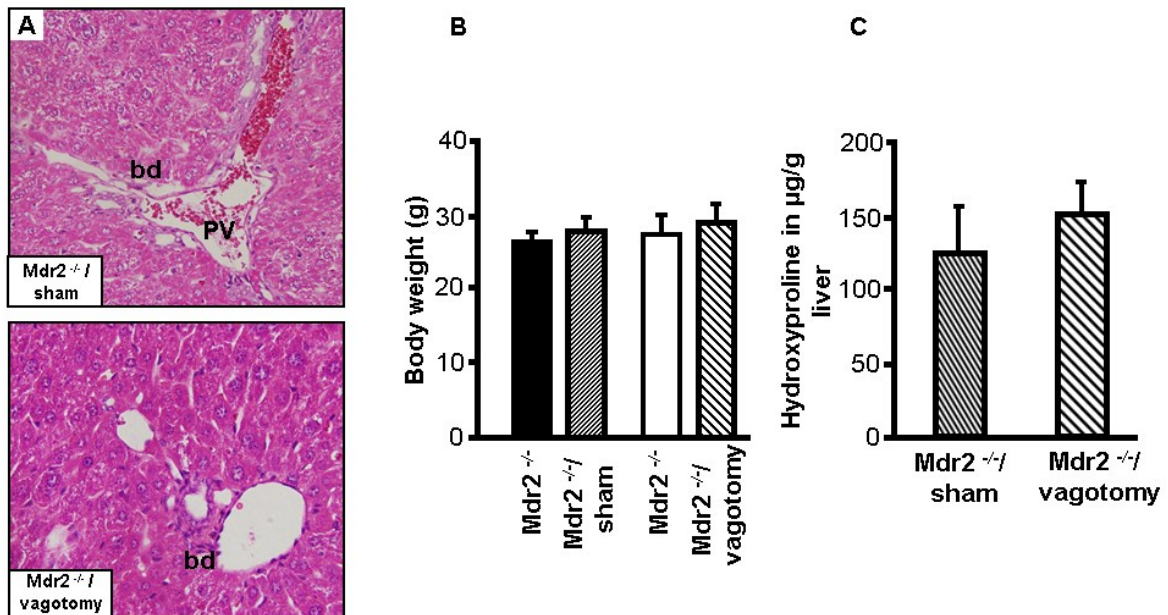


Figure 23: A) Hematoxylin / eosin staining of Mdr2^{-/-} with sham operation versus vagotomy for 4 weeks showing no difference between the two experimental groups. B) Body weight during the experiment did not differ between the two groups. C) Comparing hepatic hydroxyproline levels of Mdr2^{-/-} treated with sham operation versus vagotomy for 4 weeks showing similar liver fibrosis. Original magnification, x 20. **pv**, portal vein, **bd**, bile duct.

After 8 weeks vagotomy, $Mdr2^{-/-}$ mice showed reduced serum ALT levels compared to sham operated mice but without reaching statistical significance (531 ± 194 vs. 414 ± 68 U/l, sham vs. vagotomy, $p > 0.05$). Besides vagotomized $Mdr2^{-/-}$ mice showed significant lower serum BA compared to sham operated mice (63 ± 34 vs. 24 ± 8 $\mu\text{mol/l}$, sham vs. vagotomy, $p = 0.05$). Bilirubin levels were also decreased in $Mdr2^{-/-}$ with vagotomy compared to sham operated mice but without reaching statistical significance (0.2 ± 0.1 vs. 0.1 ± 0.03 mg/dl, sham vs. vagotomy, $p = 0.06$) (figure 24). These findings are similar to the serum parameters after 4 weeks vagotomy.

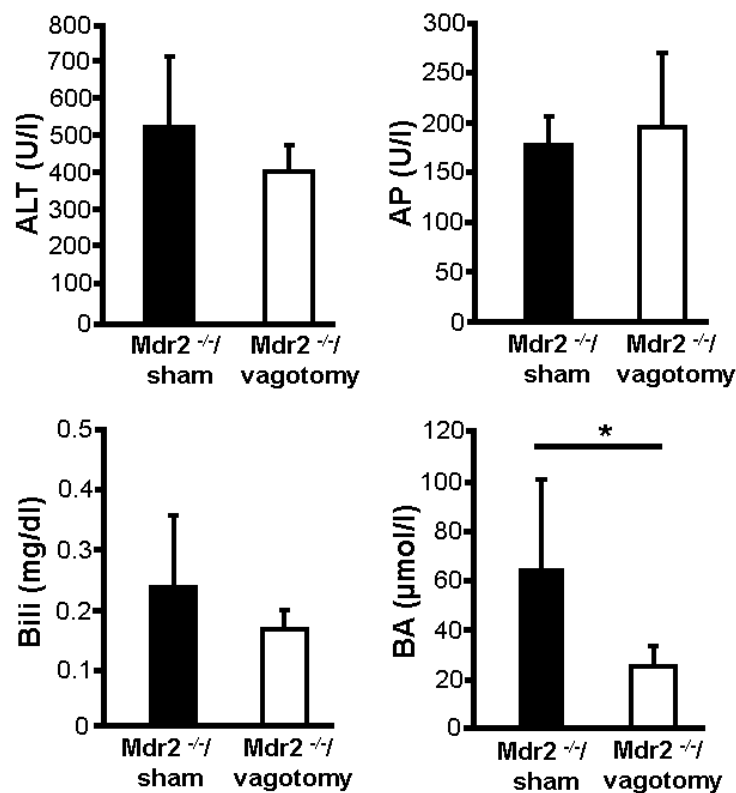


Figure 24: Serum parameters of $Mdr2^{-/-}$ treated with vagotomy for 8 weeks showing significant lower serum BA levels compared to the sham operated mice. Serum bilirubin levels were also reduced in the vaotomized animals, but without reaching statistical significane. * $P < 0.05$ vagotomy versus sham operation.

Comparing liver histology of both groups, vagotomized $Mdr2^{-/-}$ mice showed less ductular proliferation compared to sham operated mice (figure 25A). Immunohistochemical staining of bile duct epithelial cells by using anti-CK19 antibody showed reduced ductular proliferation in $Mdr2^{-/-}$ mice after 8 weeks vagotomy compared to sham operated $Mdr2^{-/-}$ (figure 25 B).

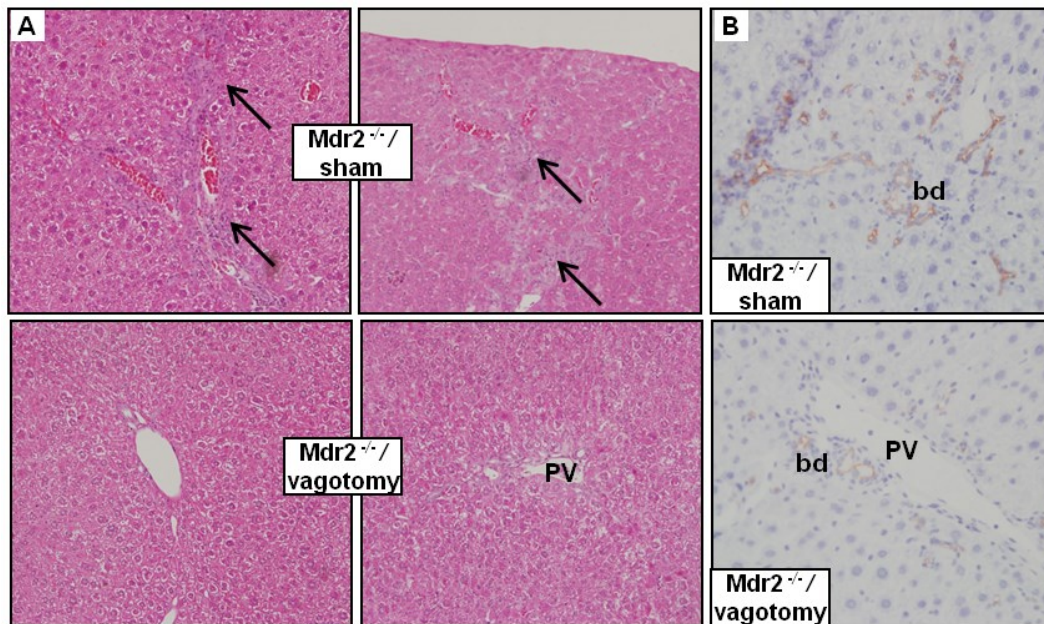


Figure 25: A) Hematoxylin / eosin staining, of $Mdr2^{-/-}$ after sham operation versus $Mdr2^{-/-}$ after vagotomy for 8 weeks. In the sham operated group more ductular proliferation was detectable compared to the vagotomized animals (black arrows). B) Immunohistochemical staining of bile duct epithelial cells by using anti-CK19 antibody. There was significant less ductular proliferation detectable in the vagotomized animals compared to the sham-operated group. Original magnification, x 20. **pv**, portal vein, **bd**, bile duct.

Besides both groups gain similar amount of BW during the experiment (figure 26A). In order to quantify liver fibrosis hepatic hydroxyproline content was determined in liver homogenates from the two groups. $Mdr2^{-/-}$ after 8 weeks vagotomy showed similar hydroxyproline levels compared to sham operated $Mdr2^{-/-}$ mice (212 ± 81 vs. 230 ± 125 μg hydroxyproline/g liver, sham vs. vagotomy, >0.05) (figure 26B). Liver weight of both groups was similar after 8 weeks hepatic vagotomy (figure 27A)

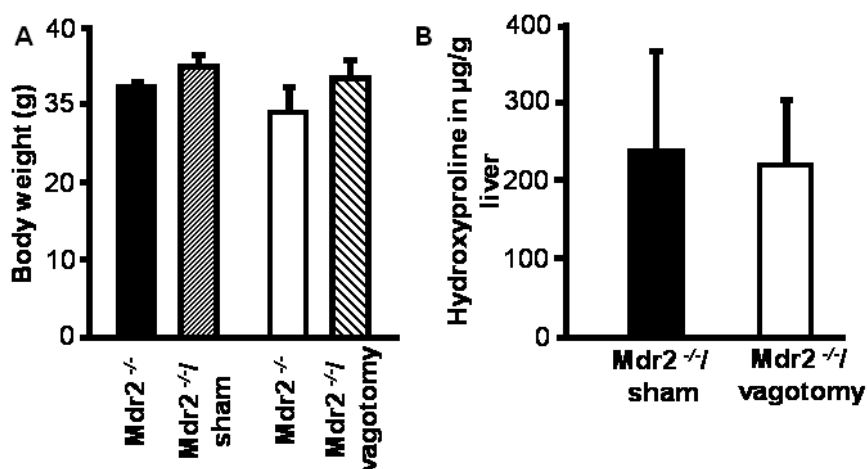


Figure 26A/B: BW and hepatic hydroxyproline of $Mdr2^{-/-}$ treated with sham operation versus vagotomy for 8 weeks showing no difference between the two groups.

As after 4 and 8 weeks serum bile acids were significantly reduced in vagotomized *Mdr2*^{-/-} mice we determined the mRNA expression of the Cyp7a1. The enzyme Cyp7a1 is the rate-limiting enzyme in the classical pathway for bile acid synthesis. It converts cholesterol into 7 α -hydroxycholesterol (187).

There was no statistical significant difference in the Cyp7a1 expression between sham operated and vagotomized *Mdr2*^{-/-} after 4 as well as after 8 weeks (0.87 \pm 0.47 vs. 0.63 \pm 0.37 μ mol/l, sham vs. vagotomy for 4 weeks, $p > 0.05$ and 1.44 \pm 1.17 vs. 0.78 \pm 0.42 μ mol/l, sham vs. vagotomy for 8 weeks, $p > 0.05$ (figure 27B).

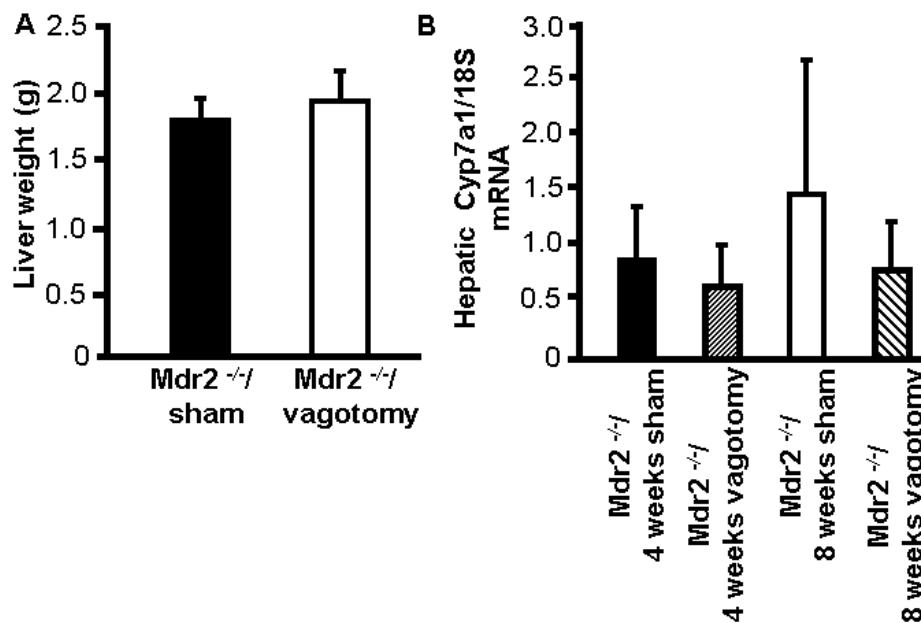


Figure 27: A) Liver weight of *Mdr2*^{-/-} after vagotomy for 8 weeks versus sham operation showing no difference. B) mRNA expression of hepatic Cyp7a1 of *Mdr2*^{-/-} after sham operation versus *Mdr2*^{-/-} after vagotomy for 4 and 8 weeks showing no difference between the two groups.

Furthermore, we assessed the hepatic mRNA expression levels of col1a1 and Mcp-1 of *mdr2*^{-/-} mice after 4 and 8 weeks sham operation versus vagotomy. No difference in gene expression of Col1a1 or Mcp-1 between the two groups was detectable (figure 28).

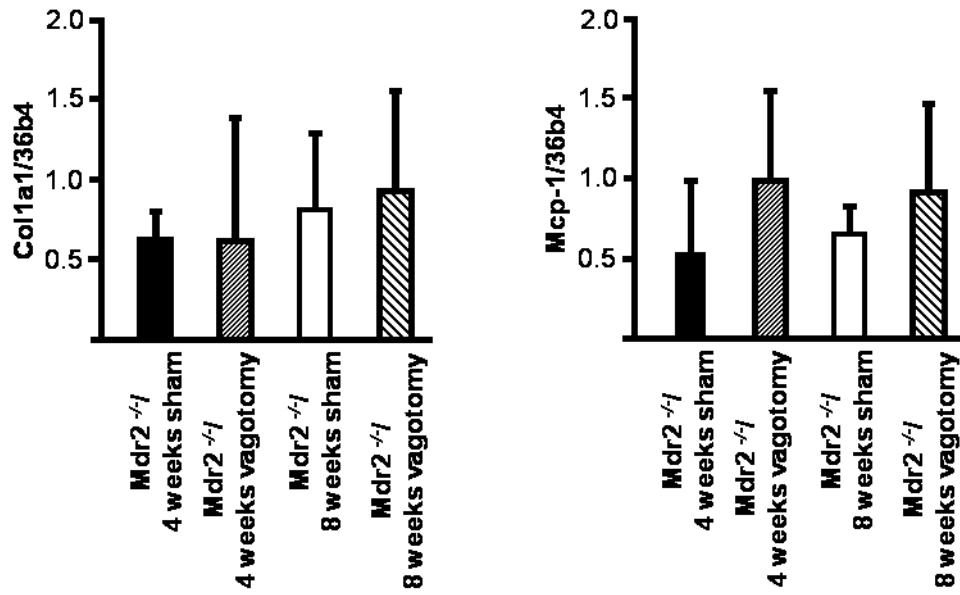


Figure 28: Hepatic mRNA expression of hepatic Col1a1 and Mcp-1 of Mdr2^{-/-} mice after sham operation versus vagotomy for 4 and 8 weeks showing no significant difference between the two groups. Expression levels of all transcripts are normalized to the housekeeping gene 36b4.

12.2.6 Comparison of liver injury in Mdr2^{-/-} after 4 weeks treatment with bethanechol (M₃-agonist) versus controls:

To determine if the liver phenotyp in Mdr2^{-/-} can be altered by treatment with a muscarinic M₃-R agonist, 4 weeks old Mdr2^{-/-} mice received bethanechol (400µg/ml) in the drinking water for 4 weeks. We compared these mice with an untreated control group. Besides we treated Mdr2^{+/+} mice with the similar experimental protocol to evaluate the effect of bethanechol in wild type mice.

In the treatment group, Mdr2^{-/-} mice showed decreased serum ALT levels compared to controls without reaching statistical significance (209.1±69.9 vs. 366.7±212.7 U/l, Mdr2^{-/-} + bethanechol vs. Mdr2^{-/-} + sham, $p>0.05$). Serum AP levels were significantly lower in the bethanechol group compared to untreated controls (122.2±26.5 vs. 170.7±12.2 U/l, Mdr2^{-/-} + bethanechol vs. Mdr2^{-/-} + sham, $p<0.05$). Furthermore bethanechol treated Mdr2^{-/-} mice showed significantly lower serum BA compared to untreated controls (18.5±15 vs. 45.6±27.2 µmol/l, Mdr2^{-/-} + bethanechol vs. Mdr2^{-/-} + sham, $p<0.05$). However, serum bilirubin levels were statistically higher in the bethanechol group compared to the control mice (0.10±0.04 vs. 0.03±0.02 mg/dl, Mdr2^{-/-} + bethanechol vs. Mdr2^{-/-} + sham, $p<0.05$) (figure 29A).

Untreated Mdr2^{-/-} showed significant higher serum AP and BA levels compared to untreated Mdr^{+/+} (serum AP 170.7±12.2 vs.93.3±9.2 U/l, Mdr2^{-/-} vs. Mdr^{+/+}, $p<0.05$ serum; serum BA 45.6±27.2 vs. 2.1±3.0 µmol/l, Mdr2^{-/-} vs. Mdr^{+/+}, $p=0.05$). Serum bilirubin as well as ALT levels were not statistical significant between the two groups (serum bilirubin 0.03±0.02 vs.0.05±0.06 mg/dl, serum ALT 366.7±221.7 vs.82.7±26.0 U/l, Mdr2^{-/-} vs. Mdr^{+/+}, $p>0.05$)(figure 29A).

During the bethanechol treatment of Mdr2^{-/-} and Mdr^{+/+} mice gained significantly more BW compared to the untreated mice (gain of body weight 0.5±1.1 vs.3.5±1.3 mg, Mdr2^{-/-} vs Mdr2^{-/-} with bethanechol, 0.6±0.9 vs.6.6±2.3 mg, Mdr^{+/+} vs Mdr^{+/+} with bethanechol, $p<0.05$ (figure 29B). Hydroxyproline levels of bethanechol treated Mdr2^{-/-} mice showed similar liver fibrosis compared to controls (figure 30B).

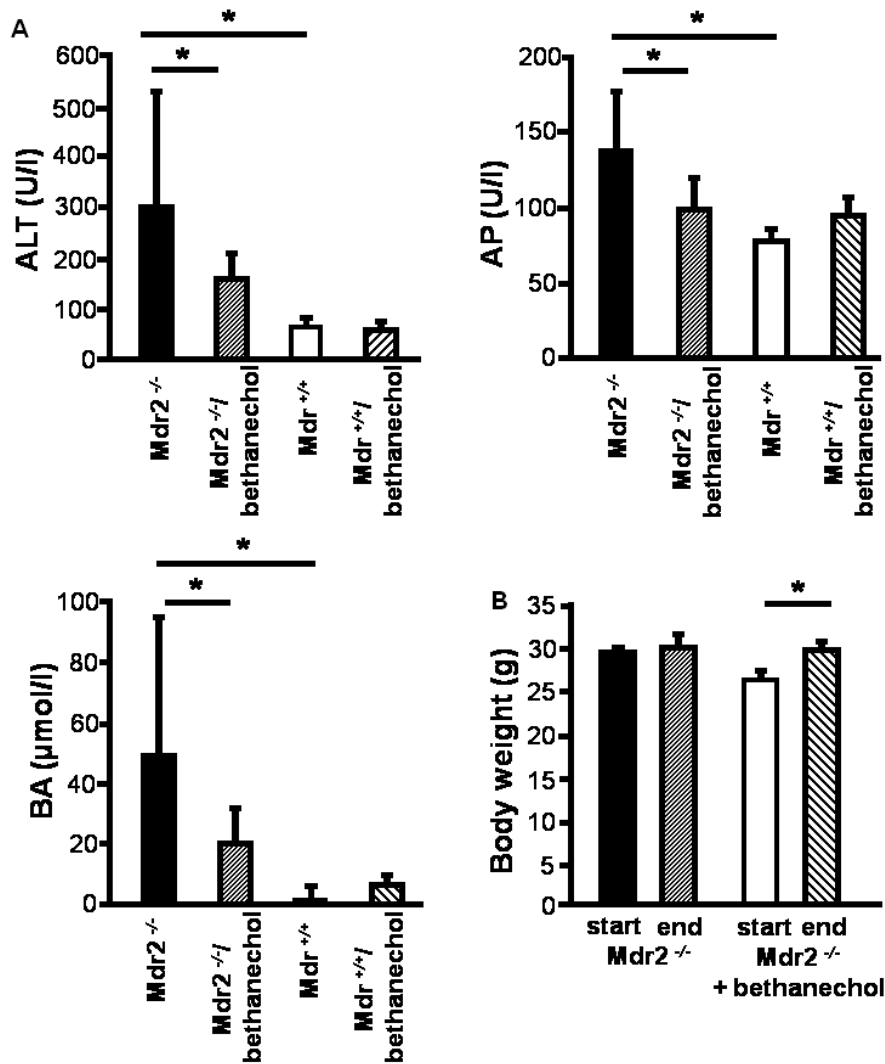


Figure 29: A) Serum parameters of 8-week-old Mdr2^{-/-} mice treated for 4 weeks with bethanechol versus untreated controls. For comparison, WT littermates (Mdr^{+/+}) were treated under the same conditions. Bethanechol-treated Mdr2^{-/-} mice showed significantly lower serum ALT, AP and BA levels compared to untreated controls. In WT littermates bethanechol treatment had no effect on liver serum parameters. B) Body weight of 8 week old Mdr2^{-/-} mice treated with bethanechol for 4 weeks versus untreated controls. Bethanechol-treated Mdr2^{-/-} mice gained significantly more BW compared to untreated controls. *p<0.05 bethanechol versus untreated Mdr2^{-/-} mice. Reproduced from Durchschein F et al. Hepatology Research. 2017; in press with permission of John Wiley & Sons Australia, ("Wiley") (1).

Comparing liver histology of both groups, the bethanechol-treated mice showed similar liver histology compared to untreated mice (figure 30A) (1).

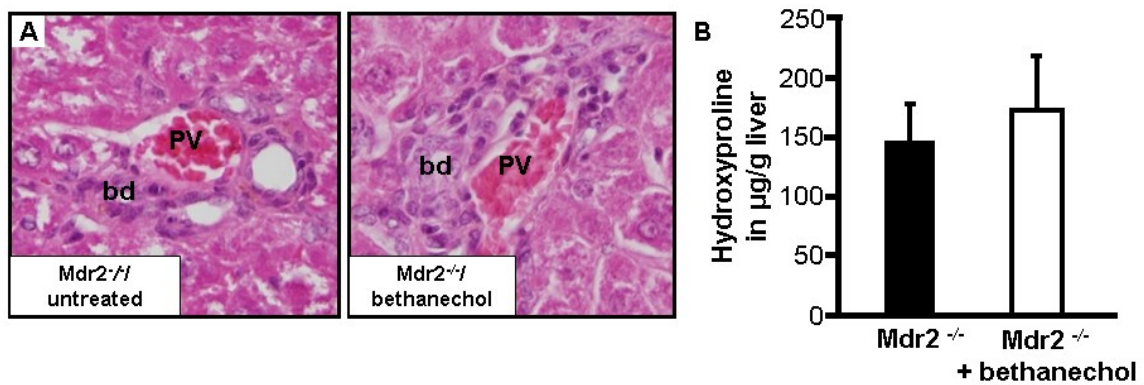


Figure 30: A) Hematoxylin/eosin staining of bethanechol-treated Mdr2^{-/-} mice showed no difference in ductular proliferation compared to untreated controls. Original magnification, x 20. **pv**, portal vein, **bd**, bile duct. B) Hepatic hydroxyproline levels were similar comparing treated versus untreated Mdr2^{-/-} mice.

Reproduced from Durchschein F et al. Hepatology Research. 2017; in press with permission of John Wiley & Sons Australia, ("Wiley") (1).

12.2.7 Comparison of bile flow in Mdr2^{-/-} mice after 1 week treatment with bethanechol (M₃-Agonist) versus untreated controls:

To determine whether bethanechol treatment alters bile flow and biliary HCO₃⁻ secretion in Mdr2^{-/-} mice, 8-week-old Mdr2^{-/-} mice and respective controls (Mdr2^{+/+} mice) received bethanechol via the drinking water for 1 week (1). Thereafter, bile flow and biliary HCO₃⁻ output was measured. In this experimental setting, bethanechol treatment did neither significantly increase bile flow nor biliary HCO₃⁻ output in Mdr2^{-/-} mice compared to untreated control mice (HCO₃⁻ output: 74.7±20.0 vs. 61.0±8.6 U/l, Mdr2^{-/-} with bethanechol vs. Mdr2^{-/-} without bethanechol, p>0.05) (1). Comparable results were obtained in WT controls (table 3) (1).

Variable	Mdr2 ^{-/-} / untreated (n=4)	Mdr2 ^{-/-} / bethanechol (n=3)	Mdr2 ^{+/+} / untreated (n=6)	Mdr2 ^{+/+} / bethanechol (n=7)
Bile flow (µl/gLW/min)	1.8 ± 0.94	2.3 ± 0,62	1.6 ± 0.37	1.6 ± 0.31
Bicarbonate output (nmol/gLW/min)	61.0 ± 8.6	74.7 ± 20.0	53.5 ± 12.4	52.9 ± 10.9

Table 3: Bile flow and biliary HCO₃⁻ output of Mdr2^{-/-} and Mdr2^{+/+} mice with and without bethanechol treatment for 1 week. Bethanechol did not result in a significant increase of bile flow and biliary HCO₃⁻ output compared to untreated controls (74.7±20.0 vs. 61.0±8.6 U/l, Mdr2^{-/-} with bethanechol vs. Mdr2^{-/-} without bethanechol, p>0.05). In Mdr2^{+/+} mice bethanechol treatment had no effect on bile flow and biliary HCO₃⁻ secretion.

Reproduced from Durchschein F et al. Hepatology Research. 2017; in press with permission of John Wiley & Sons Australia, ("Wiley") (1).

Taken together, these data indicate that the beneficial effects of bethanechol in Mdr2^{-/-} mice may not primarily be related to increased biliary HCO₃⁻ secretion (1).

12.2.8 Comparison of liver phenotyp in „aged“ $M_3-R^{-/-}$ compared to WT mice:

To determine whether $M_3-R^{-/-}$ mice develop liver injury with advancing age, we compared liver phenotypes in 50- to 56-week-old $M_3-R^{-/-}$ mice and age-matched WT mice. No statistically significant differences were detected in serum bilirubin (0.4 ± 0.03 vs. 0.3 ± 0.03 mg/dl), BA (18.1 ± 4.7 vs. 15.1 ± 8.8 μ mol/l), ALT (100.8 ± 45.0 vs. 51.3 ± 16.7 U/l) levels in WT mice compared to $M_3-R^{-/-}$ mice (all $p > 0.05$) (figure 31A) (1). Moreover, liver histology was comparable throughout the groups. Similar to WT controls, $M_3-R^{-/-}$ mice did not develop obvious liver injury at older ages (figure 31B) and did not show signs of spontaneous liver fibrosis of the biliary type (figure 31C,D) (1). Altogether these findings suggest that genetic loss of M_3-R does not alter liver morphology and function in aging mice.

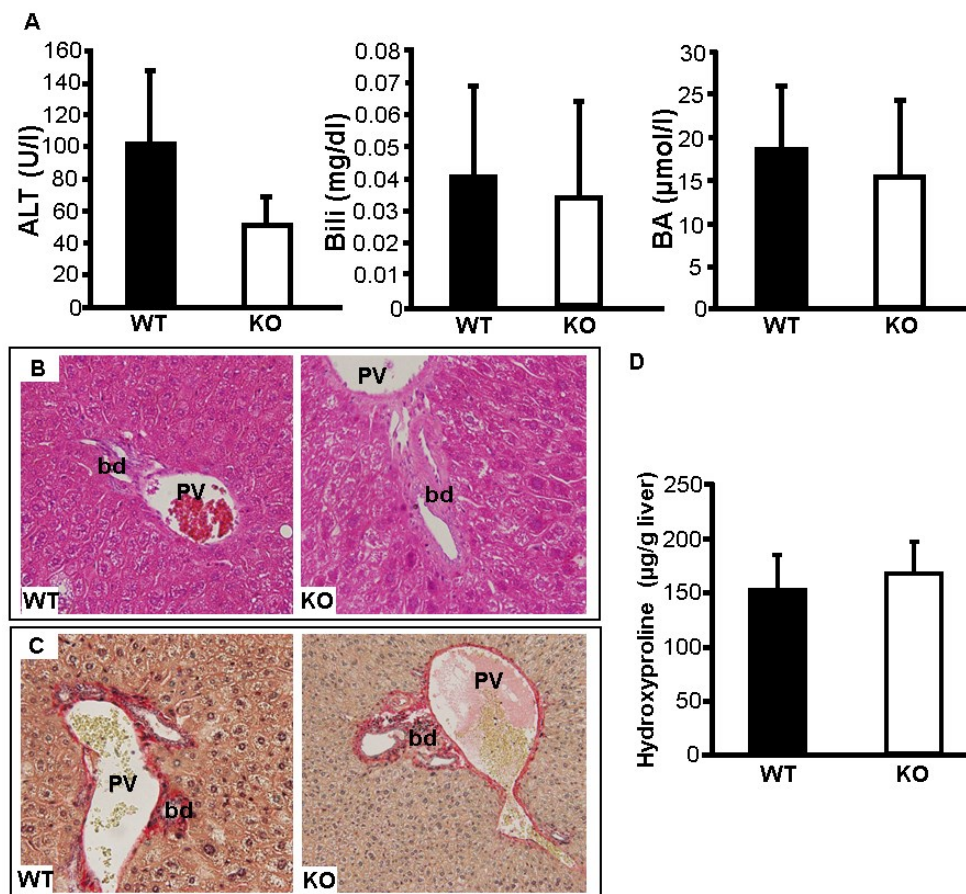


Figure 31: (A) Serum parameters of 50-week-old $M_3-R^{-/-}$ (KO) and WT mice. $M_3-R^{-/-}$ mice show similar serum ALT, bilirubin and BA levels compared to WT mice (B) Hematoxylin/Eosin and (C) Sirius Red staining of 50-week-old $M_3-R^{-/-}$ and WT mice. $M_3-R^{-/-}$ show a similar liver phenotype. Liver fibrosis, measured with Sirius red staining (C) and hydroxyproline (D), shows no difference between the two groups. **pv**, portal vein; **bd**, bile duct; Original magnification, x 20. Reproduced from Durchschein F et al. Hepatology Research. 2017; in press with permission of John Wiley & Sons Australia, ("Wiley") (1).

13 DISCUSSION

The role of hepatic innervation has been long considered as negligible, since after liver transplantation the total denervated liver continues its function without obvious problems (28). Bile ducts of transplanted livers however show significantly increased susceptibility to ischemia. This augmented vulnerability of the liver graft may be related to a lacking innervation or more specifically a defect M₃-R signaling.

The anatomical structure as well as function of hepatic innervation is despite research in last decades not fully understood. In general, the liver is innervated by afferent and efferent nerve fibers of sympathetic and parasympathetic origin (110). Besides, hepatic nerve distribution is highly species dependent with the human liver exhibiting both intraparenchymal and portal tract innervation (110). In contrast, in mice and rats hepatic innervation is evident only in portal tracts.

The parasympathetic regulation of cholangiocytes is mediated by the M₃-R, which represents the primary cholangiocyte receptor for afferent parasympathetic innervation (3). Intrahepatic parasympathetic nerve terminations release ACh, which interacts selectively with the M₃-R expressed on the basolateral membrane of cholangiocytes. This potentiates secretin-stimulated cAMP synthesis and Cl⁻/HCO₃⁻ exchanger (AE2) activity by a Ca²⁺-calcineurin-mediated modulation of adenylate cyclase with a net effect of increasing biliary HCO₃⁻ secretion (3, 127, 153). As cholangiocytes are physiologically exposed to high concentrations of potentially toxic BAs, they have developed defence mechanisms to adapt to their harsh environment. BAs are actively secreted into the canalicular lumen almost exclusively via ABCB11 (BSEP) and form mixed micelles together with phospholipids and cholesterol (188). Biliary HCO₃⁻ secretion mediated primarily via the interplay of CFTR and AE2 is an important component of bile acid-independent bile flow (189). In addition, HCO₃⁻ secretion may stabilize the glycocalyx of cholangiocytes which is sometimes referred to as the “HCO₃⁻ umbrella” (190). Consequently altered HCO₃⁻ secretion due to deficient expression or activation of M₃-R signaling may weaken this protective shield of cholangiocytes, possibly representing a first or second hit in the pathobiology of cholangiopathies. To test this hypothesis experimentally we assessed the impact of genetic loss of the M₃-R on bile formation and cholestatic liver injury in mice.

We herein demonstrate that the muscarinic M₃-R plays an essential role in bile formation. Mice lacking the M₃-R showed significantly reduced bile flow, which may originate primarily from decreased biliary HCO₃⁻ secretion. Biliary BA, phospholipid and cholesterol secretion were similar in both genotypes. Furthermore, treatment of WT mice with the parasympathetic

antagonist N-butyl scopolamine reduced biliary HCO_3^- secretion, but without reaching statistical significance.

These observations are of physiological relevance, since they underscore the importance of normal M_3 -R signaling for physiological bile formation especially for the bile acid-independent fraction of bile flow. In general, bile flow is created by an osmotic water flow in response to active solute transport (151). Both hepatocytes and cholangiocytes play a role in bile formation. In humans, hepatocytes account for approximately 60% of total bile formation. Hepatocytes can secrete BAs and other substances (like glutathione) into the ductular lumen, which is followed by osmotic entry of water. Cholangiocytes are equipped with a number of different transporters that dilute and alkalinize bile during its passage along the biliary tract (191). At their apical membrane the AE2 exchanger transports HCO_3^- into the bile duct lumen in exchange for Cl^- (151, 192). HCO_3^- secretion is followed by osmotically driven efflux of water into the ductal lumen by the aquaporine channel AQ1 (192). Consequently, the loss of the M_3 -R may result in a defective biliary HCO_3^- secretion and consequently a reduced bile flow. In addition, our findings expand earlier experimental results in dogs showing that vagotomy decreases and vagal stimulation increases bile flow (193). Pass et al. showed that vagal electrical stimulation in anaesthetized sheep enhances biliary HCO_3^- secretion (43). An interaction between secretin and ACh was shown by Alvaro et al.. He demonstrated that ACh potentiates the secretin induced biliary HCO_3^- secretion (127, 153). The interaction of secretin with its own receptor increases intracellular cAMP levels, activates PKA, and leads to an opening of CFTR Cl^- channels with activation of the $\text{Cl}^-/\text{HCO}_3^-$ exchangers (AE2), resulting in a secretion of HCO_3^- into bile (194, 195). Single ACh stimulation of cholangiocytes *in vitro* however failed to raise fluid secretion (3). Therefore, increased biliary HCO_3^- secretion by ACh takes mainly place during the digestive phase when the parasympathetic system predominates and secretin targets large bile ducts (3). According to the data of Alvaro et al. (3), it is reasonable that the reduction of biliary HCO_3^- output in M_3 -R^{-/-} mice is based on an altered secretin signaling.

To sum up, our data indicate that the M_3 -R plays a role in regulating bile flow and biliary HCO_3^- secretion. This justifies further studies to understand the function of the hepatic innervation in more detail and might help to develop new therapeutic options for cholestatic liver diseases: In our study N-butyl scopolamine treatment did not significantly reduce bile flow under the used experimental conditions. Higher concentrations however could result in significant differences in bile flow and biliary HCO_3^- output. Consequently, bile flow measurement could be repeated by using higher doses of N-butyl scopolamine. Furthermore, the influence of other M_3 -R antagonists (like darifenacin) or agonists (like carbachol,

pilocarpine) on bile flow and biliary HCO_3^- output could be tested. In our study N-butyl scopolamine was administered intraperitoneally before starting bile flow measurement. Parasympatholytics and parasympathomimetics usually have a short half-life time. To maintain a continuous drug level during bile flow measurement subcutaneous minipumps could be used for drug administration in future experiments. As ACh alone failed to increase bile flow *in vitro* (3), secretin signalling in $\text{M}_3\text{-R}^{-/-}$ mice could be investigated in more detail: For example, bile flow could be measured in $\text{M}_3\text{-R}^{-/-}$ mice after administration of bombesin (enhances secretin secretion) or somatostatin (inhibits secretin release) to evaluate secretin function in $\text{M}_3\text{-R}^{-/-}$ mice (196, 197).

In our experiments “aged” $\text{M}_3\text{-R}^{-/-}$ mice did not develop liver injury or cholestasis. There was no significant difference comparing liver phenotype of one year old $\text{M}_3\text{-R}^{-/-}$ mice and WT littermates. This is in line with earlier results showing that interruption of the hepatic parasympathetic nervous system by vagotomy alone does not affect liver phenotype (121). Rats treated with vagotomy did not develop liver injury compared to sham operated rats (117). Likewise, patients treated with truncal vagotomy for peptic ulcer disease and those undergoing liver transplantation do not develop hepatic disease despite liver denervation (28). Consequently, dysregulation of the hepatic parasympathetic nervous system without any other additional noxa seems not to affect liver phenotype.

To evaluate the effect of genetic loss of the $\text{M}_3\text{-R}$ on bile duct susceptibility to hepatic injury we compared liver damage in different cholestatic models: After 17 days DDC feeding, $\text{M}_3\text{-R}^{-/-}$ mice showed significant more liver injury compared to WT controls, accompanied by more pronounced intraductal protoporphyrin IX plugs. This changed susceptibility of $\text{M}_3\text{-R}^{-/-}$ mice may be explained by differences in biliary HCO_3^- secretion and biliary pH. Biliary HCO_3^- secretion may be an important defence mechanism for cholangiocytes to survive. The so called “ HCO_3^- umbrella”, which is created by biliary HCO_3^- secretion at the apical membrane of cholangiocytes, may play a key role in cholangiocyte protection (198). Dysfunction of any element, which is involved in biliary HCO_3^- secretion, may increase cholangiocyte susceptibility towards bile duct injury. Consequently, a defect parasympathetic innervation may weaken the “ HCO_3^- umbrella” contributing to development and progression of cholangiopathies (1). Besides changes of the biliary HCO_3^- are accompanied with changes in the biliary pH. The solubility of porphyrins critically depends on the environmental pH (199). $\text{M}_3\text{-R}^{-/-}$ mice showed more and larger porphyrin plugs in livers compared to WT littermates. Consequently, it is reasonable that aggravated liver injury in $\text{M}_3\text{-R}^{-/-}$ mice is the result of primarily diminished biliary HCO_3^- secretion and the resulting lower biliary pH (1). Such a concept however would need further experimental evidence, like measuring bile flow in both

genotypes after DDC-feeding. This approach is however technically very difficult to implement: In general, for bile flow measurement the common bile duct is ligated and the gallbladder is cannulated by a small tube for the collection of bile. The formation of porphyrin crystals after DDC-feeding can result in partial or complete occlusion of the collecting system creating imprecise values. Consequently, bile flow measurement after DDC-feeding is not feasible since the occlusion of the collecting system by porphyrin crystals would generate inaccurate data (1).

NorUDCA, a side-chainshortened derivative of ursodeoxycholic acid (UDCA), stimulates biliary HCO_3^- secretion by cholehepatic shunting (200). We showed that this increased biliary HCO_3^- output is independent of the $\text{M}_3\text{-R}$ activity. In a further step the effect of *norUDCA* in DDC-fed $\text{M}_3\text{-R}^{-/-}$ mice could be tested. Enhanced biliary HCO_3^- output in $\text{M}_3\text{-R}^{-/-}$ mice induced by *norUDCA* pretreatment may improve liver injury after DDC-feeding. This observation would strengthen the hypothesis that the increased susceptibility of $\text{M}_3\text{-R}^{-/-}$ mice is based on the reduced biliary HCO_3^- output. Finally, in our used experimental setting DDC-feeding for 17 days did not result in a significantly increased hepatic fibrosis of $\text{M}_3\text{-R}^{-/-}$ mice compared to WT littermates. In a following experiment longer treatment duration of DDC-feeding could result in a significant difference in liver fibrosis between the two genotypes.

To verify the increased susceptibility of $\text{M}_3\text{-R}^{-/-}$ mice to cholestasis, we compared both genotypes in a second cholestatic model. After LCA-feeding $\text{M}_3\text{-R}^{-/-}$ mice seem to be protected compared to WT littermates. The response of LCA-fed $\text{M}_3\text{-R}^{-/-}$ mice seem to foil our results obtained in the DDC-model at a first glance, since one may extrapolate that liver toxicity of LCA-feeding would also be aggravated due to defect biliary HCO_3^- secretion in $\text{M}_3\text{-R}^{-/-}$ mice. However, one has to remind the pathomechanisms leading LCA-induced liver injury. Upon LCA feeding a critical increase of intraductular pressure can be observed due to obstructive LCA crystals (172). This results in rupture of the canals of Herring with exposure of hepatocytes to BA concentrations like in the bile duct lumen causing hepatocyte necrosis referred to as bile infarcts as previously described in detail (172). A reduction of bile flow due to the loss of the parasympathetic innervation presumably decreases ductular pressure and consequently reduces the number of leaky bile ducts in LCA-fed $\text{M}_3\text{-R}^{-/-}$ mice. In addition, a taurine conjugate of LCA was previously shown to activate the $\text{M}_3\text{-R}$ (183, 184). Lithocholylcholine, a created molecule that combines the steroid nucleus of lithocholic acid with a choline part as is present in ACh, acts as a muscarinic receptor antagonist (184). Consequently, LCA feeding may activate the $\text{M}_3\text{-R}$ and initially induce bile flow solely in WT mice. Stimulation of the $\text{M}_3\text{-R}$ may result in an added rise of bile flow and lead to a further increase of bile duct pressure in WT mice. Consequently this may primarily explain the

higher rate of ruptured canals of Herring leading to more pronounced bile infarcts in WT littermates compared to $M_3-R^{-/-}$ mice in response to LCA-feeding.

After LCA-feeding $M_3-R^{-/-}$ mice showed significant lower degree of ductular proliferation compared to WT littermates. This may also be related to differences in bile flow and biliary pressure, which represent the main trigger of ductular proliferation in obstructive cholestasis (201). LeSage et al. demonstrated, that rats treated with CBDL and vagotomy showed significant lower ductular proliferation compared to CBDL rats without vagotomy (CBDL is the classical model of ductal proliferation increasing secretin receptor gene expression on cholangiocytes) (201). In this study vagotomized animals showed enhanced cholangiocytes' apoptosis and decreased expression levels of the M_3-R and secretin receptor (SR) expressed on cholangiocyte (121). Besides, the parasympathetic nervous system seems to play a role in liver regeneration (118). Kato et al. observed an impaired hepatic proliferation after partial hemihepatectomy and simultaneous vagotomy in rats (120, 202). Also in humans the number of oval cells in the canal of Hering and the number of atypical reactive ductular cells are significantly decreased in a transplanted denervated liver with hepatitis compared to a nontransplanted liver with viral hepatitis (202). Hepatic progenitor cells (HPC), which play a key role in hepatic regeneration, also express the M_3-R (118). Consequently, differences in ductular proliferation between LCA-fed WT and $M_3-R^{-/-}$ mice might be linked to difference in ductular pressure and/or functions of HPCs.

To sum up, in the LCA-fed mouse model WT littermates seem to be more susceptible compared to $M_3-R^{-/-}$ mice. This difference may be based on alteration in bile flow and biliary pressure. To test this hypothesis in more detail further experiments are needed, like measuring bile flow in WT mice after LCA-feeding. LCA may activate the M_3-R resulting in an enhanced bile flow compared to untreated controls. Besides next to LCA (183, 184), other BAs also seem to modulate parasympathetic function. Taurocholic acid feeding prevented the vagotomy-induced reduction of proliferation in cholangiocytes in CBDL rats (203). The same result was observed after UDCA and tauro-UDCA feeding of vagotomized CBDL rats (204). In humans, the adjuvant treatment with UDCA reduces allograft rejection after liver transplantation (205). These data argue for a modulation of the parasympathetic nervous system by BAs. In a next step $M_3-R^{-/-}$ mice and WT controls could be pretreated with UDCA before comparing liver phenotype in different cholestatic models. These experiments could help to determine if the observed effect of UDCA in vagotomized CBDL rats is reproducible in $M_3-R^{-/-}$ mice. Besides bile flow and biliary HCO_3^- secretion could be measured to see if UDCA treatment changes bile composition in $M_3-R^{-/-}$ mice. To progress on the difference in ductular proliferation between LCA-fed WT and $M_3-R^{-/-}$ mice, apoptosis of cholangiocytes and

HPC activation could be determined in both genotypes by using immunohistochemistry and/or immunofluorescence (for example using anti-activated caspase-3 antibody, anti-cytokeratin-19 (CK-19) and anti-epithelial cell adhesion molecule (EpCAM) antibodies (markers of apoptosis, bile ducts and HPCs).

We also determined the susceptibility of $M_3-R^{-/-}$ mice in response to 5 days CBDL. However, in this cholestatic model our results were ambiguous. In the first experiments $M_3-R^{-/-}$ mice showed significant more liver injury compared to WT mice. We repeated the experiment four times and the initial increased susceptibility of $M_3-R^{-/-}$ mice was not reproducible in the last two passages. We could not detect a sufficient explanation for this finding. On the one hand, $M_3-R^{-/-}$ mice should be more susceptible to liver injury caused by a debilitated “ HCO_3^- umbrella”. On the other hand a critical increase of intraductular pressure can be observed during CBDL. This results in rupture of the canals of Hering with exposure of hepatocytes to high BA concentrations derived from bile leaking into the liver parenchyma (172). The reduced bile flow and thus decreased bile duct pressure in $M_3-R^{-/-}$ mice could be protective after CBDL resulting in less liver injury compared to WT controls.

Taken together, the role of the M_3-R in the cholestatic model of CBDL is still unclear. No technical problems appeared during the operative intervention in all four independent experiments since CBDL is a frequent performed procedure in our laboratory. For further studies, the duration of the CBDL can be extended in order to find significant differences in liver injury and/or hepatic fibrosis between the two genotypes.

Muscarinic receptors are therapeutic targets in the pharmacological therapy for different diseases like chronic obstructive pulmonary disease (206), glaucoma (207) or Sjögren’s syndrome (208). To test the effect of a muscarinic receptor agonist in cholestatic liver diseases, we compared liver injury of $Mdr2^{-/-}$ mice treated with bethanechol versus untreated controls. After 4 weeks of treatment $Mdr2^{-/-}$ mice showed less liver injury as evidenced by the decline of liver serum parameters compared to untreated controls. However no significant effect on liver fibrosis was detectable and there was no significant increase in bile flow and biliary HCO_3^- output after 1 week bethanechol treatment (1). Consequently the observed beneficial effects of bethanechol may not primarily be related to increased biliary HCO_3^- secretion (1). As the M_3-R is also expressed on inflammatory cells, like T- and B-lymphocytes, neutrophils as well as macrophages, bethanechol may modulate the inflammatory response (209) also referred to as “anti-inflammatory cholinergic axis” (discussed below) (1, 82). Therefore it is attractive to speculate that the observed beneficial bethanechol effects may be related to antiinflammatory properties of M_3-R activation (1).

Consequently, targeting the muscarinic receptor on cholangiocytes may represent a new option in the therapy of cholestatic liver diseases. Such a concept however would need further experimental evidence, like treating $Mdr2^{-/-}$ mice with different concentrations of the muscarinic agonist bethanechol. Besides the treatment duration can be extended to investigate the long-term effect of this agonist on hepatic injury and liver fibrosis. Other M_3 -R agonists (like carbachol, pilocarpine) and also M_3 -R antagonists (like darifenacin) can be used to determine the therapeutic role of the M_3 -R in cholangiopathies. Next to the $Mdr2^{-/-}$ mouse model, “gain and loss of function” of the M_3 -R can be studied in other cholestatic mouse models.

One limitation of our study is the administration of the used M_3 -R agonist. We have chosen bethanechol because it can be administered in the drinking water. Mice were freely allowed to drink water with or without bethanechol (without gavage) for 4 weeks (1, 182). Volumes of water consumed by each group were measured weekly and were not significantly different between the groups during the study period (1). Differences in application rate between the single animals however cannot be totally excluded. Parasympatholytics and parasympathomimetics usually have a short half-life time. Consequently, the use of subcutaneous minipumps could help to maintain a continuous drug level and represent a better way of administration.

Next to alterations in bile flow, changes in immune response could be a further hypothesis to explain the altered susceptibility of M_3 -R^{-/-} mice in the different cholestatic models. The parasympathetic nervous system can alter the immune system (209, 210). The so called “anti-inflammatory cholinergic axis” describes the interaction between neurotransmitters and inflammatory cells expressing nicotinic as well as muscarinic receptors (82). The neurotransmitter ACh, released by nerve terminals, can attenuate inflammatory processes by paracrine and/or autocrine mechanisms (209, 211). As the M_3 -R is expressed on inflammatory cells like T- and B-lymphocytes, neutrophils as well as macrophages (209), activation or loss of this receptor may modulate inflammatory response. This effect varies among different tissues. In the bronchial system for example, activation of the muscarinic receptors results in an enhanced inflammatory response. In contrast, activation of the muscarinic receptors in the colon leads to an attenuated inflammation response (80). As ACh can react with both nicotinic and muscarinic receptors, it is difficult to determine whether the effect reflects its interaction with muscarinic and/or nicotinic receptors (212). Consequently loss of the parasympathetic nervous system may alter hepatic inflammatory response in cholangiopathies. This hypothesis however needs further experimental evidence, like analysing inflammatory response in WT and M_3 -R^{-/-} mice in different cholestatic models. For

example, the accumulation of granulocytes and monocytes/macrophages after LCA-feeding can be characterized in the two genotypes by using immunohistochemistry for CD11b⁺ and F4/80⁺.

In order to evaluate the effect of the parasympathetic nervous system in cholestatic liver diseases in general, we performed vagotomy in different cholestatic models. Results of these experiments however are not totally comparable with those generated in M₃-R^{-/-} mice. The M₃-R^{-/-} mouse is a genetically engineered mouse model with a systemic inactive M₃-R gene. In contrast, hepatic vagotomized mice have exclusively an interrupted hepatic parasympathetic innervation. Additionally, hepatic vagotomy may change functions of other parasympathetic receptors in the liver, like other muscarinic receptors or nicotinic receptors, which are all involved in inflammatory response. Furthermore, the disconnection of parasympathetic nerve fibers by vagotomy affects other neurotransmitters than ACh, which are also localized in parasympathetic nerve fibers. Consequently, the results gained in M₃-R^{-/-} mice are not automatically comparable to those generated after hepatic vagotomy.

First, we performed hepatic vagotomy in WT mice and compared liver injury to sham operated controls after 17 days DDC-feeding. Hepatic injury of vagotomized WT mice was similar to sham operated controls. These findings are comparable to results of Hajiasgharzadeh et al. who performed selective hepatic vagotomy in long-term CBDL rats (213). Vagotomized animals showed no difference to sham operated rats in the development of portal hypertension, hepatic fibrosis or inflammation (213). Heider et al. reported that an anterior trunk vagotomy did not raise the risk of inflammatory response in surgical patients with complicated ulcer diseases (214). Cholangiopathies are characterized by a dysbalance of cholangiocyte's proliferation and apoptosis leading to chronic cholestasis, ductopenia and hepatic fibrosis (204). The parasympathetic nervous system seems to alter this dysbalance. Vagotomized CBDL rats showed less ductular proliferation compared to sham operated CBDL rats (120, 202). We performed hepatic vagotomy in Mdr2^{-/-} mice and compared liver injury to sham operative controls after 4 and 8 weeks. Hepatic vagotomy for 8 weeks resulted in a reduced hepatic injury in Mdr2^{-/-} mice as evidenced by the decline of liver serum parameters compared to sham operated controls. Besides, vagotomized mice showed less ductular proliferation compared to sham operated controls. As this effect was more pronounced after 8 weeks compared to 4 weeks, loss of the parasympathetic innervation may alter hepatic injury in a time-dependent manner. To study the effect of hepatic vagotomy in Mdr2^{-/-} mice in more detail, the duration of the experiment could be extended. A longer time period of hepatic vagotomy may show differences in hepatic injury more obviously and may even result in significant alterations of hepatic fibrosis. Besides, earlier studies revealed

that vagotomy in dogs decreases bile flow (193). Consequently, bile flow could be measured in vagotomized $Mdr2^{-/-}$ mice and sham operated controls to determine if changes in bile flow cause the observed difference in hepatic phenotype. Furthermore, the effect of hepatic vagotomy in other cholestatic mouse models, like DDC- or LCA-feeding, could be studied. To progress on the observed difference in ductular proliferation between vagotomized and sham-operated $mdr2^{-/-}$ mice, apoptosis and proliferation of cholangiocytes could be determined in both groups (for example by using immunohistochemical staining for caspase-3, CK-19 and EpCAM).

One limitation of our vagotomy experiments is the missing verification of a complete hepatic parasympathetic denervation. As hepatic innervation is a complex system with a high interspecies and individual variability, in some mice hepatic vagotomy may be incomplete. Some hepatic nerves also derive from the right phrenic nerve. Therefore, it is possible that not all nerve fibers were cutted during the hepatic vagotomy.

To sum up, the M_3 -R seems to play an important role in regulating bile flow and composition. In the cholestatic model of DDC-feeding M_3 -R $^{-/-}$ mice showed increased susceptibility compared to WT littermates. After treatment with a M_3 -R agonist liver injury in $Mdr2^{-/-}$ mice improved compared to that in untreated controls (1). After LCA-feeding M_3 -R $^{-/-}$ mice however seemed to be protected. The herein observed significant difference in cholestatic liver injury between M_3 -R $^{-/-}$ and WT mice argues for a significant effect of the M_3 -R in modulating cholestatic liver injury (1). Dysfunction of the parasympathetic nervous system may be a “second” hit which aggravates liver injury. These findings may have important clinical relevance for the pathophysiology of the transplanted and so denervated liver, where ischemic insults against intrahepatic bile ducts are not adequately counteracted, due to the lack of nerve modulation of cholangiocyte functions. With the increasing number of individuals affected by cholestatic liver diseases and the limited therapeutic options, the role of the autonomic nervous system in liver regeneration is becoming more prominent. Further studies are necessary to evaluate the role and mechanisms of action by which the neurotransmitters may regulate cholangiocyte functions in cholestasis. Future research should be directed towards an understanding of the neurotransmitters, signalling molecules and cell types innervated by the hepatic nervous system. These processes are potential drug targets for clinical practice. Furthermore, creating hybrid molecules of BAs and ACh might provide new selective muscarinic receptor ligands as a therapeutic option (184). The manipulation of nerve impulses and synaptic mediators can possibly allow direct control over hepatic function.

Outlook: Cholangiocytes are major victims in human cholangiopathies. Inflammation or relative ischemia of bile ducts (e.g. in PBC, PSC, SSC-CIP) may alter M₃-R function of these cells, which may render bile ducts more susceptible. M₃-R activation may be impaired due to pericholangitis and a thickened periductal fibrotic shield leading to altered innervation of bile ducts and cholangiocytes. Consequently altered M₃-R function may represent a causative factor in cholangiopathies, may modify disease progression, and most importantly may represent a therapeutic target. Aim of next experiments could be to determine M₃-R tissue distribution in prototypic human cholangiopathies at different stages of diseases (e.g. PBC, PSC), disease controls (CHC, CHB, ASH), and normal liver tissue by immunohistochemistry. Additionally, protein expression levels could be analyzed by Western blotting. Since M₃-R expression is primarily awaited to be altered in interlobular and lobular bile ducts, M₃-R expression could be characterized in explant liver tissue and surgical resected liver tissue. As the M₃-R might also be involved in the development of cholangiocarcinoma (CCC) surgical resected liver tissue from CCC and HCC, especially tumour margins, could be analysed. Besides analysing M₃-R expression pattern, parasympathetic nerve fibres could be stained using specific antibodies against neurofilaments and could be compared to disease controls and normal liver tissue.

Our preliminary data on reduced biliary bicarbonate secretion in M₃-R^{-/-} mice and increased susceptibility of M₃-R^{-/-} mice in response to DDC-feeding strongly argue for a central role of M₃-R signaling in cholangiopathies and justify more detailed studies. However, the hepatic innervation is a very complex system with a high inter- and intraspecies differences. As in the liver also other neurotransmitters like noradrenalin or dopamine are presented, they may be also involved in the regulation of hepatic metabolism and liver disease. Cholangiocytes also express the dopamine (D₂) receptor and receptors of the adrenergic system. Since activation of these receptors results in the inhibition of the secretin-induced choleresis and consequently reduced biliary bicarbonate secretion, usage of high dose vasoactive drugs may increase the vulnerability of bile ducts in critically ill patients. Such a concept could be investigated with the aid of catecholamine application via mini pumps in the models outlined above with and without selective hepatic denervation. In addition, nicotinic receptor malfunction may prone the liver to cholangiopathies via an increased susceptibility for apoptotic liver injury or direct effects on bile flow and composition. Such a concept could be studied with the aid of respective gene knock-out animals and the application of nicotine via minipumps in our model systems.

Acknowledgment: I want to thank Dr. Wolfgang Erwa (Graz) and colleagues for performing liver tests and Judith Gumhold, Dagmar Silbert, Andrea Deutschmann, Dietmar Glänzer, Caroline Rast and Katharina Kinslechner for excellent technical assistance.

This doctoral thesis is affiliated with the Doctoral School General and Clinical Pathophysiology of the Medical University of Graz with no financial support.

12 REFERENCES

1. Durchschein F, Krones E, Pollheimer M, Zollner G, Wagner M, Raufmann JP, Fickert P: Genetic loss of the muscarinic m3 receptor (M₃-R) markedly alters bile formation and cholestatic liver injury in mice. *Hepatology Research*. 2017; in press
2. Konturek PC, Konturek SJ. The history of gastrointestinal hormones and the Polish contribution to elucidation of their biology and relation to nervous system. *Journal of physiology and pharmacology : an official journal of the Polish Physiological Society*. 2003;54 Suppl 3:83-98.
3. Alvaro D, Alpini G, Jezequel AM, Bassotti C, Francia C, Fraioli F, et al. Role and mechanisms of action of acetylcholine in the regulation of rat cholangiocyte secretory functions. *The Journal of clinical investigation*. 1997;100(6):1349-62.
4. Yoneda M, Watanobe H, Terano A. Central regulation of hepatic function by neuropeptides. *Journal of Gastroenterology*. 2001;36(6):361-7.
5. Yokoyama HO, Wilson ME, Tsuboi KK, Stowell RE. Regeneration of Mouse Liver after Partial Hepatectomy *Cancer Research* 1953 13 (1):80-5
6. Vatamaniuk MZ, Horyn OV, Vatamaniuk OK, Doliba NM. Acetylcholine affects rat liver metabolism via type 3 muscarinic receptors in hepatocytes. *Life sciences*. 2003;72(16):1871-82.
7. Ohtake M, Sakaguchi T, Yoshida K, Muto T. Hepatic branch vagotomy can suppress liver regeneration in partially hepatectomized rats. *HPB surgery : a world journal of hepatic, pancreatic and biliary surgery*. 1993;6(4):277-86.
8. Kiba T, Tanaka K, Numata K, Hoshino M, Inoue S. Facilitation of liver regeneration after partial hepatectomy by ventromedial hypothalamic lesions in rats. *Pflugers Archiv : European journal of physiology*. 1994;428(1):26-9.
9. Teff KL. Visceral nerves: vagal and sympathetic innervation. *JPEN Journal of parenteral and enteral nutrition*. 2008;32(5):569-71.
10. Miyazawa Y, Fukuda Y, Imoto M, Koyama Y, Nagura H. Immunohistochemical studies on the distribution of nerve fibers in chronic liver diseases. *The American journal of gastroenterology*. 1988;83(10):1108-14.
11. Berthoud HR, Fox EA, Powley TL. Localization of vagal preganglionics that stimulate insulin and glucagon secretion. *The American journal of physiology*. 1990;258(1 Pt 2):R160-8.
12. Forssmann WG, Ito S. Hepatocyte innervation in primates. *The Journal of cell biology*. 1977;74(1):299-313.
13. Skaaring P, Bierring F. On the intrinsic innervation of normal rat liver. *Histochemical and scanning electron microscopical studies*. *Cell and tissue research*. 1976;171(2):141-55.
14. Timmermans JP, Geerts A. Nerves in liver: superfluous structures? A special issue of *The Anatomical Record* updating our views on hepatic innervation. *Anatomical record Part B, New anatomist*. 2005;282(1):4.
15. Kiba T. The role of the autonomic nervous system in liver regeneration and apoptosis-recent developments. *Digestion*. 2002;66(2):79-88.
16. Roskams T, Cassiman D, De Vos R, Libbrecht L. Neuroregulation of the neuroendocrine compartment of the liver. *The anatomical record Part A, Discoveries in molecular, cellular, and evolutionary biology*. 2004;280(1):910-23.
17. Jensen KJ, Alpini G, Glaser S. Hepatic nervous system and neurobiology of the liver. *Comprehensive Physiology*. 2013;3(2):655-65.
18. Abdel-Misih SR, Bloomston M. Liver anatomy. *The Surgical clinics of North America*. 2010;90(4):643-53.
19. Tiniakos DG, Lee JA, Burt AD. Innervation of the liver: morphology and function. *Liver*. 1996;16(3):151-60.
20. Balemba OB, Salter MJ, Mawe GM. Innervation of the extrahepatic biliary tract. *The anatomical record Part A, Discoveries in molecular, cellular, and evolutionary biology*. 2004;280(1):836-47.

21. Akiyoshi H, Gonda T, Terada T. A comparative histochemical and immunohistochemical study of aminergic, cholinergic and peptidergic innervation in rat, hamster, guinea pig, dog and human livers. *Liver*. 1998;18(5):352-9.
22. Thurman, RG, Kauffman, FC, and Jungermann, K. Regulation of hepatic metabolism. Intra- and intercellular compartmentation. Springer Verlag; 2012:3-25.
23. Streba LA, Vere CC, Ionescu AG, Streba CT, Rogoveanu I. Role of intrahepatic innervation in regulating the activity of liver cells. *World journal of hepatology*. 2014;6(3):137-43.
24. Uyama N, Geerts A, Reynaert H. Neural connections between the hypothalamus and the liver. *The Anatomical Record Part A: Discoveries in Molecular, Cellular, and Evolutionary Biology*. 2004;280A(1):808-20.
25. Shimazu T. Neuronal regulation of hepatic glucose metabolism in mammals. *Diabetes/metabolism reviews*. 1987;3(1):185-206.
26. Shimazu T. Reciprocal innervation of the liver: its significance in metabolic control. *Advances in metabolic disorders*. 1983;10:355-84.
27. Shimazu T, Ogasawara S. Effects of hypothalamic stimulation on gluconeogenesis and glycolysis in rat liver. *The American journal of physiology*. 1975;228(6):1787-93.
28. Boon AP, Hubscher SG, Lee JA, Hines JE, Burt AD. Hepatic reinnervation following orthotopic liver transplantation in man. *The Journal of pathology*. 1992;167(2):217-22.
29. Shimazu T. Central nervous system regulation of liver and adipose tissue metabolism. *Diabetologia*. 1981;20 Suppl:343-56.
30. Berthoud HR, Kressel M, Neuhuber WL. An anterograde tracing study of the vagal innervation of rat liver, portal vein and biliary system. *Anatomy and embryology*. 1992;186(5):431-42.
31. Magni F, Carobi C. The afferent and preganglionic parasympathetic innervation of the rat liver, demonstrated by the retrograde transport of horseradish peroxidase. *Journal of the autonomic nervous system*. 1983;8(3):237-60.
32. Lechner SG, Markworth S, Poole K, Smith ES, Lapatsina L, Frahm S, et al. The molecular and cellular identity of peripheral osmoreceptors. *Neuron*. 2011;69(2):332-44.
33. May M, Gueler F, Barg-Hock H, Heiringhoff KH, Engeli S, Heusser K, et al. Liver afferents contribute to water drinking-induced sympathetic activation in human subjects: a clinical trial. *PloS one*. 2011;6(10):e25898.
34. Niiijima A. Afferent impulse discharges from glucoceptors in the liver of the guinea pig. *Annals of the New York Academy of Sciences*. 1969;157(2):690-700.
35. McCuskey RS. Anatomy of efferent hepatic nerves. *The anatomical record Part A, Discoveries in molecular, cellular, and evolutionary biology*. 2004;280(1):821-6.
36. Ueno T, Tanikawa K. Intralobular innervation and lipocyte contractility in the liver. *Nutrition*. 1997;13(2):141-8.
37. Balabaud, C, Boulard, A, Quinton, A et al. Light and transmission electron microscopy of sinusoids in human liver¹⁴ P Bioulac-Sage, C Balabaud (Eds.) *Sinusoids in Human Liver: Health and Disease*. Kupffer Cell Foundation, Rijswijk, The Netherlands; 1988: 87-110.
38. Bioulac-Sage P, Lafon ME, Saric J, Balabaud C. Nerves and perisinusoidal cells in human liver. *Journal of hepatology*. 1990;10(1):105-12.
39. Akiyoshi H. Ultrastructure of cholinergic innervation in the cirrhotic liver in guinea pigs. *Virchows Archiv B Cell Pathology Zell-pathologie*. 1989;57(1):81-90.
40. Strazzabosco M, Fabris L. Functional anatomy of normal bile ducts. *Anatomical record*. 2008;291(6):653-60.
41. Terada T, Nakanuma Y. Innervation of intrahepatic bile ducts and peribiliary glands in normal human livers, extrahepatic biliary obstruction and hepatolithiasis. An immunohistochemical study. *Journal of hepatology*. 1989;9(2):141-8.
42. Jones RS, Grossman MI. Choleric effects of secretin and histamine in the dog. *The American journal of physiology*. 1969;217(2):532-5.
43. Pass M, Heath T. Effect of electrical stimulation of the vagus nerves on bile secretion in Anaesthetized sheep. *Australian journal of biological sciences*. 1976;29(4):351-5.

44. Takahashi A, Ishimaru H, Ikarashi Y, Kishi E, Maruyama Y. Effects of hepatic nerve stimulation on blood glucose and glycogenolysis in rat liver: studies with in vivo microdialysis. *Journal of the autonomic nervous system*. 1996;61(2):181-5.
45. Oben JA, Yang S, Lin H, Ono M, Diehl AM. Norepinephrine and neuropeptide Y promote proliferation and collagen gene expression of hepatic myofibroblastic stellate cells. *Biochemical and biophysical research communications*. 2003;302(4):685-90.
46. Hamasaki K, Nakashima M, Naito S, Akiyama Y, Ohtsuru A, Hamanaka Y, et al. The sympathetic nervous system promotes carbon tetrachloride-induced liver cirrhosis in rats by suppressing apoptosis and enhancing the growth kinetics of regenerating hepatocytes. *Journal of gastroenterology*. 2001;36(2):111-20.
47. Oben JA, Roskams T, Yang S, Lin H, Sinelli N, Li Z, et al. Sympathetic nervous system inhibition increases hepatic progenitors and reduces liver injury. *Hepatology*. 2003;38(3):664-73.
48. Glaser S, Alvaro D, Francis H, Ueno Y, Marucci L, Benedetti A, et al. Adrenergic receptor agonists prevent bile duct injury induced by adrenergic denervation by increased cAMP levels and activation of Akt. *American journal of physiology Gastrointestinal and liver physiology*. 2006;290(4):G813-26.
49. LeSage GD, Alvaro D, Glaser S, Francis H, Marucci L, Roskams T, et al. Alpha-1 adrenergic receptor agonists modulate ductal secretion of BDL rats via Ca(2+)- and PKC-dependent stimulation of cAMP. *Hepatology*. 2004;40(5):1116-27.
50. Nathanson MH, Burgstahler AD, Mennone A, Boyer JL. Characterization of cytosolic Ca²⁺ signaling in rat bile duct epithelia. *The American journal of physiology*. 1996;271(1 Pt 1):G86-96.
51. Glaser S, Alvaro D, Roskams T, Phinizy JL, Stoica G, Francis H, et al. Dopaminergic inhibition of secretin-stimulated choleresis by increased PKC-gamma expression and decrease of PKA activity. *American journal of physiology Gastrointestinal and liver physiology*. 2003;284(4):G683-94.
52. Lundberg JM, Terenius L, Hokfelt T, Martling CR, Tatemoto K, Mutt V, et al. Neuropeptide Y (NPY)-like immunoreactivity in peripheral noradrenergic neurons and effects of NPY on sympathetic function. *Acta physiologica Scandinavica*. 1982;116(4):477-80.
53. Burt AD, Tiniakos D, MacSween RN, Griffiths MR, Wisse E, Polak JM. Localization of adrenergic and neuropeptide tyrosine-containing nerves in the mammalian liver. *Hepatology*. 1989;9(6):839-45.
54. Ohata M. Electron microscope study on the innervation of guinea pig liver--proposal of sensory nerve terminals in the hepatic parenchyme. *Archivum histologicum Japonicum = Nihon soshikigaku kiroku*. 1984;47(2):149-78.
55. Metz W, Forssmann WG. Innervation of the liver in guinea pig and rat. *Anatomy and embryology*. 1980;160(3):239-52.
56. Stoyanova, II, Gulubova MV. Peptidergic nerve fibres in the human liver. *Acta histochemica*. 1998;100(3):245-56.
57. Ding WG, Fujimura M, Mori A, Tooyama I, Kimura H. Light and electron microscopy of neuropeptide Y-containing nerves in human liver, gallbladder, and pancreas. *Gastroenterology*. 1991;101(4):1054-9.
58. Gray TS, Morley JE. Neuropeptide Y: anatomical distribution and possible function in mammalian nervous system. *Life sciences*. 1986;38(5):389-401.
59. DeMorrow S, Onori P, Venter J, Invernizzi P, Frampton G, White M, et al. Neuropeptide Y inhibits cholangiocarcinoma cell growth and invasion. *American journal of physiology Cell physiology*. 2011;300(5):C1078-89.
60. Feher E, Fodor M, Feher J. Ultrastructural localization of somatostatin- and substance P-immunoreactive nerve fibers in the feline liver. *Gastroenterology*. 1992;102(1):287-94.
61. Gong AY, Tietz PS, Muff MA, Splinter PL, Huebert RC, Strowski MZ, et al. Somatostatin stimulates ductal bile absorption and inhibits ductal bile secretion in mice via SSTR2 on cholangiocytes. *American journal of physiology Cell physiology*. 2003;284(5):C1205-14.

62. Tietz PS, Alpini G, Pham LD, Larusso NF. Somatostatin inhibits secretin-induced ductal hypercholerisis and exocytosis by cholangiocytes. *The American journal of physiology*. 1995;269(1 Pt 1):G110-8.
63. Tanikawa K. Hepatic sinusoidal cells and sinusoidal circulation. *Journal of gastroenterology and hepatology*. 1995;10 Suppl 1:S8-11.
64. Goehler LE, Sternini C, Brecha NC. Calcitonin gene-related peptide immunoreactivity in the biliary pathway and liver of the guinea-pig: distribution and colocalization with substance P. *Cell and tissue research*. 1988;253(1):145-50.
65. Goehler LE, Sternini C. Neuropeptide Y immunoreactivity in the mammalian liver: pattern of innervation and coexistence with tyrosine hydroxylase immunoreactivity. *Cell and tissue research*. 1991;265(2):287-95.
66. Ueno T, Inuzuka S, Torimura T, Sakata R, Sakamoto M, Gondo K, et al. Distribution of substance P and vasoactive intestinal peptide in the human liver: light and electron immunoperoxidase methods of observation. *The American journal of gastroenterology*. 1991;86(11):1633-7.
67. Nyberg B, Einarsson K, Sonnenfeld T. Evidence that vasoactive intestinal peptide induces ductular secretion of bile in humans. *Gastroenterology*. 1989;96(3):920-4.
68. Cho WK, Boyer JL. Vasoactive intestinal polypeptide is a potent regulator of bile secretion from rat cholangiocytes. *Gastroenterology*. 1999;117(2):420-8.
69. Delalande JM, Milla PJ, Burns AJ. Hepatic nervous system development. The anatomical record Part A, Discoveries in molecular, cellular, and evolutionary biology. 2004;280(1):848-53.
70. Kandilis AN, Koskinas J, Vlachos I, Skaltsas S, Karandrea D, Karakitsos P, et al. Liver regeneration: immunohistochemical study of intrinsic hepatic innervation after partial hepatectomy in rats. *BMC gastroenterology*. 2014;14(1):202.
71. Dhillon AP, Sankey EA, Wang JH, Wightman AK, Mathur S, Burroughs AK, et al. Immunohistochemical studies on the innervation of human transplanted liver. *The Journal of pathology*. 1992;167(2):211-6.
72. Iwai M, Miyashita T, Shimazu T. Inhibition of glucose production during hepatic nerve stimulation in regenerating rat liver perfused in situ. Possible involvement of gap junctions in the action of sympathetic nerves. *European journal of biochemistry / FEBS*. 1991;200(1):69-74.
73. Kumar NM, Gilula NB. Cloning and characterization of human and rat liver cDNAs coding for a gap junction protein. *The Journal of cell biology*. 1986;103(3):767-76.
74. Amenta F, Cavallotti C, Ferrante F, Tonelli F. Cholinergic nerves in the human liver. *The Histochemical journal*. 1981;13(3):419-24.
75. Lutt WW. *Hepatic Circulation: Physiology and Pathophysiology*. San Rafael (CA): Morgan & Claypool Life Sciences; 2009. Available from: <https://www.ncbi.nlm.nih.gov/books/NBK53073/>
76. Fuller RW, Felten SY, Perry KW, Snoddy HD, Felten DL. Sympathetic noradrenergic innervation of guinea-pig liver: histofluorescence and pharmacological studies. *The Journal of pharmacology and experimental therapeutics*. 1981;218(1):282-8.
77. Andersson U, Tracey KJ. Neural reflexes in inflammation and immunity. *The Journal of experimental medicine*. 2012;209(6):1057-68.
78. Rittirsch D, Flierl MA, Ward PA. Harmful molecular mechanisms in sepsis. *Nature reviews Immunology*. 2008;8(10):776-87.
79. Munoz-Ortega M, Quintanar-Stephano A, Garcia Lorenzana M, Campos-Esparza MR, Silva-Briano M, Adabache-Ortiz A, et al. Modulation of amoebic hepatic abscess by the parasympathetic system. *Parasite immunology*. 2011;33(1):65-72.
80. Ghia JE, Blennerhassett P, Kumar-Ondiveeran H, Verdu EF, Collins SM. The vagus nerve: a tonic inhibitory influence associated with inflammatory bowel disease in a murine model. *Gastroenterology*. 2006;131(4):1122-30.
81. Ek M, Kurosawa M, Lundberg T, Ericsson A. Activation of vagal afferents after intravenous injection of interleukin-1beta: role of endogenous prostaglandins. *The Journal of neuroscience : the official journal of the Society for Neuroscience*. 1998;18(22):9471-9.
82. Tracey KJ. The inflammatory reflex. *Nature*. 2002;420(6917):853-9.

83. Goehler LE, Gaykema RP, Hansen MK, Anderson K, Maier SF, Watkins LR. Vagal immune-to-brain communication: a visceral chemosensory pathway. *Autonomic neuroscience : basic & clinical*. 2000;85(1-3):49-59.
84. Bluthé RM, Michaud B, Kelley KW, Dantzer R. Vagotomy attenuates behavioural effects of interleukin-1 injected peripherally but not centrally. *Neuroreport*. 1996;7(9):1485-8.
85. Bluthé RM, Michaud B, Kelley KW, Dantzer R. Vagotomy blocks behavioural effects of interleukin-1 injected via the intraperitoneal route but not via other systemic routes. *Neuroreport*. 1996;7(15-17):2823-7.
86. van Westerloo DJ, Giebelen IA, Florquin S, Daalhuisen J, Bruno MJ, de Vos AF, et al. The cholinergic anti-inflammatory pathway regulates the host response during septic peritonitis. *The Journal of infectious diseases*. 2005;191(12):2138-48.
87. Guarini S, Altavilla D, Cainazzo MM, Giuliani D, Bigiani A, Marini H, et al. Efferent vagal fibre stimulation blunts nuclear factor-kappaB activation and protects against hypovolemic hemorrhagic shock. *Circulation*. 2003;107(8):1189-94.
88. Bernik TR, Friedman SG, Ochani M, DiRaimo R, Susarla S, Czura CJ, et al. Cholinergic antiinflammatory pathway inhibition of tumor necrosis factor during ischemia reperfusion. *Journal of vascular surgery*. 2002;36(6):1231-6.
89. Eliakim R, Karmeli F, Rachmilewitz D, Cohen P, Fich A. Effect of chronic nicotine administration on trinitrobenzene sulphonic acid-induced colitis. *European journal of gastroenterology & hepatology*. 1998;10(12):1013-9.
90. McCafferty DM, Wallace JL, Sharkey KA. Effects of chemical sympathectomy and sensory nerve ablation on experimental colitis in the rat. *The American journal of physiology*. 1997;272(2 Pt 1):G272-80.
91. Hirota CL, McKay DM. M3 muscarinic receptor-deficient mice retain bethanechol-mediated intestinal ion transport and are more sensitive to colitis. *Canadian journal of physiology and pharmacology*. 2006;84(11):1153-61.
92. Sanchez-Aleman E, Quintanar-Stephano A, Escobedo G, Campos-Esparza MD, Campos-Rodriguez R, Ventura-Juarez J. Vagotomy Induces Deregulation of the Inflammatory Response during the Development of Amoebic Liver Abscess in Hamsters. *Neuroimmunomodulation*. 2014.
93. Borovikova LV, Ivanova S, Zhang M, Yang H, Botchkina GI, Watkins LR, et al. Vagus nerve stimulation attenuates the systemic inflammatory response to endotoxin. *Nature*. 2000;405(6785):458-62.
94. Gottwald TP, Lhotak S, Stead RH. Effects of subdiaphragmatic vagotomy on mucosal mast cell densities in stomach and jejunum of rats. *Advances in experimental medicine and biology*. 1995;371A:303-6.
95. D'Mello C, Swain MG. Liver-brain inflammation axis. *American journal of physiology Gastrointestinal and liver physiology*. 2011;301(5):G749-61.
96. Luo L, Xu T, Wang P, Mao L, Xi C, Huang J, et al. Expression of muscarinic acetylcholine receptors in hepatocytes from rat fibrotic liver. *Experimental and toxicologic pathology : official journal of the Gesellschaft fur Toxikologische Pathologie*. 2017;69(2):73-81.
97. Jadcherla SR. Inflammation inhibits muscarinic signaling in in vivo canine colonic circular smooth muscle cells. *Pediatric research*. 2002;52(5):756-62.
98. Ohama T, Hori M, Ozaki H. Mechanism of abnormal intestinal motility in inflammatory bowel disease: how smooth muscle contraction is reduced? *Journal of smooth muscle research = Nihon Heikatsukin Gakkai kikanishi*. 2007;43(2):43-54.
99. Akiho H, Khan WI, Al-Kaabi A, Blennerhassett P, Deng Y, Collins SM. Cytokine modulation of muscarinic receptors in the murine intestine. *American journal of physiology Gastrointestinal and liver physiology*. 2007;293(1):G250-5.
100. Tobin G, Giglio D, Lundgren O. Muscarinic receptor subtypes in the alimentary tract. *Journal of physiology and pharmacology : an official journal of the Polish Physiological Society*. 2009;60(1):3-21.
101. Profita M, Giorgi RD, Sala A, Bonanno A, Riccobono L, Mirabella F, et al. Muscarinic receptors, leukotriene B4 production and neutrophilic inflammation in COPD patients. *Allergy*. 2005;60(11):1361-9.

102. Lee JA, Ahmed Q, Hines JE, Burt AD. Disappearance of hepatic parenchymal nerves in human liver cirrhosis. *Gut*. 1992;33(1):87-91.
103. Jaskiewicz K, Voigt MD, Robson SC. Distribution of hepatic nerve fibers in liver diseases. *Digestion*. 1994;55(4):247-52.
104. Ueno T, Bioulac-Sage P, Balabaud C, Rosenbaum J. Innervation of the sinusoidal wall: regulation of the sinusoidal diameter. *The anatomical record Part A, Discoveries in molecular, cellular, and evolutionary biology*. 2004;280(1):868-73.
105. Jaskiewicz K, Robson SC, Banach L. Toxic hepatic injury is associated with proliferation of portal nerve fibers. *Pathology, research and practice*. 1993;189(10):1191-4.
106. Dubuisson L, Desmouliere A, Decourt B, Evade L, Bedin C, Boussarie L, et al. Inhibition of rat liver fibrogenesis through noradrenergic antagonism. *Hepatology*. 2002;35(2):325-31.
107. Inoue N, Sakai H, Magari S, Sakanaka M. Distribution and possible origins of substance P-containing nerve fibers in the rat liver. *Annals of anatomy = Anatomischer Anzeiger : official organ of the Anatomische Gesellschaft*. 1992;174(6):557-60.
108. Terada T, Nakanuma Y, Ohta G. Glandular elements around the intrahepatic bile ducts in man; their morphology and distribution in normal livers. *Liver*. 1987;7(1):1-8.
109. Terada T, Nakanuma Y. Morphological examination of intrahepatic bile ducts in hepatolithiasis. *Virchows Archiv A, Pathological anatomy and histopathology*. 1988;413(2):167-76.
110. Kandilis AN, Papadopoulou IP, Koskinas J, Sotiropoulos G, Tiniakos DG. Liver innervation and hepatic function: new insights. *The Journal of surgical research*. 2015;194(2):511-9.
111. Pietroletti R, Chamuleau RA, Speranza V, Lygidakis NJ. Immunocytochemical study of the hepatic innervation in the rat after partial hepatectomy. *The Histochemical journal*. 1987;19(6-7):327-32.
112. Thorgeirsson SS. Hepatic stem cells in liver regeneration. *FASEB journal : official publication of the Federation of American Societies for Experimental Biology*. 1996;10(11):1249-56.
113. Yokoyama HO, Wilson ME, Tsuboi KK, Stowell RE. Regeneration of mouse liver after partial hepatectomy. *Cancer research*. 1953;13(1):80-5.
114. Fausto N, Campbell JS. The role of hepatocytes and oval cells in liver regeneration and repopulation. *Mechanisms of development*. 2003;120(1):117-30.
115. Yokoyama Y, Nagino M, Nimura Y. Mechanism of impaired hepatic regeneration in cholestatic liver. *Journal of hepato-biliary-pancreatic surgery*. 2007;14(2):159-66.
116. Ohtake M, Sakaguchi T, Yoshida K, Muto T. Hepatic Branch Vagotomy Can Suppress Liver Regeneration in Partially Hepatectomized Rats. *HPB Surgery*. 1993;6(4):277-86.
117. LeSage* G, Alvaro D, Benedetti A, Glaser S, Luca M, Baiocchi L, et al. Cholinergic system modulates growth, apoptosis, and secretion of cholangiocytes from bile duct ligated rats. *Gastroenterology*. 1999;117(1):191-9.
118. Roskams T, Cassiman D, De Vos R, Libbrecht L. Neuroregulation of the neuroendocrine compartment of the liver. *The Anatomical Record Part A: Discoveries in Molecular, Cellular, and Evolutionary Biology*. 2004;280A(1):910-23.
119. Kiba T, Tanaka K, Numata K, Hoshino M, Inoue S. Facilitation of liver regeneration after partial hepatectomy by ventromedial hypothalamic lesions in rats. *Pflügers Archiv European Journal of Physiology*. 1994;428(1):26-9.
120. Kato H, Shimazu T. Effect of autonomic denervation on DNA synthesis during liver regeneration after partial hepatectomy. *European journal of biochemistry / FEBS*. 1983;134(3):473-8.
121. LeSage EG, Alvaro D, Benedetti A, Glaser S, Marucci L, Baiocchi L, et al. Cholinergic system modulates growth, apoptosis, and secretion of cholangiocytes from bile duct-ligated rats. *Gastroenterology*. 1999;117(1):191-9.
122. Frucht H, Jensen RT, Dexter D, Yang W-L, Xiao Y. Human Colon Cancer Cell Proliferation Mediated by the M3 Muscarinic Cholinergic Receptor *Clinical Cancer Research* 1999 5 (9):2532-9

123. Guizzetti M, Costa P, Peters J, Costa LG. Acetylcholine as a mitogen: muscarinic receptor-mediated proliferation of rat astrocytes and human astrocytoma cells. *European Journal of Pharmacology*. 1996;297(3):265-73.
124. Wess J. Novel insights into muscarinic acetylcholine receptor function using gene targeting technology. *Trends in Pharmacological Sciences*. 2003;24(8):414-20.
125. Uchiyama T, Chess-Williams R. Muscarinic receptor subtypes of the bladder and gastrointestinal tract. *Journal of smooth muscle research = Nihon Heikatsukin Gakkai kikanishi*. 2004;40(6):237-47.
126. Cassiman D, Libbrecht L, Sinelli N, Desmet V, Deneef C, Roskams T. The Vagal Nerve Stimulates Activation of the Hepatic Progenitor Cell Compartment via Muscarinic Acetylcholine Receptor Type 3. *The American journal of pathology*. 2002;161(2):521-30.
127. Kanno N, LeSage G, Glaser S, Alpini G. Regulation of cholangiocyte bicarbonate secretion. *American journal of physiology Gastrointestinal and liver physiology*. 2001;281(3):G612-25.
128. Alpini G, Glaser SS, Ueno Y, Pham L, Podila PV, Caligiuri A, et al. Heterogeneity of the proliferative capacity of rat cholangiocytes after bile duct ligation. *The American journal of physiology*. 1998;274(4 Pt 1):G767-75.
129. Nathanson MH, Boyer JL. Mechanisms and regulation of bile secretion. *Hepatology*. 1991;14(3):551-66.
130. Elsing C, Hubner C, Fitscher BA, Kassner A, Stremmel W. Muscarinic acetylcholine receptor stimulation of biliary epithelial cells and its effect on bile secretion in the isolated perfused liver. *Hepatology*. 1997;25(4):804-13.
131. Pauli-Magnus C, Meier PJ. Hepatobiliary transporters and drug-induced cholestasis. *Hepatology*. 2006;44(4):778-87.
132. Strazzabosco M, Spirlí C, Okolicsanyi L. Pathophysiology of the intrahepatic biliary epithelium. *Journal of Gastroenterology and Hepatology*. 2000;15(3):244-53.
133. Kanno N, LeSage G, Glaser S, Alvaro D, Alpini G. Functional heterogeneity of the intrahepatic biliary epithelium. *Hepatology*. 2000;31(3):555-61.
134. Alpini G, Glaser S, Robertson W, Rodgers RE, Phinizy JL, Lasater J, et al. Large but not small intrahepatic bile ducts are involved in secretin-regulated ductal bile secretion. *The American journal of physiology*. 1997;272(5 Pt 1):G1064-74.
135. Ludwig J. New concepts in biliary cirrhosis. *Seminars in liver disease*. 1987;7(4):293-301.
136. Alpini G, Lenzi R, Zhai WR, Slott PA, Liu MH, Sarkozi L, et al. Bile secretory function of intrahepatic biliary epithelium in the rat. *The American journal of physiology*. 1989;257(1 Pt 1):G124-33.
137. LeSage GD, Benedetti A, Glaser S, Marucci L, Tretjak Z, Caligiuri A, et al. Acute carbon tetrachloride feeding selectively damages large, but not small, cholangiocytes from normal rat liver. *Hepatology*. 1999;29(2):307-19.
138. LeSage GD, Glaser SS, Marucci L, Benedetti A, Phinizy JL, Rodgers R, et al. Acute carbon tetrachloride feeding induces damage of large but not small cholangiocytes from BDL rat liver. *The American journal of physiology*. 1999;276(5 Pt 1):G1289-301.
139. Benedetti A, Bassotti C, Rapino K, Marucci L, Jezequel AM. A morphometric study of the epithelium lining the rat intrahepatic biliary tree. *Journal of hepatology*. 1996;24(3):335-42.
140. Sugiura H, Nakanuma Y. Secretory component and immunoglobulins in the intrahepatic biliary tree and peribiliary gland in normal livers and hepatolithiasis. *Gastroenterologia Japonica*. 1989;24(3):308-14.
141. Alvaro D, Benedetti A, Marucci L, Delle Monache M, Monterubbianesi R, Di Cosimo E, et al. The function of alkaline phosphatase in the liver: regulation of intrahepatic biliary epithelium secretory activities in the rat. *Hepatology*. 2000;32(2):174-84.
142. Alpini G, Ulrich C, Roberts S, Phillips JO, Ueno Y, Podila PV, et al. Molecular and functional heterogeneity of cholangiocytes from rat liver after bile duct ligation. *The American journal of physiology*. 1997;272(2 Pt 1):G289-97.

143. Alvaro D, Mennone A, Boyer JL. Role of kinases and phosphatases in the regulation of fluid secretion and Cl-/HCO₃⁻ exchange in cholangiocytes. *The American journal of physiology*. 1997;273(2 Pt 1):G303-13.
144. Kato A, Gores GJ, LaRusso NF. Secretin stimulates exocytosis in isolated bile duct epithelial cells by a cyclic AMP-mediated mechanism. *The Journal of biological chemistry*. 1992;267(22):15523-9.
145. LeSage G, Glaser S, Alpini G. Regulation of cholangiocyte proliferation. *Liver*. 2001;21(2):73-80.
146. Baiocchi L, LeSage G, Glaser S, Alpini G. Regulation of cholangiocyte bile secretion. *Journal of hepatology*. 1999;31(1):179-91.
147. Alpini G, Ueno Y, Glaser SS, Marzioni M, Phinizy JL, Francis H, et al. Bile acid feeding increased proliferative activity and apical bile acid transporter expression in both small and large rat cholangiocytes. *Hepatology*. 2001;34(5):868-76.
148. Marzioni M, Fava G, Benedetti A. Nervous and Neuroendocrine regulation of the pathophysiology of cholestasis and of biliary carcinogenesis. *World journal of gastroenterology : WJG*. 2006;12(22):3471-80.
149. Heitz P, Polak JM, Kasper M, Timson CM, Pearse AG. Immunoelectron cytochemical localization of motilin and substance P in rabbit bile duct enterochromaffin (EC) cells. *Histochemistry*. 1977;50(4):319-25.
150. Roskams T, van den Oord JJ, De Vos R, Desmet VJ. Neuroendocrine features of reactive bile ductules in cholestatic liver disease. *The American journal of pathology*. 1990;137(5):1019-25.
151. Banales JM, Prieto J, Medina JF. Cholangiocyte anion exchange and biliary bicarbonate excretion. *World journal of gastroenterology : WJG*. 2006;12(22):3496-511.
152. Akiyoshi H, Terada T. Mast cell, myofibroblast and nerve terminal complexes in carbon tetrachloride-induced cirrhotic rat livers. *Journal of Hepatology*. 1998;29(1):112-9.
153. Alvaro D, Alpini G, Jezequel AM, Bassotti C, Francia C, Fraioli F, et al. Role and mechanisms of action of acetylcholine in the regulation of rat cholangiocyte secretory functions. *The Journal of Clinical Investigation*. 1997;100(6):1349-62.
154. Witz M, Schneider A, Novis B, Engelberg M, Dinbar A. Bile composition and bile acid pool size. Comparison after truncal, selective, and highly selective vagotomy. *Archives of surgery*. 1985;120(11):1306-9.
155. Shaffer EA. The effect of vagotomy on gallbladder function and bile composition in man. *Annals of surgery*. 1982;195(4):413-8.
156. Fletcher DM, Clark CG. Changes in canine bile-flow and composition after vagotomy. *The British journal of surgery*. 1969;56(2):103-6.
157. Bouchier IA. The vagus, the bile, and gallstones. *Gut*. 1970;11(9):799-803.
158. Trauner M, Fickert P, Halilbasic E, Moustafa T. Lessons from the toxic bile concept for the pathogenesis and treatment of cholestatic liver diseases. *WMW Wiener Medizinische Wochenschrift*. 2008;158(19):542-8.
159. Beuers U, Hohenester S, de Buy Wenniger LJM, Kremer AE, Jansen PLM, Elferink RPJO. The biliary HCO₃ umbrella: A unifying hypothesis on pathogenetic and therapeutic aspects of fibrosing cholangiopathies. *Hepatology*. 2010;52(4):1489-96.
160. Hohenester S, Maillette de Buy Wenniger L, Paulusma CC, van Vliet SJ, Jefferson DM, Oude Elferink RP, et al. A biliary HCO₃ umbrella constitutes a protective mechanism against bile acid-induced injury in human cholangiocytes. *Hepatology*. 2012;55(1):173-83.
161. Bernik TR, Friedman SG, Ochani M, DiRaimo R, Susarla S, Czura CJ, et al. Cholinergic antiinflammatory pathway inhibition of tumor necrosis factor during ischemia reperfusion. *Journal of Vascular Surgery*. 2002;36(6):1231-6.
162. JADCHERLA SR, editor Inflammation inhibits muscarinic signaling in in vivo canine colonic circular smooth muscle cells. *Pediatric Research*; 2002.
163. TAKASHI O. Mechanism of abnormal intestinal motility in inflammatory bowel disease: how smooth muscle contraction is reduced? *Journal of Smooth Muscle Research*. 2007;43(2):43-54.
164. Medina JF. Role of the Anion Exchanger 2 in the Pathogenesis and Treatment of Primary Biliary Cirrhosis. *Digestive Diseases*. 2011;29(1):103-12.

165. Berg C, Blume K, Lauber K, Gregor M, Berg P, Wesselborg S, et al. Autoantibodies to muscarinic acetylcholine receptors found in patients with primary biliary cirrhosis. *BMC Gastroenterology*. 2010;10(1):120.
166. Bacman S, Perez Leiros C, Sterin-Borda L, Hubscher O, Arana R, Borda E. Autoantibodies against lacrimal gland M3 muscarinic acetylcholine receptors in patients with primary Sjögren's syndrome. *Investigative Ophthalmology & Visual Science*. 1998;39(1):151-6.
167. Gelbmann CM, Rummele P, Wimmer M, Hofstadter F, Gohlmann B, Endlicher E, et al. Ischemic-Like Cholangiopathy With Secondary Sclerosing Cholangitis in Critically Ill Patients. *2007;102(6):1221-9*.
168. Chand N, Sanyal AJ. Sepsis-induced cholestasis. *Hepatology*. 2007;45(1):230-41.
169. Kjaer M, Jurlander J, Keiding S, Galbo H, Kirkegaard P, Hage E. No reinnervation of hepatic sympathetic nerves after liver transplantation in human subjects. *Journal of hepatology*. 1994;20(1):97-100.
170. Colle I, Van Vlierberghe H, Troisi R, De Hemptinne B. Transplanted liver: Consequences of denervation for liver functions. *The Anatomical Record Part A: Discoveries in Molecular, Cellular, and Evolutionary Biology*. 2004;280A(1):924-31.
171. Fickert P, Stöger U, Fuchsbichler A, Moustafa T, Marschall H-U, Weiglein AH, et al. A New Xenobiotic-Induced Mouse Model of Sclerosing Cholangitis and Biliary Fibrosis. *The American Journal of Pathology*. 2007;171(2):525-36.
172. Fickert P, Fuchsbichler A, Marschall HU, Wagner M, Zollner G, Krause R, et al. Lithocholic Acid Feeding Induces Segmental Bile Duct Obstruction and Destructive Cholangitis in Mice. *The American Journal of Pathology*. 2006;168(2):410-22.
173. Fickert P, Zollner G, Fuchsbichler A, Stumptner C, Weiglein A, Lammert F, et al. Ursodeoxycholic acid aggravates bile infarcts in bile duct-ligated and Mdr2 knockout mice via disruption of cholangioles. *Gastroenterology*. 2002;123(4):1238-51.
174. Fickert P, Fuchsbichler A, Wagner M, Zollner G, Kaser A, Tilg H, et al. Regurgitation of bile acids from leaky bile ducts causes sclerosing cholangitis in Mdr2 (Abcb4) knockout mice. *Gastroenterology*. 2004;127(1):261-74.
175. Fickert P, Wagner M, Marschall HU, Fuchsbichler A, Zollner G, Tsybrovskyy O, et al. 24-norUrsodeoxycholic Acid Is Superior to Ursodeoxycholic Acid in the Treatment of Sclerosing Cholangitis in Mdr2 (Abcb4) Knockout Mice. *Gastroenterology*. 2006;130(2):465-81.
176. Yamada M, Miyakawa T, Duttaroy A, Yamanaka A, Moriguchi T, Makita R, et al. Mice lacking the M3 muscarinic acetylcholine receptor are hypophagic and lean. *Nature*. 2001;410(6825):207-12.
177. Wess J, Eglen RM, Gautam D. Muscarinic acetylcholine receptors: mutant mice provide new insights for drug development. *2007;6(9):721-33*.
178. Fickert P, Trauner M, Fuchsbichler A, Zollner G, Wagner M, Marschall H, et al. Oncosis represents the main type of cell death in mouse models of cholestasis. *J Hepatol*. 2005;42(3):378-85.
179. Wagner M, Fickert P, Zollner G, Fuchsbichler A, Silbert D, Tsybrovskyy O, et al. Role of farnesoid X receptor in determining hepatic ABC transporter expression and liver injury in bile duct-ligated mice. *Gastroenterology*. 2003;125(3):825-38.
180. Fickert P, Zollner G, Fuchsbichler A, Stumptner C, Pojer C, Zenz R, et al. Effects of ursodeoxycholic and cholic acid feeding on hepatocellular transporter expression in mouse liver. *Gastroenterology*. 2001;121(1):170-83.
181. Davit-Spraul A, Gonzales E, Baussan C, Jacquemin E. The Spectrum of Liver Diseases Related to ABCB4 Gene Mutations: Pathophysiology and Clinical Aspects. *Semin Liver Dis*. 2010;30(02):134,46.
182. Peng Z, Heath J, Drachenberg C, Raufman JP, Xie G. Cholinergic muscarinic receptor activation augments murine intestinal epithelial cell proliferation and tumorigenesis. *BMC cancer*. 2013;13:204.
183. Raufman JP, Cheng K, Zimniak P. Activation of muscarinic receptor signaling by bile acids: physiological and medical implications. *Digestive diseases and sciences*. 2003;48(8):1431-44.

184. Cheng K, Khurana S, Chen Y, Kennedy RH, Zimniak P, Raufman JP. Lithocholylcholine, a bile acid/acetylcholine hybrid, is a muscarinic receptor antagonist. *The Journal of pharmacology and experimental therapeutics*. 2002;303(1):29-35.
185. Raufman JP, Zimniak P, Bartoszko-Malik A. Lithocholyltaurine interacts with cholinergic receptors on dispersed chief cells from guinea pig stomach. *The American journal of physiology*. 1998;274(6 Pt 1):G997-1004.
186. Halilbasic E, Fiorotto R, Fickert P, Marschall HU, Moustafa T, Spirli C, et al. Side chain structure determines unique physiologic and therapeutic properties of norursodeoxycholic acid in Mdr2^{-/-} mice. *Hepatology*. 2009;49(6):1972-81.
187. Beigneux A, Hofmann AF, Young SG. Human CYP7A1 deficiency: progress and enigmas. *The Journal of clinical investigation*. 2002;110(1):29-31.
188. Pollheimer MJ, Fickert P, Stieger B. Chronic cholestatic liver diseases: clues from histopathology for pathogenesis. *Molecular aspects of medicine*. 2014;37:35-56.
189. Boyer JL. Bile formation and secretion. *Comprehensive Physiology*. 2013;3(3):1035-78.
190. Maillette de Buy Wenniger LJ, Hohenester S, Maroni L, van Vliet SJ, Oude Elferink RP, Beuers U. The Cholangiocyte Glycocalyx Stabilizes the 'Biliary HCO₃ Umbrella': An Integrated Line of Defense against Toxic Bile Acids. *Digestive diseases*. 2015;33(3):397-407.
191. Esteller A. Physiology of bile secretion. *World journal of gastroenterology : WJG*. 2008;14(37):5641-9.
192. Tabibian JH, Masyuk AI, Masyuk TV, O'Hara SP, LaRusso NF. Physiology of cholangiocytes. *Comprehensive Physiology*. 2013;3(1):541-65.
193. White TT, Tournut RA, Scharplatz D, Kavlie H, Olson AD, Hopton DS. The effect of vagotomy on biliary secretions and bile salt pools in dogs. *Annals of surgery*. 1974;179(4):406-11.
194. Alpini G, Ulrich CD, 2nd, Phillips JO, Pham LD, Miller LJ, LaRusso NF. Upregulation of secretin receptor gene expression in rat cholangiocytes after bile duct ligation. *The American journal of physiology*. 1994;266(5 Pt 1):G922-8.
195. Barbaro B, Glaser S, Francis H, et al. Nerve Regulation of Cholangiocyte Functions. In: *Madame Curie Bioscience Database [Internet]*. Austin (TX): Landes Bioscience;2000-2013. Available from: <https://www.ncbi.nlm.nih.gov/books/NBK6626/>
196. Afroze S, Meng F, Jensen K, McDaniel K, Rahal K, Onori P, et al. The physiological roles of secretin and its receptor. *Annals of translational medicine*. 2013;1(3):29.
197. Kaminski DL, Deshpande YG. Effect of somatostatin and bombesin on secretin-stimulated ductular bile flow in dogs. *Gastroenterology*. 1983;85(6):1239-47.
198. Beuers U, Hohenester S, de Buy Wenniger LJ, Kremer AE, Jansen PL, Elferink RP. The biliary HCO₃⁽⁻⁾ umbrella: a unifying hypothesis on pathogenetic and therapeutic aspects of fibrosing cholangiopathies. *Hepatology*. 2010;52(4):1489-96.
199. Hofmann AF, Hagey LR. Key discoveries in bile acid chemistry and biology and their clinical applications: history of the last eight decades. *Journal of lipid research*. 2014;55(8):1553-95.
200. Halilbasic E, Steinacher D, Trauner M. Nor-Ursodeoxycholic Acid as a Novel Therapeutic Approach for Cholestatic and Metabolic Liver Diseases. *Digestive diseases*. 2017;35(3):288-92.
201. Wagner M, Fickert P, Zollner G, Fuchsbichler A, Silbert D, Tsybrovskyy O, et al. Role of farnesoid X receptor in determining hepatic ABC transporter expression and liver injury in bile duct-ligated mice. *Gastroenterology*. 2003;125(3):825-38.
202. Cassiman D, Libbrecht L, Sinelli N, Desmet V, Deneef C, Roskams T. The vagal nerve stimulates activation of the hepatic progenitor cell compartment via muscarinic acetylcholine receptor type 3. *The American journal of pathology*. 2002;161(2):521-30.
203. Marzioni M, LeSage GD, Glaser S, Patel T, Marienfeld C, Ueno Y, et al. Taurocholate prevents the loss of intrahepatic bile ducts due to vagotomy in bile duct-ligated rats. *American journal of physiology Gastrointestinal and liver physiology*. 2003;284(5):G837-52.
204. Marzioni M, Francis H, Benedetti A, Ueno Y, Fava G, Venter J, et al. Ca²⁺-dependent cytoprotective effects of ursodeoxycholic and tauroursodeoxycholic acid on the biliary

- epithelium in a rat model of cholestasis and loss of bile ducts. *The American journal of pathology*. 2006;168(2):398-409.
205. Friman S, Persson H, Schersten T, Svanvik J, Karlberg I. Adjuvant treatment with ursodeoxycholic acid reduces acute rejection after liver transplantation. *Transplantation proceedings*. 1992;24(1):389-90.
206. Qaseem A, Wilt TJ, Weinberger SE, Hanania NA, Criner G, van der Molen T, et al. Diagnosis and management of stable chronic obstructive pulmonary disease: a clinical practice guideline update from the American College of Physicians, American College of Chest Physicians, American Thoracic Society, and European Respiratory Society. *Annals of internal medicine*. 2011;155(3):179-91.
207. Ackland D, Kumaran N, Zia R. Treating glaucoma: the not-so-nice guidance. *The British journal of ophthalmology*. 2014;98(9):1139-40.
208. Vivino FB, Carsons SE, Foulks G, Daniels TE, Parke A, Brennan MT, et al. New Treatment Guidelines for Sjogren's Disease. *Rheumatic diseases clinics of North America*. 2016;42(3):531-51.
209. Gosens R, Zaagsma J, Meurs H, Halayko AJ. Muscarinic receptor signaling in the pathophysiology of asthma and COPD. *Respiratory research*. 2006;7:73.
210. Zhao M, He X, Bi XY, Yu XJ, Gil Wier W, Zang WJ. Vagal stimulation triggers peripheral vascular protection through the cholinergic anti-inflammatory pathway in a rat model of myocardial ischemia/reperfusion. *Basic research in cardiology*. 2013;108(3):345.
211. Strom TB, Deisseroth A, Morganroth J, Carpenter CB, Merrill JP. Alteration of the cytotoxic action of sensitized lymphocytes by cholinergic agents and activators of adenylate cyclase. *Proceedings of the National Academy of Sciences of the United States of America*. 1972;69(10):2995-9.
212. Razani-Boroujerdi S, Behl M, Hahn FF, Pena-Philippides JC, Hutt J, Sopori ML. Role of muscarinic receptors in the regulation of immune and inflammatory responses. *Journal of neuroimmunology*. 2008;194(1-2):83-8.
213. Hajiasgharzadeh K, Tavangar SM, Javan M, Dehpour AR, Mani AR. Does hepatic vagus nerve modulate the progression of biliary fibrosis in rats? *Autonomic neuroscience : basic & clinical*. 2014;185:67-75.
214. Heider TR, Koruda MJ, Farrell TM, Behrns KE. Acute vagotomy does not augment the systemic inflammatory response in patients with peptic ulcer disease. *The American surgeon*. 2004;70(4):342-6.